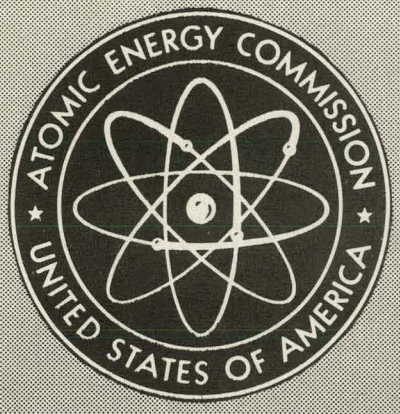

APAE-105

THERMAL ANALYSIS OF TYPE 3 ELEMENTS IN THE SM-1, SM-1A AND PM-2A CORES

By
S. L. Davidson
I. Segalman

March 30, 1962

Nuclear Power Engineering Department
Alco Products, Inc.
Schenectady, New York

UNITED STATES ATOMIC ENERGY COMMISSION • DIVISION OF TECHNICAL INFORMATION

DISCLAIMER

LEGAL NOTICE

Printed in USA. Price $2.50. Available from the Office of Technical Services, Department of Commerce, Washington 25, D. C.

USAEC Division of Technical Information Extension, Oak Ridge, Tennessee

APAE-105

REACTOR TECHNOLOGY

THERMAL ANALYSIS OF TYPE 3 ELEMENTS IN THE SM-1, SM-1A and PM-2A CORES

By
S. L. Davidson
I. Segalman

Approved by:
M. H. Dixon, Project Engineer

Issued: March 30, 1962

Contract No. AT(30-1)-2639
with U. S. Atomic Energy Commission
New York Operations Office

ALCO PRODUCTS, INC.
Nuclear Power Engineering Department
Post Office Box 414
Schenectady 1, N. Y.

THIS PAGE

WAS INTENTIONALLY

LEFT BLANK

ABSTRACT

Thermal characteristics of Type 3 elements planned for installation in the SM-1, SM-1A and PM-2A plants were analyzed for both steady state and loss of flow transient conditions. Results of this analysis for steady state conditions indicate that the SM-1, SM-1A and PM-2A Type 3 cores will operate safely at design and scram conditions. All steady state analyses indicated minimum DNBR's for both design and scram conditions above the minimum criteria of 1.5. Local nucleate boiling was noted in the SM-1 and SM-1A Type 3 cores. Loss of flow transient results indicate that all three Type 3 cores have minimum DNBR's above 1.5 and are safe from burnout. Only the SM-1A Type 3 core indicates bulk nucleate boiling during the loss of flow accident.

THIS PAGE

WAS INTENTIONALLY

LEFT BLANK

TABLE OF CONTENTS

TABLE OF CONTENTS (CONT'D)

TABLE OF CONTENTS (CONT'D)

LIST OF FIGURES

LIST OF FIGURES (CONT'D)

LIST OF FIGURES (CONT'D)

LIST OF TABLES

LIST OF TABLES (CONT'D)

SUMMARY

A steady state and transient thermal analysis has been performed on the Type 3 replacement cores for the SM-1, SM-1A and PM-2A plants. The fundamental criterion for acceptable thermal design is the minimum departure from nucleate boiling ratio (DNBR). The minimum design DNBR at design power conditions and scram power conditions for concurrent transient and steady state analyses is currently specified at 1.5.

The steady state thermal analysis indicates that the SM-1 Type 3 core will operate safely at design conditions of 10.77 MW and scram power of 13.45 MW with minimum DNBR s above 1.5. Stationary elements in some peripheral core positions experience local nucleate boiling.

The steady state thermal analysis indicates that the SM-1A Type 3 core will operate safely at design conditions of 20.2 MW and scram power of 24.2 MW with minimum DNBR's above 1.5. At scram power conditions a minute amount of local nucleate boiling in the hot channel was evident at the exit end of the most critical control rod and stationary element.

Results of the thermal analysis indicate that the PM-2A Type 3 core will operate safely at design conditions of 10.0 MW and scram power of 12.0 MW with minimum DNBR's greater than 1.5.

The analysis of all Type 3 cores shows they are safe during the early critical period (first 3 sec) of a loss of low transient. The corresponding minimum DNBR produced is 1.96 in the SM-1A Type 3 core at the peak power level (scram power level) with the scram mechanism inoperative. Since this minimum DNBR occurs under the severest conditions and the minimum DNBR produced is greater than the design criteria of 1.50, all Type 3 cores are considered thermally safe. Under similar conservative conditions the SM-1 Type 3 core has a minimum loss of flow transient DNBR of 4.08 and the PM-2A Type 3 core has a minimum loss of flow transient DNBR of 4.59.

At nominal power levels the SM-1 and SM-1A Type 3 cores indicate local nucleate boiling in the hot channel while the PM-2A Type 3 core indicates no local nucleate boiling. At the scram power level all Type 3 cores indicate steady state local nucleate boiling in the hot channels. However, only the SM-1A Type 3 core indicates any bulk nucleate boiling in the hot channel during the first 5 sec of the loss of flow accident.

In the evaluation of the SM-1 Type 3 core it has been determined that increasing the flow coastdown time or scramming the reactor due to reduced flow does not appreciably affect the minimum DNBR but helps to impede the bulk fluid temperature rise during the loss of flow transient.

1.0 STEADY STATE ANALYSIS

1.1 INTRODUCTION

Steady state and transient analyses have been performed on the SM-1, SM-1A and PM-2A full size Type 3 cores as a part of the Army Replacement Core Development Program under item 3.3 of AP Note 286, Addendum 1, Revision 1.* The principal effort in this program was devoted to utilization of Type 3 (SM-2) fuel plates in the above mentioned cores. Due to an increase in fuel content, the Type 3 fuel elements offer significant improvements in core life over the initial cores.

Various elements within each core have been analyzed to insure safe core operation for both steady state and transient conditions. The limitations imposed upon the preliminary thermal analysis [1] have been removed by the following:

A. The analytical predictions and measured nuclear power distributions have been improved. Good agreement was found between predicted values and critical experiment [2] values using the exact SM-1, SM-1A and PM-2A core arrays.

B. Channel-to-channel flow distribution was established as a result of single element flow testing. Previous to this analysis, channel-to-channel maldistributions were estimated [4]

C. Improved and more realistic transient results were obtained for the loss of pump accident by the use of the transient code ART-02 [17]. Previous analysis treated this as a quasi-steady state problem.

This analysis has presented the important thermal and hydraulic characteristics associated with SM-1, SM-1A and PM-2A cores in order to verify safe core operation with Type 3 elements installed. The design data for these cores is listed in Table 1.1. Fig. 1.1 and 1.2 show the Type 3 stationary fuel element and control rod element, respectively.

---

* Subsequent to the completion of these analyses a decision had been made to make the first SM-1 Type 3 core as a prototype of a PM-2A Type 3 core. The analysis of this 37 element Type 3 core in the SM-1 will be covered in a supplement to this report.

TABLE 1.1
THERMAL, HYDRAULIC AND MECHANICAL DESIGN DATA
FOR THE SM-1, SM-1A AND PM-2A TYPE 3 CORES

1. DRAWINGS

The following drawings show the final Type 3 element configurations for installation in the SM-1, SM-1A and PM-2A Type 3 Cores.

Fuel Element Control Rod - SM Type 3 Core	D9-13-1047
Assembly - Fuel Element (Stationary) - SM Type 3 Core	R9-13-1052
Type 3 Fuel Element (Stationary) for PM-2A Core	R9-13-1049

2. HYDRAULIC DESIGN DATA

A. SM-1 Type 3 Core

Primary System pressure	psia	1200
Primary system flow rate	gpm	3862
Average nominal channel mass flow	lb/hr-ft^2 x 10^6	0.752
Average hot channel mass flow	lb/hr-ft^2 x 10^5	0.573
Maximum average channel pressure drop	ft. H_2O	0.99
Maximum hot channel pressure drop	ft. H_2O	0.89

B. SM-1A Type 3 Core

Primary system pressure	psia	1200
Primary system flow rate	gpm	7400
Average nominal channel mass flow	lb/hr-ft^2 x 10^6	1.52
Average hot channel mass flow	lb/hr-ft^2 x 10^6	1.36
Maximum average channel pressure drop	ft. H_2O	1.40
Maximum hot channel pressure drop	ft. H_2O	1.30

C. PM-2A Type 3 Core

Primary system pressure	psia	1750
Primary system flow rate	gpm	4890
Average nominal channel mass flow	lb/hr-ft^2 x 10^6	1.10
Average hot channel mass flow	lb/hr-ft^2 x 10^6	0.951
Maximum average channel pressure drop	ft H_2O	1.01
Maximum hot channel pressure drop	ft H_2O	0.91

3. THERMAL DESIGN DATA

A. SM-1 Type 3 Core

Core Inlet Temperature	^{o}F	427.7
Maximum bulk water temp.	^{o}F	529.7
Maximum plate surface temperature	^{o}F	576.4
Maximum meat temperature	^{o}F	603.2
Average plate surface temperature	^{o}F	529.5
Average meat temperature for hot element	^{o}F	566.5
Effective core heat transfer area	ft^2	589.32
Average core heat flux	Btu-hr ft^2	64,557
Maximum Core Heat Flux	Btu-hr-ft^2	2.578×10^5
Minimum, DNBR (steady State)		4.06
Minimum, DNBR (transient state)		4.08

B. SM-1A Type 3 Core

Core inlet temperature	^{o}F	423
Maximum bulk water temperature	^{o}F	479.5
Maximum plate surface temperature	^{o}F	578.5
Maximum meat temperature	^{o}F	638.3
Average plate surface temperature	^{o}F	534.0
Average meat temperature for hot element	^{o}F	566.0
Effective core heat transfer area	ft^2	593.1
Average core heat flux	Btu-hr-ft^2	120,320
Maximum Core heat flux	Btu-hr-ft^2	5.149×10^5
Minimum DNBR (steady state)		1.98
Minimum DNBR (transient state)		1.96

C. PM-2A Type 3 Core

Core inlet temperature	^{o}F	500
Maximum bulk water temperature	^{o}F	545
Maximum plate surface temperature	^{o}F	610.3
Maximum meat temperature	^{o}F	620.9
Average plate surface temperature	^{o}F	572
Average meat temperature for hot element	^{o}F	586.5
Effective core heat transfer area	ft^2	513.07
Average core heat flux	Btu-hr-ft^2	68,849
Maximum core heat flux	Btu-hr-ft^2	2.016×10^5
Minimum DNBR (steady-state)		4.66
Minimum DNBR (transient-state)		4.59

4. MECHANICAL DESIGN DATA - DIMENSIONS OF FUEL ASSEMBLIES

A. SM-1, SM-1A, PM-2A Type 3 Cores

		Stationary	Control Rod
Meat width	in.	2.650	2.40
Plate width	in.	2.839	2.589
Active length	in.	22.0	21.5
Total plate length	in.	23.5	23
Overall thickness (max)	in.	2.865	2.618
Overall width (max)	in.	2.874	2.624

Two outside plates are 27 in. long.

1.2 STEADY STATE METHODS OF ANALYSIS

The final steady state analysis was performed using the STDY-3 Code[3]. It is the authors' intent in this report to discuss in general the input parameters of the code and how the code uses these parameters to arrive at a solution. A discussion of this code and the correlations programmed in the code appear in Appendix A.

1.3 POWER DISTRIBUTION

1.3.1 Maximum Power for Each Core

The steady state analysis was performed at both design power and scram power level. This places the analysis for the SM-1, SM-1A and PM-2A Type 3 cores on the most conservative basis. The scram power level condition may be obtained by operator's error, such as slow rod withdrawal. Design power level for the SM-1 is 10.77 MW, SM-1A - 20.2 MW, and PM-2A, 10.0 MW. Scram power level setting for the SM-1 is 13.45 MW[5], SM-1A - 24.2 MW[6], and PM-2A - 12 MW[7]. These power levels and core heat transfer areas listed in Table 1.2 were used to calculate average core heat flux.

1.3.2 Radial and Axial Power Distributions

The radial peaking factors used in the thermal analysis were calculated using the IBM-650 Code, VALPROD. The analytical values were compared with experiment to obtain correction factors to apply to the calculated most adverse power distributions.

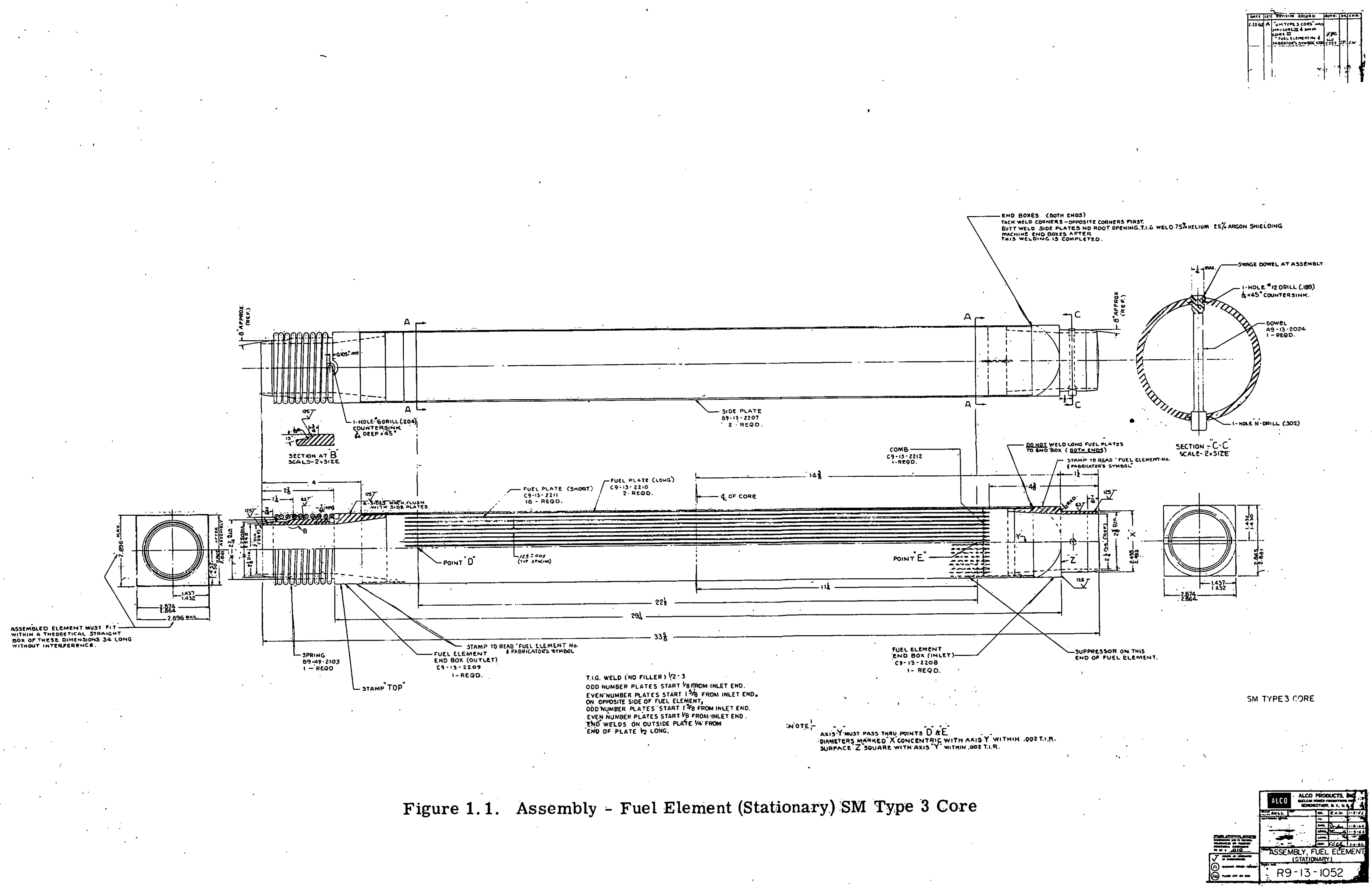

Figure 1.1. Assembly - Fuel Element (Stationary) SM Type 3 Core

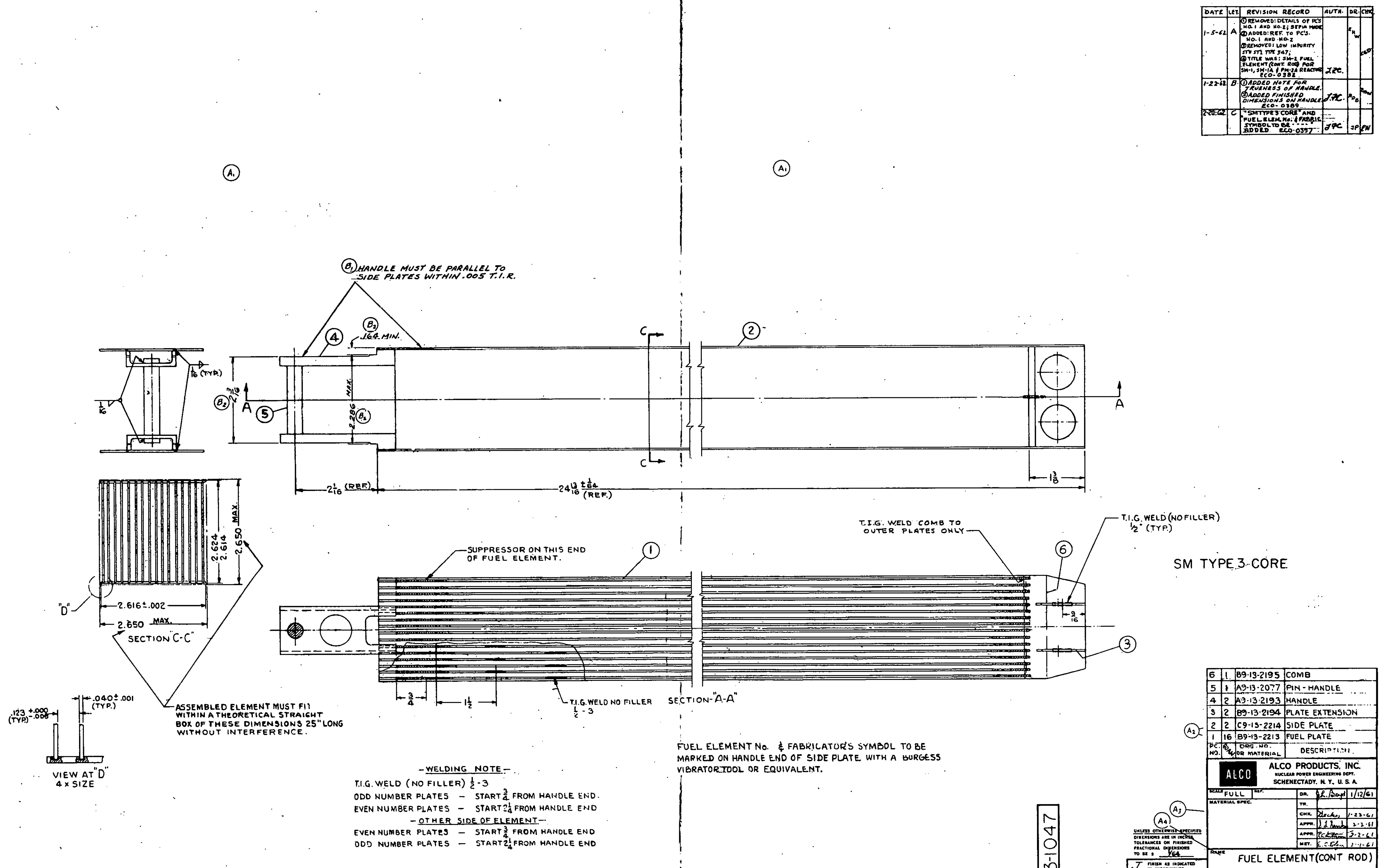

Figure 1.2A. Fuel Elements (Control Rod) SM Type 3 Core

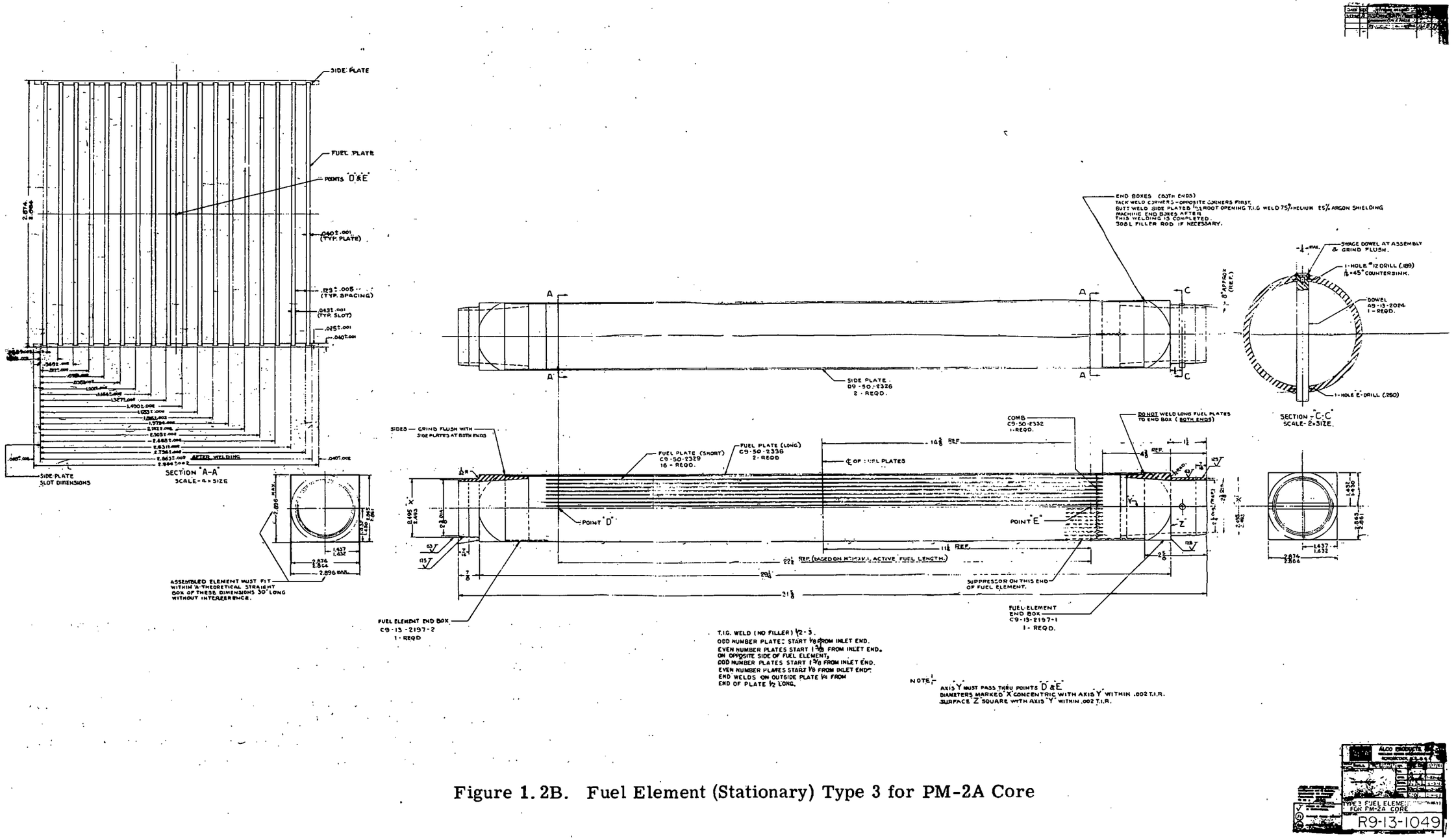

Figure 1.2B. Fuel Element (Stationary) Type 3 for PM-2A Core

The average and local radial peaking factors listed in Tables 1.3, 1.4, and 1.5 were used to determine hot channel factors for both the nominal and hot channel. These are applied as follows to obtain the mechanical hot channel factors for both the nominal and local channels used in the channel description input parameters described in Appendix A.

For the nominal channel: $F_{\Delta T_N} = F_N F_\psi \bar{Q}_{\Delta T}$

$F_{\Delta \theta_N} = F_N F_\psi Q_{\Delta \theta}$

For the hot channel $F_{\Delta T_H} = F_N F_\psi Q_{\Delta \theta}$

$F_{\Delta \theta_H} = F_N F_\psi Q_{\Delta \theta} F_{M\Delta \theta}$

where $F_{\Delta T_N}$, $F_{\Delta \theta_N}$, $F_{\Delta T_H}$, $F_{\Delta \theta_H}$ = the average and local hot channel factors respectively

F_N = nuclear uncertainty factor for average or local condition

F_ψ = power generation factor for average or local condition

$Q_{\Delta T}$ = average radial peaking factor in the hot channel

$\bar{Q}_{\Delta T}$ = average radial peaking factor in the nominal or average channel

$Q_{\Delta \theta}$ = local radial peaking factor

$F_{M\Delta T}$, $F_{M\Delta \theta}$ = mechanical hot channel factor excluding plate spacing factor and plenum maldistribution factor. Average and local, respectively.

The relative axial power distributions for each core are shown on Fig. 1.3, 1.4, 1.5 for control rod elements and Fig. 1.6 and 1.7 for stationary elements. These values are normalized to a core average of one. One value for each axial channel increment is used in the analysis as described in Appendix A.

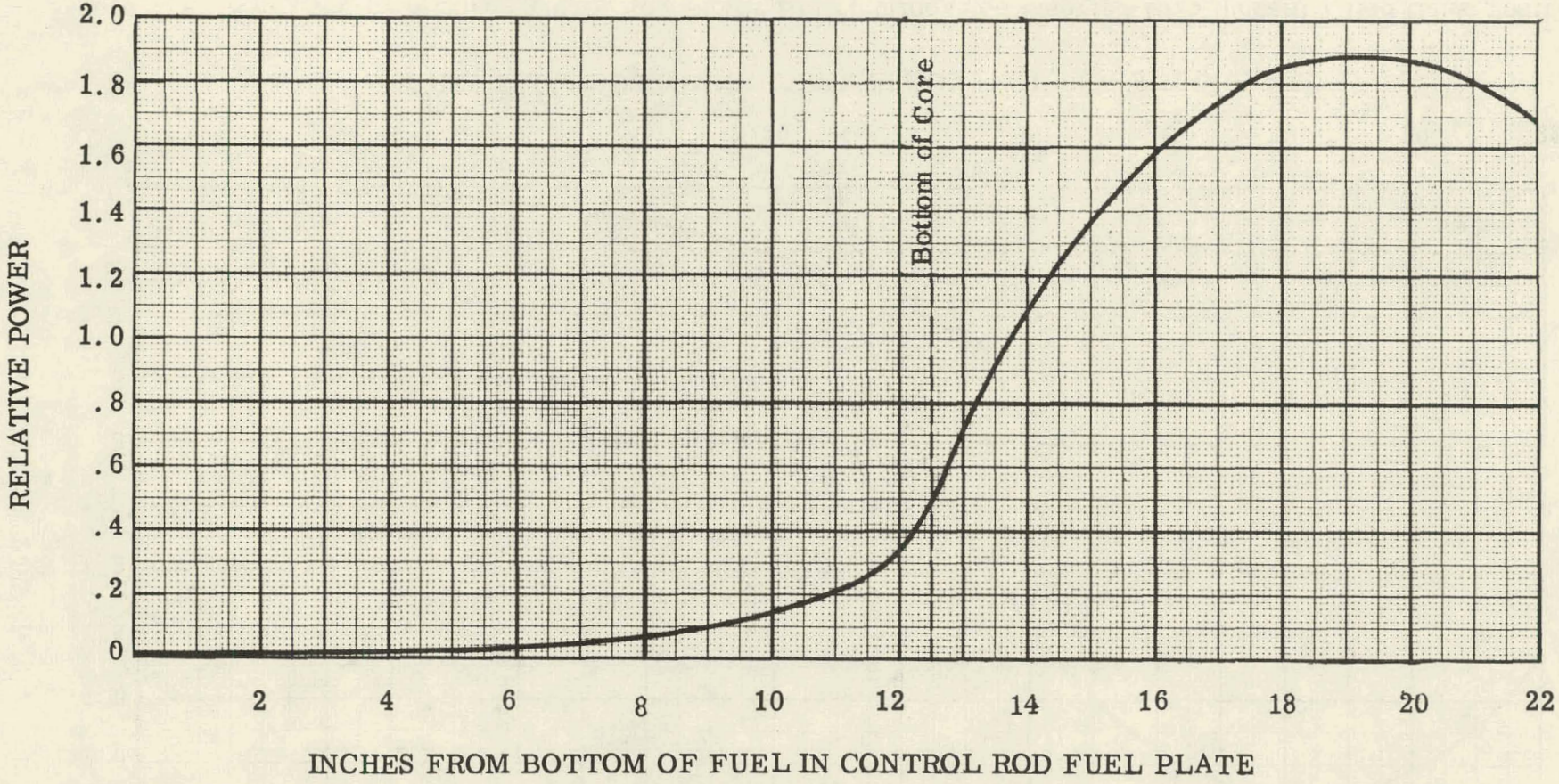

Figure 1.3. SM-1 Type 3 Core Control Rod Axial Power Distribution (Rod inserted 9.5 inches) 7 Rod Bank Position

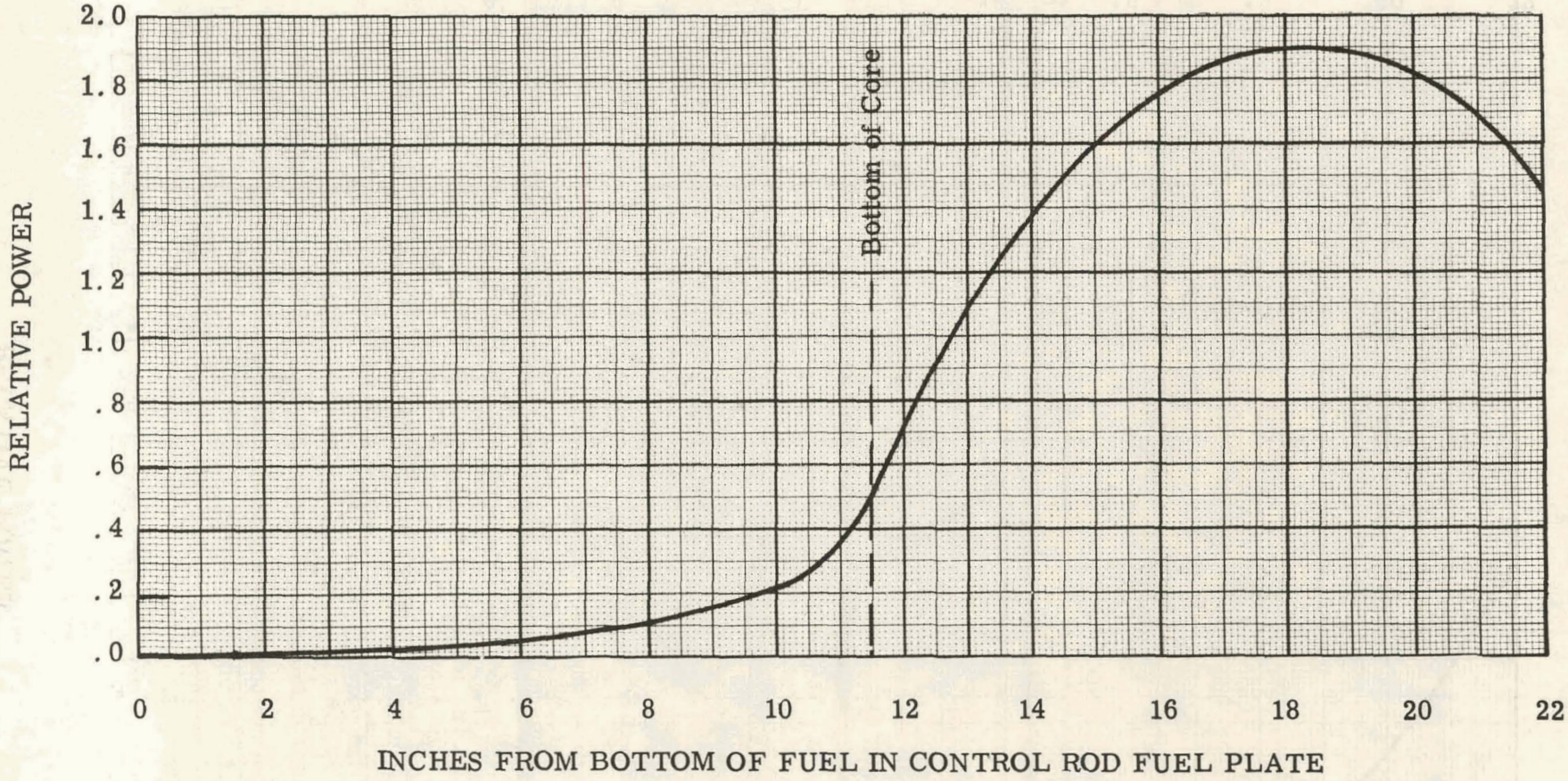

Figure 1.4. SM-1A Type 3 Core Control Rod Power Distribution (Rod Inserted 10.5 Inches) 7 Rod Bank Position.

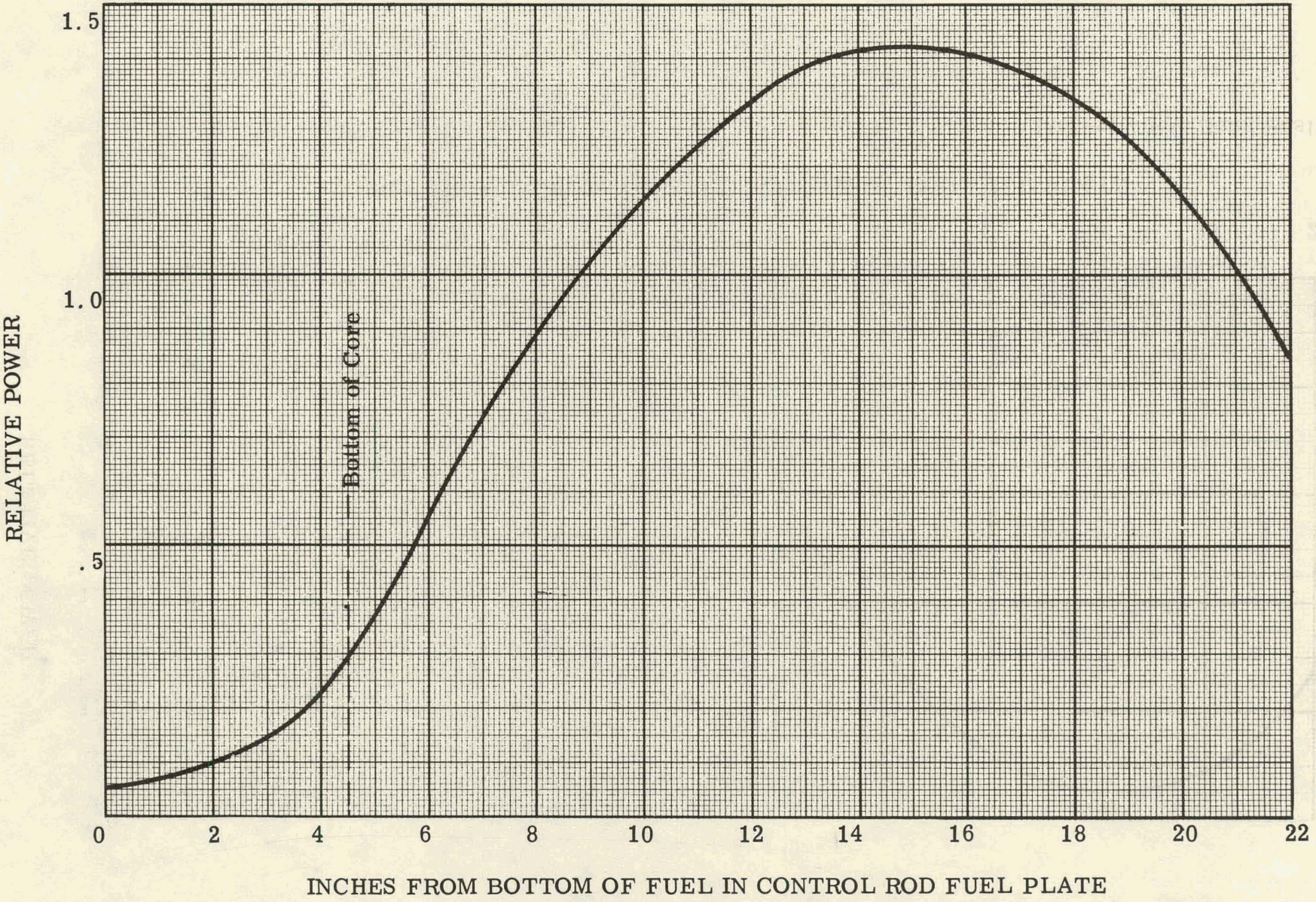

Figure 1.5. PM-2A Type 3 Core Control Rod Power Distribution (Rod Inserted 17.5 Inches)

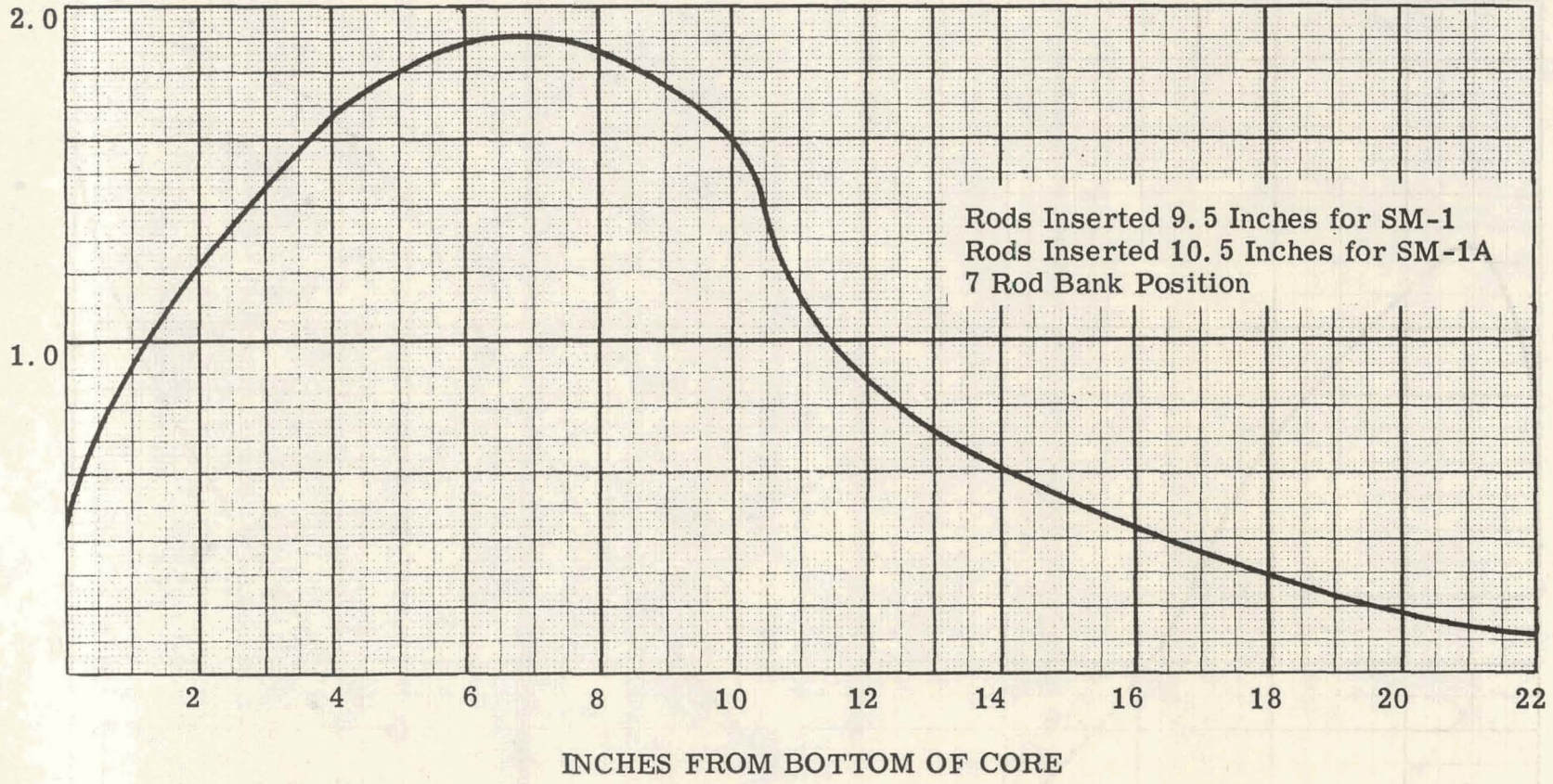

Figure 1.6. SM-1 and SM-1A Type 3 Cores Axial Power Distribution (Stationary Element)

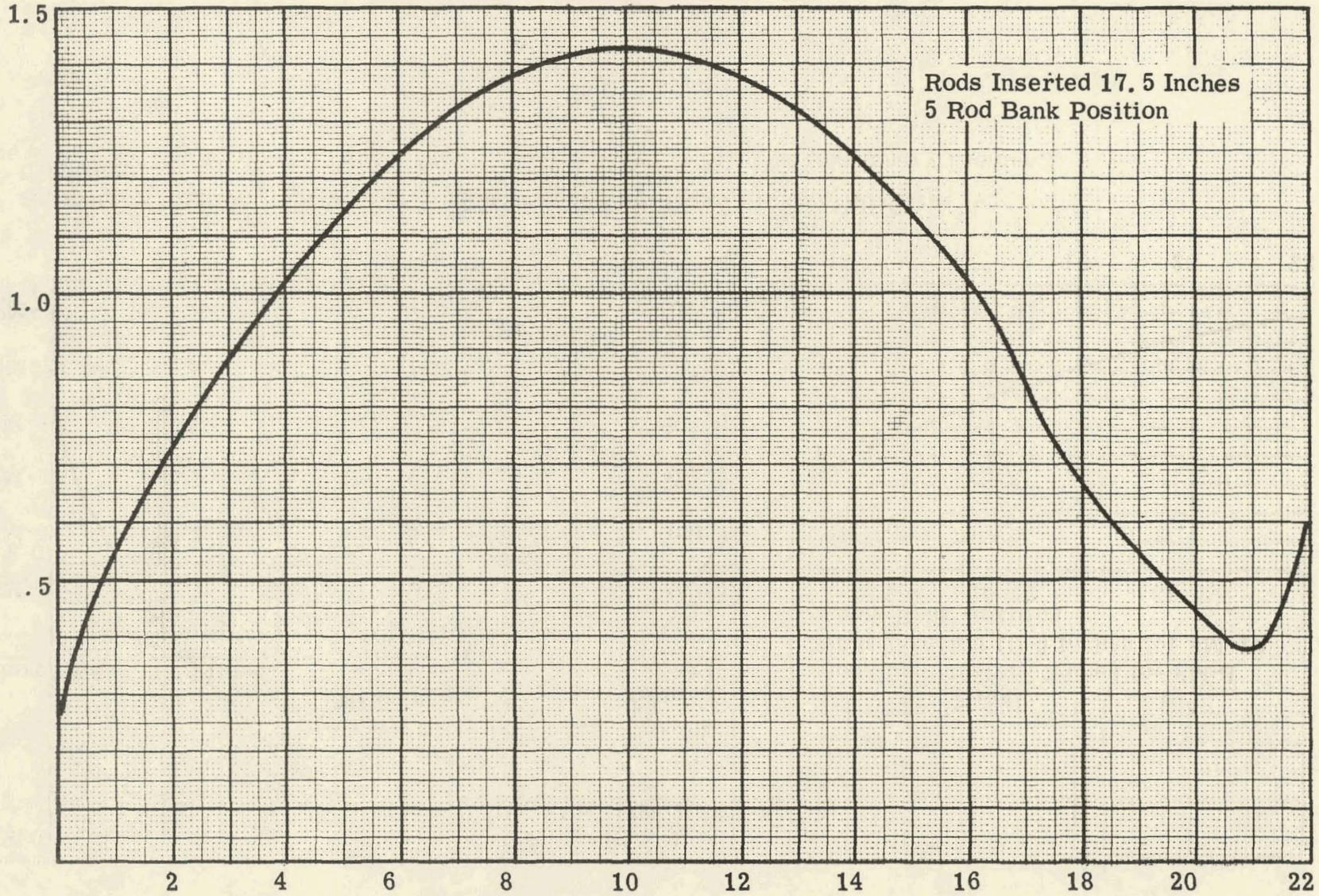

Figure 1.7. PM-2A Type 3 Core Axial Power Distribution (Stationary Element)

TABLE 1.2
CORE AVERAGE HEAT FLUX

Core	Rod Bank	Control Rod Meat Insertion Inches	Core Heat Transfer Area Ft^2	Power MW	*Core Average Heat Flux Btu/hr-ft^2
SM-1	7	9.5	589.32	10.77	64,557
SM-1	7	9.5	589.32	13.45	77,920
SM-1A	7	10.5	593.05	20.2	120,320
SM-1A	7	10.5	593.05	24.2	144,143
PM-2A	5	17.5	513.07	10.0	68,849
PM-2A	5	17.5	513.07	12.0	82,619

* An instrumentation tolerance of 3.5% was applied to the core power for both design and scram level conditions.

TABLE 1.3
RADIAL POWER FACTORS FRO SM-1 TYPE 3 CORE - 440°F

Element No.	$\overline{Q}_{(\Delta T)}$	$Q_{(\Delta T)_{0\,MWYR}}$*	$Q_{(\Delta \theta)_{0\,MWYR}}$	$Q_{(\Delta T)_B}$**	$Q_{(\Delta \theta)_B}$
12, 76	0.795	1.22	1.73	1.29	1.83
13, 75	0.827	0.93	1.73	0.98	1.83
14, 74	0.897	0.94	1.83	0.99	1.93
15, 73	0.919	1.05	1.79	1.11	1.89
16, 72	0.872	1.18	1.83	1.24	1.93
21, 67	0.854	1.28	1.91	1.35	2.02
22, 66	0.815	1.03	1.30	1.09	1.37
23, 65	0.915	1.20	1.70	1.27	1.79
24, 64	1.07	1.27	1.62	1.34	1.71
25, 63	1.043	1.23	1.57	1.30	1.66
26, 62	0.924	1.08	1.36	1.14	1.43
27, 61	0.906	1.22	1.97	1.29	2.08
31, 57	0.870	1.47	1.98	1.55	2.09
32.56	0.901	1.31	1.65	1.38	1.74
33, 55	1.20	1.55	1.90	1.64	2.00
34, 54	1.202	1.59	1.88	1.68	1.98
35, 53	1.247	1.53	1.81	1.61	1.91
36, 52	1.086	1.38	1.66	1.46	1.75
37, 51	0.870	1.28	1.55	1.35	1.64
41, 47	0.942	1.61	1.82	1.70	1.92
42, 46	1.07	1.33	1.64	1.40	1.73
43	1.200	1.59	1.89	1.68	1.99
44	1.35	1.49	1.81	1.57	1.91
45	1.214	1.62	1.81	1.71	1.91

* Subscript zero refers to Power Factor at Start of Life
** Subscript B refers to Power Factor During Life

TABLE 1.4
RADIAL POWER FACTORS FOR SM-1A TYPE 3 CORE - 440°F

Element No.	$\overline{Q}_{(\Delta T)}$	$Q_{(\Delta T)_{0\ MWYR}}$	$Q_{(\Delta \theta)_{0\ MWYR}}$	$Q_{(\Delta T)_B}$	$Q_{(\Delta \theta)_B}$
12, 76	0.79	1.30	1.94	1.50	2.24
13, 75	0.84	0.96	1.81	1.11	2.09
14, 74	0.88	0.95	1.90	1.10	2.19
15, 73	0.94	0.93	1.88	1.07	2.17
16, 72	0.85	1.21	1.97	1.40	2.27
21, 67	0.73	1.15	1.90	1.33	2.19
22, 66	0.80	0.99	1.32	1.14	1.52
23, 65	0.91	1.17	1.68	1.34	1.94
24, 64	0.87	1.23	1.75	1.42	2.02
25, 63	1.07	1.26	1.69	1.45	1.95
26, 62	0.92	1.07	1.39	1.23	1.60
27, 61	0.84	1.20	1.90	1.38	2.19
31, 57	0.81	0.90	1.89	1.04	2.18
32, 56	0.96	1.20	1.53	1.38	1.76
33, 55	1.22	1.56	1.94	1.80	2.24
34, 54	1.21	1.55	1.92	1.79	2.21
35, 53	1.26	1.52	1.85	1.75	2.13
36, 52	1.05	1.29	1.64	1.49	1.89
37, 51	0.86	1.03	1.81	1.19	2.09
41, 47	0.82	0.88	1.84	1.01	2.12
42, 46	0.97	1.20	1.46	1.38	1.68
43	1.21	1.57	1.93	1.81	2.23
44	1.34	1.54	1.85	1.78	2.13
45	1.24	1.67	1.82	1.93	2.10

TABLE 1.5
RADIAL POWER FACTORS FOR PM-2A TYPE 3 CORE - 510°F

Element No.	$\overline{Q}_{(\Delta T)}$	$Q_{(\Delta T)_{0\ MWYR}}$	$Q_{(\Delta \theta)_{0\ MWYR}}$	$Q_{(\Delta T)_B}$	$Q_{(\Delta \theta)_B}$
13, 15, 73, 75	0.760	1.31	1.39	1.52	1.61
14, 74	0.739	0.75	1.22	0.87	1.41
22, 26, 62, 66	1.017	1.39	1.74	1.61	2.01
23, 25, 63, 65	0.983	1.21	1.60	1.40	1.85
24, 64	0.508	1.26	1.67	1.46	1.93
31, 37, 51, 57	0.839	0.83	1.32	0.96	1.53
32, 36, 52, 56	0.993	1.17	1.53	1.35	1.77
33, 35, 53, 55	1.190	1.27	1.75	1.47	2.03
34, 54	1.180	1.27	1.70	1.47	1.97
41, 47	0.792	0.96	1.02	1.11	1.18
42, 46	0.508	1.33	1.57	1.54	1.82
43, 45	1.200	1.40	1.67	1.62	1.93
44	0.678	1.51	1.77	1.75	2.05

1.4 HOT CHANNEL FACTORS

The mechanical hot channel factors used in this final analysis include average and local deviations for active core length, uranium content, and clad thickness. The preceding factors were calculated by methods described in Appendix B. The results of these calculations are listed in Table 1.6.

The plate spacing and flow maldistribution factors do not appear in the STDY-3 code as hot channel factors. Plate spacing appears in the hot and nominal channel description input parameters as an average and local dimension. This is shown on cards 81 and 82 in Table A.1. Flow maldistribution and its associated hot channel factor are discussed in Section 1.5.

TABLE 1.6
COMPOSITE TYPE 3 FUEL ELEMENT HOT CHANNEL FACTORS

	Stationary Element		Control Rod Element	
	$F_{M\,\Delta T}$	$F_{M\,\Delta\,\theta}$	$F_{M\,\Delta T}$	$F_{M\,\Delta\,\theta}$
Meat Length	1.0233	1.0233	1.0233	1.0233
Uranium content	1.005	1.025	1.005	1.025
Clad thickness	1.007	1.012	1.007	1.012
Composite Mechanical factor as applied in STDY-3 Analysis	1.0357	1.0615	1.0357	1.0615

1.4.1 Instrumentation Tolerances

The worst reactor conditions were considered in the thermal analysis and tolerances applied to the reactor instrumentation. These instrumentation tolerances are listed in Table 1.7.

TABLE 1.7
INSTRUMENTATION TOLERANCES

SM-1 Core	Instrumentation Tolerance	Value Used In Analysis
Core Power	± 3.5% at scram power level	13.45
Inlet Temp.	± 4.0 at core inlet 427.7°F	431.7°F
System Pressure	± 25 psia at 1200 psia	1175 psia
PM-2A		
Core Power	± 3.5% at scram power level	12
Inlet Temp.	± 4.0 at core inlet 500°F	504°F
System Pressure	± 35 psia at 1750 psia	1715 psia
SM-1A		
Core Power	± 3.5% at scram power level	24.2
Inlet Temp.	± 4.0 at core inlet 423°F	427°F
System Pressure	± 25 psia at 1200 psia	1175 psia

1.4.2 Fuel Plate Rippling

Compressive stresses result from the temperature differential between the meat and side plate causing ripples in the fuel plates. To account for the growth of these ripples, growth factors were taken from the rippling analysis of SM-2 elements and applied to the local hot channel dimension.

Element	Ripple Ratio	Hot Channel Spacing
Stationary	1.55	0.136
Control Rod	1.20	0.133

1.4.3 Additional Factors

1.4.3.1 Nuclear Uncertainty Factor

To allow for uncertainties in the calculated power distribution, a nuclear uncertainty factor of 1.05 was used for the nominal channel and 1.10 for the hot channel.

1.4.3.2 Core Power Generation Factor

In order to account for the fraction of fission heat liberated in the coolant directly (F_{ψ}^{I}) a factor of 0.95 was applied to the power generated in the fuel plates for local conditions. The fraction of power generated in the core (F_{ψ}) is 1.00 for average conditions.

1.5 FLOW DISTRIBUTION

1.5.1 Core Flow Distribution

Element-to-element core flow distributions for Cores I are shown in Fig. 1.8, 1.9, and 1.10. It is expected that the flow distribution within the Type 3 cores will be identical with SM-2 elements installed.[10] Core flow distributions were obtained from full scale air flow rigs described in Ref. (11), (12), and (13). Orifice plates were developed for each core to give the required element flows. The orifice plate schedules are also shown on Fig. 1.8, 1.9 and 1.10.

1.5.2 Channel-to-Channel Flow Distribution

In the preliminary thermal analysis [1] a maldistribution of 12 percent was assumed. This was based on past experience of SM-2 single element flow testing [14] excluding end box effects. MTR and ETR [15], [16] single element flow tests have shown channel to channel maldistribution as high as 25%.

A single element flow test program was conducted at Alco's General Engineering and Test Laboratory to provide channel-to-channel maldistribution factors for the steady state and transient thermal analysis. The basic philosophy for optimum channel distribution is that any departure from the desired uniform profile must not cause below average flow at the outermost channels and lattices where flux peaks are expected to occur.

The flow test program was set up to provide factors for the three cores to insure conservatism in the analysis. The most adverse flow distribution was mocked up by testing each core with its stationary element of minimum orifice diameter. The unorificed control rod elements for each core were also tested.

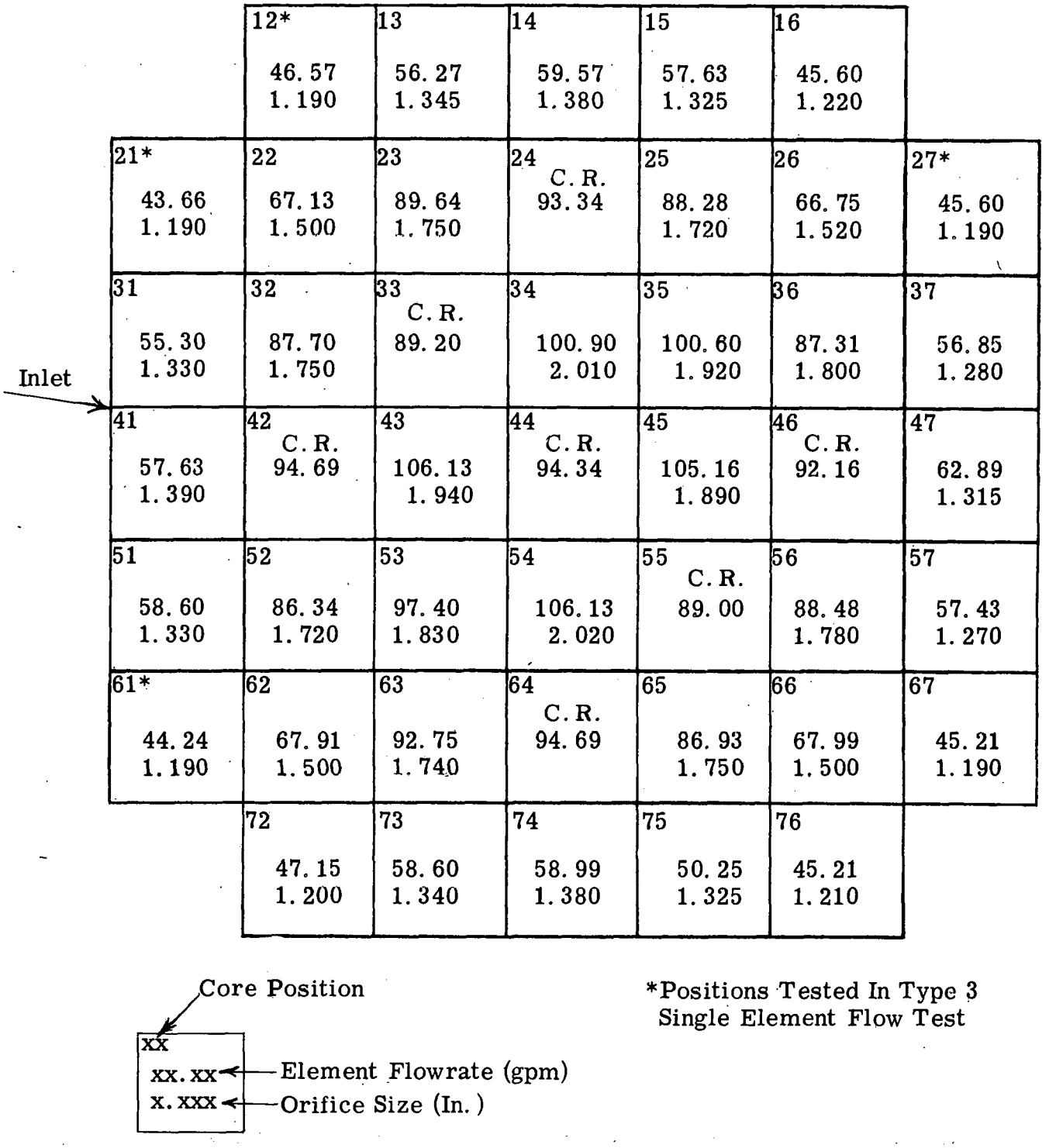

Figure 1.8. SM-1 Core Flow Distribution and Orifice Size

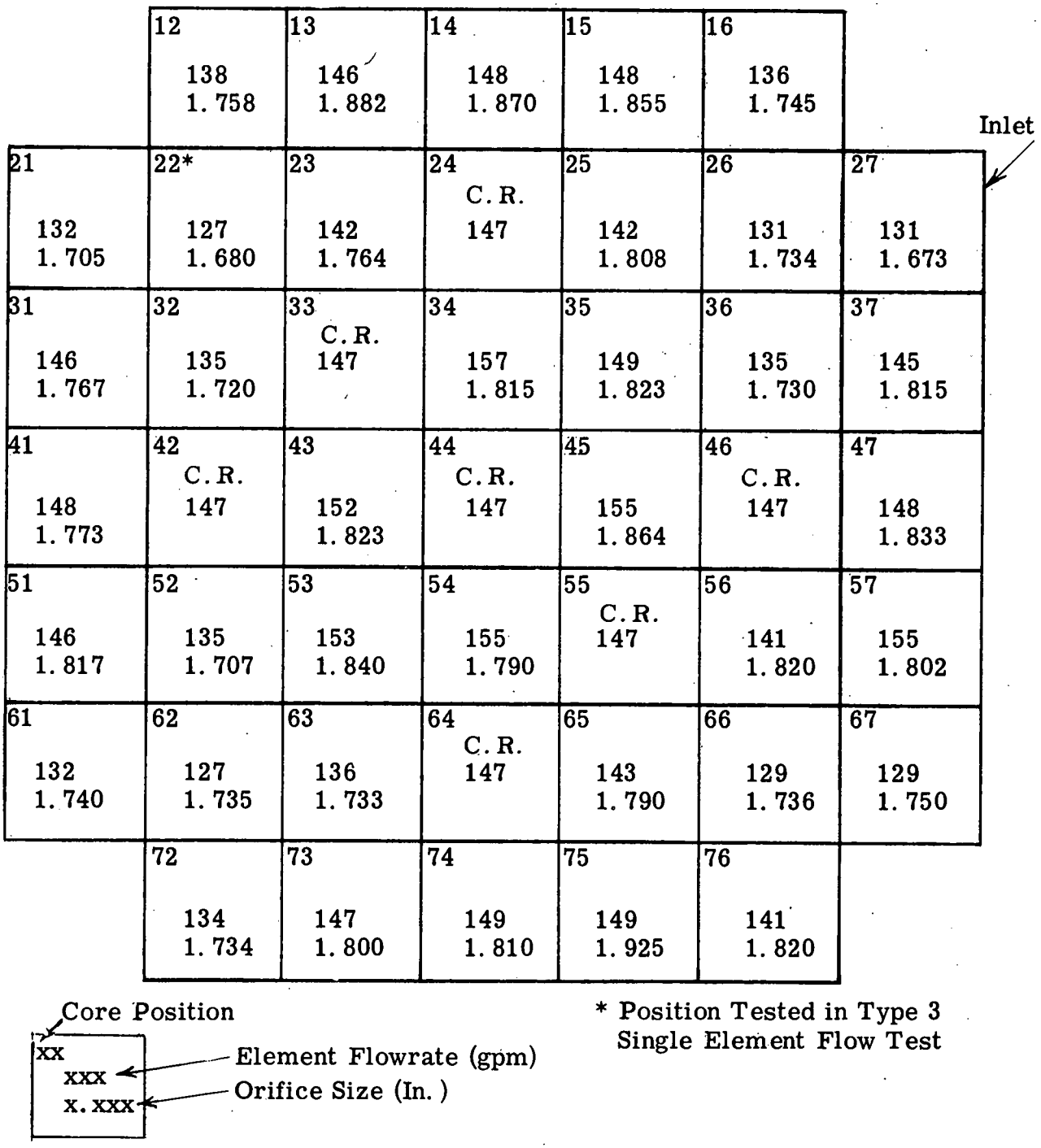

Figure 1.9. SM-1A Core Flow Distribution and Orifice Size

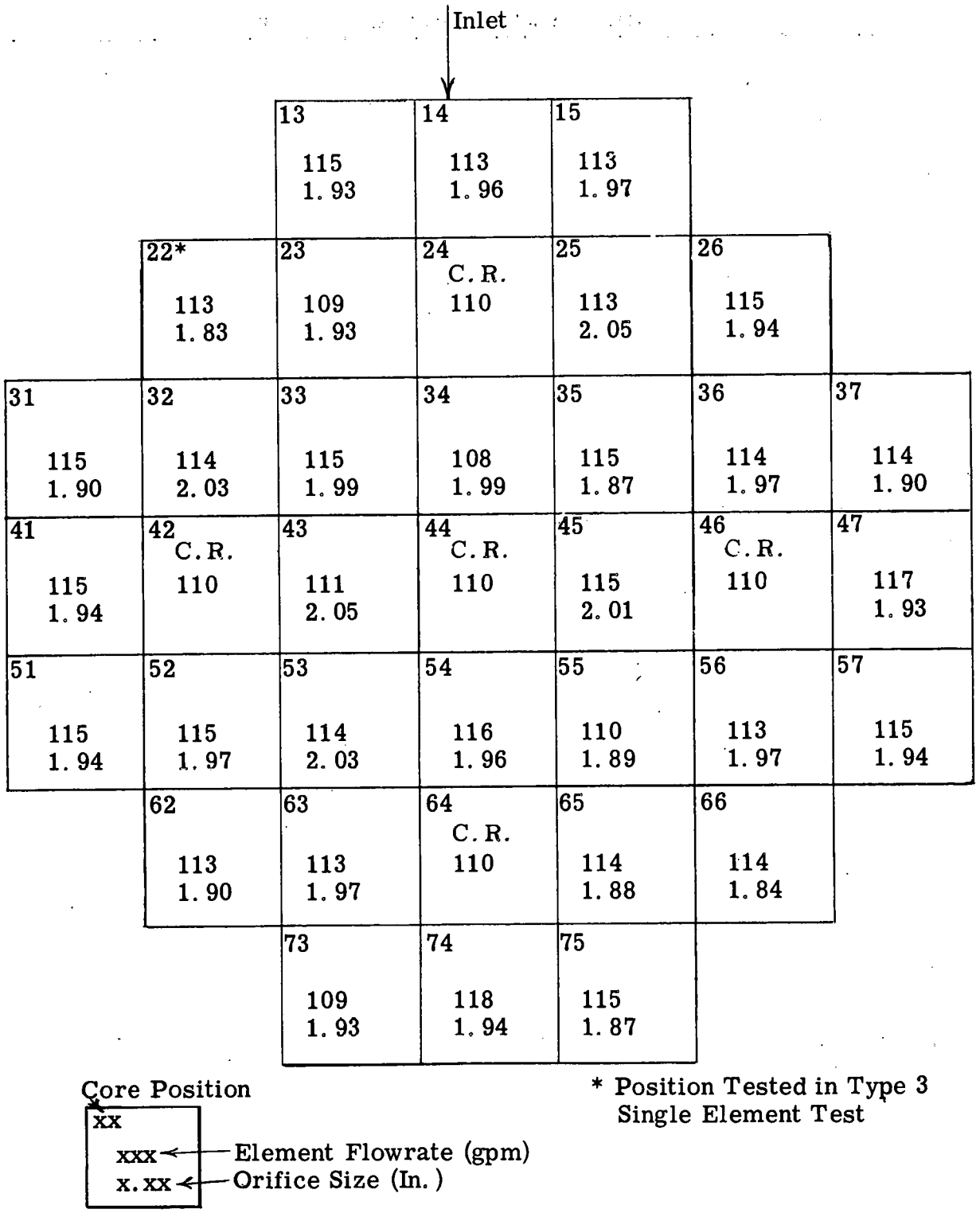

Figure 1.10. PM-2A Core Flow Distribution and Orifice Size

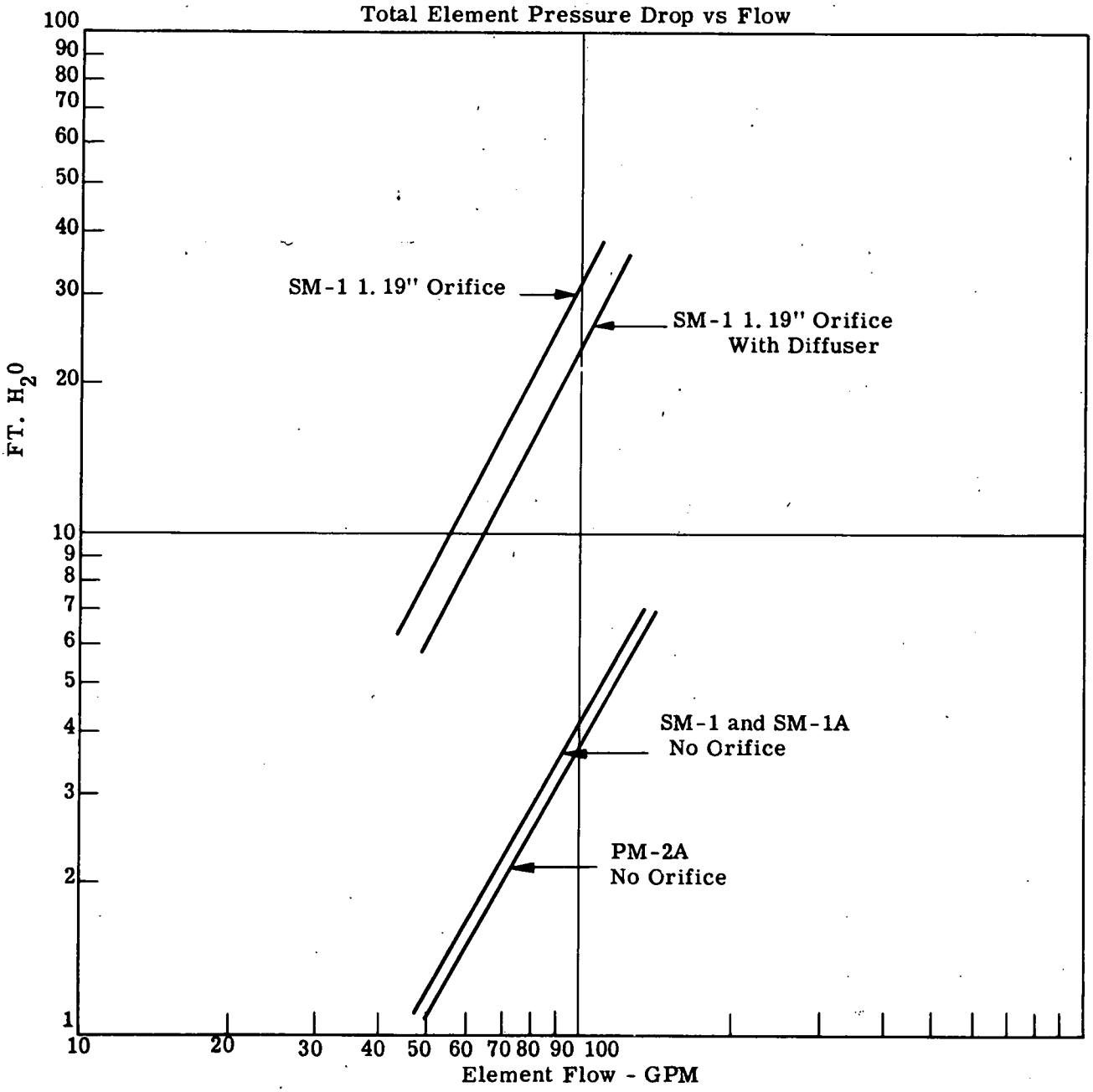

Figure 1.11.

Results of Pressure Drop, Single Element
Flow Test, Stationary Type 3 Fuel Elements

Velocity probes in each channel were connected by tubing to a manometer board and the element installed in the test rig with its appropriate orifice plate at the inlet of the end box for SM-1 elements and the exit of the end box for SM-1A and PM-2A cores. Water was circulated through the elements at flow rates corresponding to those obtained in full scale flow testing. Velocity head measurements were obtained for each probed channel and graphed for ease of investigation. A detailed test report, Ref. (4) contains these graphs along with a complete summary of the test program. Table 1.8 lists maldistribution results obtained from single element flow tests. The maldistribution results are the maximum percentage deviation from the average channel flow. This table lists the data which was used for calculating the maldistribution factors in the thermal analysis.

TABLE 1.8
MALDISTRIBUTION RESULTS FROM SINGLE ELEMENT FLOW TESTS FOR TYPE 3 ELEMENTS

Core	Type of Element	Orifice Diam, In.	Flow GPM	Percent Maldistribution
SM-1	Stationary	1.19	87	+70.5 -70.0
SM-1	Stationary	1.19	75	+44.0 -58.0
SM-1	Stationary	1.19	52	+44.0 -55.0
SM-1	Control Rod	No orifice	99	+23.5 -27.8
SM-1	Control Rod	No orifice	76	+21.6 -25.9
SM-1	Control Rod	No orifice	50	+18.0 -21.0
SM-1A	Stationary	1.68	125	+6.1 -6.7
SM-1A	Control Rod	No orifice	120	+13.2 -22.8
SM-1A	Control Rod	No orifice	100	+12.0 -21.2
PM-2A	Stationary	1.83	125	+6.2 -11.1
PM-2A	Stationary	1.83	100	+5.8 -10.8
PM-2A	Control Rod	No orifice	120	+13.2 -22.8
PM-2A	Control Rod	No orifice	100	+12.0 -21.2

To insure conservatism in the final analysis, maldistribution data was obtained from the minimum orificed elements. The poor distribution in the SM-1 stationary elements is attributed to the orifice plate being on the inlet side of the element. The SM-1A and PM-2A cores have orifice plates on the exit side of the elements. The maldistribution results, excluding the SM-1 stationary elements, are in good agreement with previous single element flow testing conducted on the MTR and ETR elements which had similar end box configurations.(14),(15)

Overall element pressure drop was measured for the stationary elements. This data was not used in the final thermal analysis, however it served as an indication of the magnitude of overall pressure drop for the SM-1, SM-1A and PM-2A cores with no orifices and the range of pressure drops for the SM-1 from minimum orifice 1.19 to no orifice. These results are shown on Fig. 1.11.

To improve the flow distribution within the SM-1 stationary element several flow fixes were tested. The most successful, a conical diffuser located in the inlet end box improved the maldistribution and element flow profile from a -55% to a -23%. The overall element pressure drop was thus reduced as shown on Fig. 1.11. Further details of this test and other flow fixes are contained in Ref. (4).

As a result of the single element flow testing of Type 3 SM-1 elements, a maldistribution study was performed to determine the effects of varying the channel to channel flow distribution on an element's thermal performance. Various channel to channel maldistributions were inserted into the STDY-3 code. Since only changes in frictional pressure drop are considered;

$$\Delta P \text{ friction} = (G)^{1.8}$$

$$K_1 = (1 - \delta)^{1.8}$$

where G = mass flow rate - lb/hr - ft^2

δ = channel-to-channel flow maldistribution -%

K_1 = plenum factor used in the STDY-3 code

Results of this analysis are shown in Table 1.9 for SM-1 element position 37. The 42% maldistribution was extrapolated from experimental data. The results indicate very small variations in DNBR due to increases in flow maldistribution. Plate surface temperatures and meat centerline temperatures remained essentially the same along the length of the channel with the largest variation of these parameters occurring in the first few inches at the entrance of the channels. The hot channel flow and the hot channel pressure drop decreased with increases in maldistribution. Local nucleate boiling does not occur for maldistribution less than 20%. The inception of local nucleate boiling in the hot channel is approximately 6 in. at 42%, 8 in. at 60% and 9 in. with bulk nucleate boiling at 80%.

It is apparent that no major improvements in DNBR could be made by improving channel flow distribution. This is likewise true for plate surface temperatures and meat centerline temperatures. DNBR's are well above the design minimum of 1.5 for steady state operation at 13.45 MW. However, local nucleate boiling is evident for maldistributions above 20% and improvements could be made to reduce the extent of local nucleate boiling in the hot channel. This can be accomplished with the conical diffuser mentioned above.

1.6 SELECTION OF ELEMENTS FOR ANALYSIS

An analysis has been presented (8) in which a basis for element selection has been determined. A burnout index was established for each core in which

$$I_{DNBR} = \left[1 \neq \left(\frac{5}{2} \quad \frac{K}{H_o} \right) \frac{Q \Delta T}{G} \right] Q \Delta \theta$$

$$\text{and } K = \frac{\phi_{avg} \, A_H \sum_{n=o}^{m=j} f'(Z)}{\rho}$$

where

I_{DNBR} = burnout index

H_o = reactor inlet enthalpy, Btu/lb

G = volumetric flow rate, gpm

A_H = effective core heat transfer area, ft^2

ϕ_{avg} = average core heat flux Btu/hr-ft^2

f'(Z) = axial power distribution for the j^{th} position

ρ = fluid density, lb/ft^3

For the SM-1 core this equation is

$$I_{DNBR} = \left(1 \neq 16.67 \frac{Q \Delta T}{G} \right) Q \Delta \theta \qquad (1.1)$$

For the SM-1A core this equation is

$$I_{DNBR} = \left(1 \neq 31.01 \frac{Q \Delta T}{G} \right) Q \Delta \theta \qquad (1.2)$$

For the PM-2A core this equation is

$$I_{DNBR} = 1 \neq 15.76 \frac{Q \Delta T}{G} Q \Delta \theta \qquad (1.3)$$

TABLE 1.9
RESULTS OF MALDISTRIBUTION SURVEY ON ELEMENT 37 - SM-1 TYPE 3 CORE, 13.45 MW

% Mal-Distr.	Nominal Channel Flow lb/hr-ft^2	Hot Channel Flow lb/hr-ft^2	Avg. Hot Channel Pressure Drop-psi	Hot Channel Bulk Temp. Rise ^oF	Hot Channel Enthalpy Rise Btu/lb	Max. T_S-^oF	Max. T_M-^oF	T_M-T_S (max)	Min. DNBR	Hot Channel Local Boiling	Bulk Boiling	Quality %
20	5.90×10^5	5.17×10^5	0.736	82.0	95.3	575.90	600.49	24.6	6.14	No	No	0
42	5.90×10^5	4.06×10^5	0.703	103.0	121.28	575.90	600.49	24.6	5.97	J=11*	0	0
60	5.90×10^5	3.32×10^5	0.688	124.22	148.23	575.90	600.49	24.6	5.88	J=8*	0	0
80	5.90×10^5	2.95×10^6	0.669	135.70	166.76	575.90	600.49	24.6	5.75	J=7*	J=22*	0.4

* Axial increment at which nucleate boiling begins, measured in inches from bottom of core

TABLE 1.10

I_{DNBR} INDEXES FOR THE SM-1 TYPE 3 CORE

Core Position	G, GPM	$Q\Delta_T$	$Q\Delta_\theta$	$I_{DNBR} = (1/16.67 \frac{Q\Delta T}{G}) Q\Delta\theta$
12	46.57	1.29	1.83	2.68
13	56.27	0.98	1.83	2.36
14	59.59	0.99	1.93	2.46
15	57.63	1.11	1.89	2.50
16	45.60	1.24	1.93	2.80
21	43.66	1.35	2.02	3.06
22	67.13	1.09	1.37	1.74
23	89.64	1.27	1.79	2.21
24	94.34	1.34	1.71	2.12
25	88.28	1.30	1.66	2.07
26	66.75	1.44	1.43	1.94
*27	45.60	1.29	2.08	3.07
*31	55.30	1.55	2.09	3.07
32	87.70	1.38	1.74	2.19
33	89.20	1.64	2.00	2.61
*34	100.90	1.68	1.98	2.53
35	100.60	1.61	1.91	2.42
*36	87.31	1.46	1.75	2.24
37	56.85	1.35	1.64	2.29
*41	57.63	1.70	1.92	2.86
42	94.69	1.40	1.73	2.16
43	106.13	1.68	1.99	2.58
*44	94.34	1.57	1.91	2.44
45	105.16	1.71	1.91	2.43
46	92.16	1.40	1.73	2.27
*47	62.89	1.70	1.92	2.79
51	58.60	1.35	1.64	2.17
52	86.34	1.46	1.75	2.24
*53	97.40	1.61	1.91	2.44
54	106.13	1.68	1.98	2.50
*55	89.00	1.64	2.00	2.61
56	88.48	1.38	1.74	2.19
*57	57.43	1.55	2.09	3.03
*61	44.24	1.29	2.08	3.09
62	67.91	1.14	1.43	1.83
63	92.75	1.30	1.66	2.05
64	94.69	1.34	1.71	2.11
65	86.93	1.27	1.79	2.23
66	67.99	1.09	1.37	1.74
67	45.21	1.35	2.02	3.03
72	47.15	1.24	1.93	2.78
73	58.60	1.11	1.89	2.49
*74	58.99	0.99	1.93	2.47
75	50.25	0.98	1.83	2.42
76	45.21	1.29	1.83	2.70

TABLE 1.11

I_{DNBR} INDEXES FOR THE SM-1A TYPE 3 CORE

Core Position	G, GPM	$Q_{\Delta T}$	$Q_{\Delta\theta}$	$I_{DNBR} = \left[1/31.01 \frac{Q\Delta T}{G}\right] Q_{\Delta\theta}$
12	138	1.50	2.24	2.99
13	146	1.11	2.09	2.58
14	148	1.10	2.19	2.69
15	148	1.07	2.17	2.66
*16	136	1.40	2.27	2.99
21	132	1.33	2.19	2.87
22	127	1.40	1.52	2.04
23	142	1.34	1.94	2.51
24	147	1.42	2.02	2.62
25	142	1.45	1.95	2.57
26	131	1.23	1.60	2.07
*27	131	1.38	2.19	2.90
31	146	1.04	2.18	2.66
32	135	1.38	1.76	2.32
*33	147	1.80	2.24	3.09
*34	157	1.79	2.21	2.99
35	149	1.75	2.13	2.91
36	135	1.49	1.89	2.54
37	145	1.19	2.09	2.62
41	148	1.01	2.12	2.57
42	147	1.38	1.68	2.17
*43	152	1.81	2.23	3.05
44	147	1.78	2.13	2.93
45	155	1.93	2.10	2.91
46	147	1.38	1.68	2.17
47	148	1.01	2.12	2.57
51	146	1.19	2.09	2.62
52	135	1.49	1.89	2.54
53	153	1.75	2.13	2.89
*54	155	1.79	2.21	3.00
*55	147	1.80	2.24	3.09
56	141	1.38	1.76	2.29
57	155	1.04	2.18	2.63
*61	132	1.38	2.19	2.90
*62	127	1.23	1.60	2.08
63	136	1.45	1.95	2.59
64	147	1.42	2.02	2.62
65	143	1.34	1.94	2.50
66	129	1.14	1.52	1.94
67	129	1.33	2.19	2.89
*72	134	1.40	2.27	3.01
73	147	1.07	2.17	2.66
74	149	1.10	2.19	2.69
75	149	1.11	2.09	2.57
76	141	1.50	2.24	2.98

TABLE 1.12
I_{DNBR} INDEXES FOR THE PM-2A TYPE 3 CORE

Core Position	G, GPM	$Q_{\Delta T}$	$Q_{\Delta\theta}$	$I_{DNBR} = \left[1/15.76 \frac{Q\Delta T}{G}\right] Q\Delta\theta$
*13	115	1.52	1.61	1.95
14	113	0.87	1.41	1.58
15	113	1.52	1.61	1.95
*22	113	1.61	2.01	2.46
23	109	1.40	1.85	2.22
24	110	1.46	1.93	2.26
25	113	1.40	1.85	2.18
*26	115	1.61	2.01	2.45
31	115	0.56	1.53	1.73
32	114	1.35	1.77	2.10
*33	115	1.47	2.03	2.44
34	108	1.47	1.97	2.39
35	115	1.47	2.03	2.44
36	114	1.35	1.77	2.10
*37	114	0.96	1.53	1.73
41	115	1.11	1.18	1.36
42	110	1.54	1.82	2.22
*43	111	1.62	1.93	2.37
*44	110	1.77	2.05	2.57
45	115	1.62	1.93	2.36
46	110	1.54	1.82	2.22
47	117	1.11	1.18	1.36
51	115	0.96	1.53	1.73
52	115	1.35	1.77	2.10
53	114	1.47	2.03	2.44
54	116	1.47	1.97	2.36
*55	110	1.47	2.03	2.46
56	113	1.35	1.77	2.10
57	115	0.96	1.53	1.73
*62	113	1.61	2.01	2.46
63	113	1.40	1.85	2.21
64	110	1.46	1.93	2.34
65	114	1.40	1.85	2.21
*66	114	1.61	2.01	2.47
73	109	1.52	1.61	1.96
74	118	0.87	1.41	1.58
75	115	1.52	1.61	1.95

The above correlations were used to determine the relative values of the DNBR between elements. To insure the thermal safety of the cores the most critical elements for each core were analyzed. These elements appear with an asterisk in Tables 1.10, 1.11, and 1.12. With the selection of these elements a complete thermal history of each core was obtained.

1.7 STEADY STATE PERFORMANCE OF TYPE 3 ELEMENTS IN THE SM-1 CORE

A steady state thermal analysis was performed on 12 elements within the SM-1 core. These elements were selected based on their burnout indexes presented in Table 1.10. In some instances elements even with low burnout indexes were selected because of their critical location, such as element number 74. adjacent to the core reflector.

The analysis included studies at both design power 10.77 MW and at scram power 13 MW with average core heat fluxes of 64,557 Btu/hr-ft^2 and 77,920 Btu/hr-ft^2 respectively. Plate surface temperature, bulk water temperature, departure from nucleate boiling and quality were calculated for one-inch increments up the 22 in. channel. The results of this analysis at 10.77 MW are shown on Table 1.13 and at 13.45 MW on Table 1.14.

Local boiling is indicated at design power and design flow conditions for element positions 27, 31, 41,47, 57 and 61. Local boiling is also indicated at scram power for the identical element positions with the inception of boiling occurring slightly below that indicated at design conditions. The inception of local boiling is characterized by a flat plate surface temperature profile. This profile for element position 61 is shown on Fig. 1.13. Element 55 shown on Fig. 1.12 is marginally away from local boiling as shown by the flatness of the plate surface temperature curve at the exit end of the element and the fact that 11.0 degrees of superheat exists between saturation temperature and maximum plate surface temperature.

The results of this analysis indicate that no SM-1 element is in danger of burnout since the most critical control rod element, #55, and the most critical stationary element, #61, exhibit minimum DNBR's of 4.91 and 5.21, respectively. This is based on DNBR's well above the steady state minimum DNBR of 1.5, when a transient analysis is performed. See Section 2.10.

TABLE 1.13
RESULTS OF THE STEADY STATE THERMAL
ANALYSIS OF THE SM-1 TYPE 3 CORE, POWER 10.77 MW

Core Position	G-Nominal Channel Flow X 10^6 lb/hr-ft^2	G-Hot Channel Flow X 10^5, lb/hr-ft^2	Hot Channel Bulk Outlet Temp., ^oF	Hot Channel Maximum Plate Surface Temp., ^oF	Min DNBR	Qlty.	*Local Boiling
27	0.474	3.259	521.2	575.6	5.22	0	7
31	0.574	3.946	521.0	576.1	5.24	0	9
34	1.048	9.17	474.3	551.9	5.74	0	0
36	0.907	7.936	474.5	550.9	6.51	0	0
41	0.598	4.859	517.8	576.4	5.72	0	9
44	1.076	7.397	465.7	571.7	5.17	0	0
47	0.653	4.489	517.7	576.4	5.68	0	7
53	1.011	8.846	474.0	550.9	5.96	0	0
55	1.015	6.978	469.1	576.3	4.91	0	0
57	0.596	4.097	517.8	576.1	5.22	0	7
61	0.459	3.156	524.0	575.6	5.21	0	7
74	0.613	4.597	486.1	575.0	5.85	0	0

* Axial increment at which nucleate boiling begins, measured in inches from bottom of the element.

TABLE 1.14
RESULTS OF THE STEADY STATE THERMAL
ANALYSIS OF THE SM-1 TYPE 3 CORE, POWER 13.45

Core Position	G-Nominal Channel Flow X 10^6 lb/hr-ft^2	G-Hot Channel Flow X 10^5, lb/hr-ft^2	Hot Channel Bulk Outlet Temp., ^oF	Hot Channel Maximum Plate Surface Temp., ^oF	Min DNBR	Qlty.	*Local Boiling
27	0.474	3.259	535.3	576.1	4.28	0	6
31	0.574	3.946	535.0	576.7	3.75	0	6
34	1.048	9.170	476.0	565.0	4.76	0	0
36	0.907	7.936	479.6	571.9	5.38	0	0
41	0.598	4.485	531.3	576.9	4.66	0	5
44	1.076	7.397	469.0	576.7	4.31	0	0
47	0.653	4.859	531.2	576.9	4.66	0	5
53	1.011	8.846	479.0	571.8	4.93	0	0
55	1.015	6.978	473.2	576.8	4.06	0	0
57	0.596	4.097	531.3	576.7	4.28	0	6
61	0.459	3.156	538.6	576.1	4.27	0	5
74	0.613	4.597	493.5	575.5	4.84	0	0

* Axial increment at which mucleate boiling begins, measured in inches from bottom of the element.

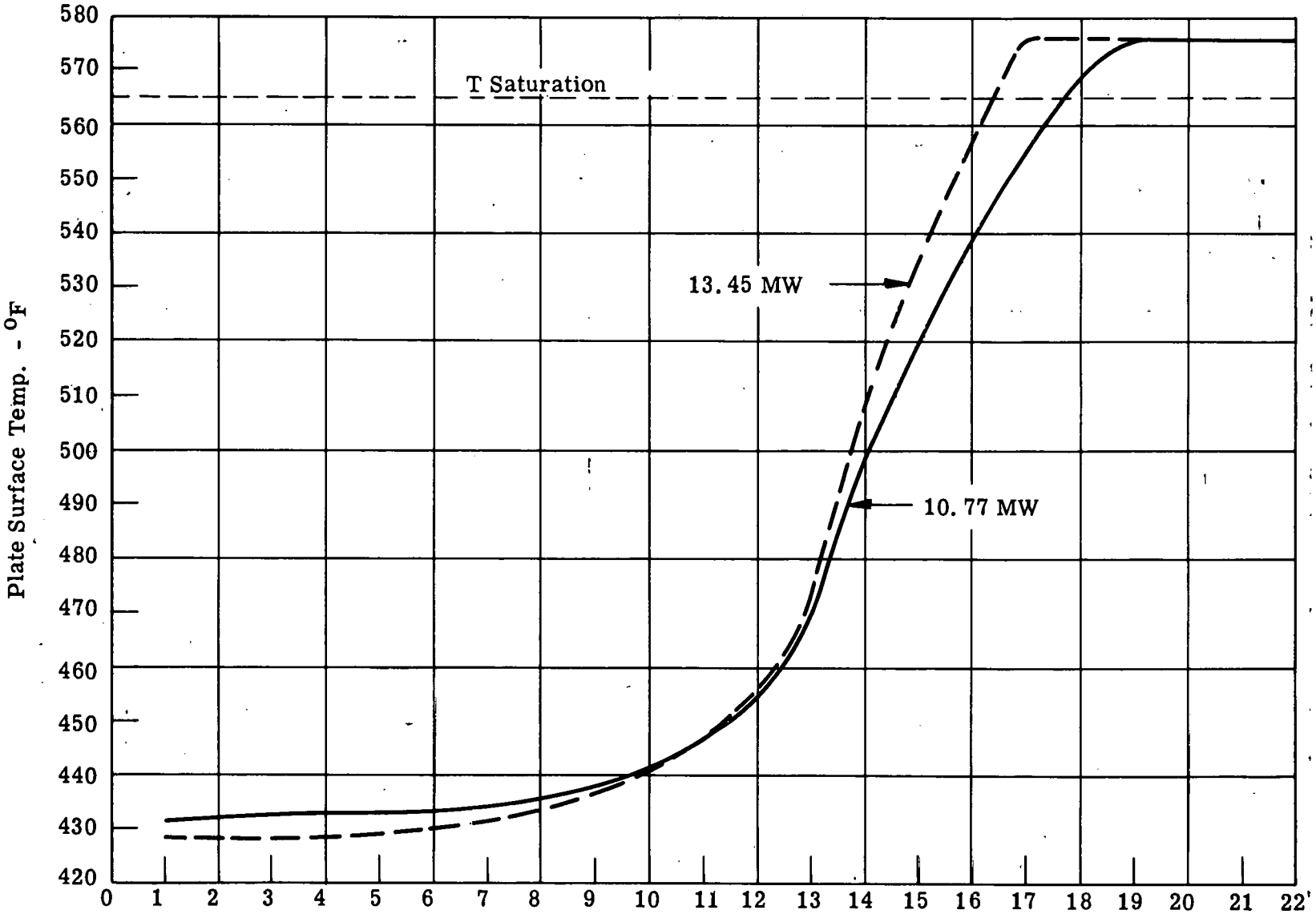

Figure 1.12

Plate Surface Temperature of Type 3 Elements in the SM-1 Core
Core Position 55

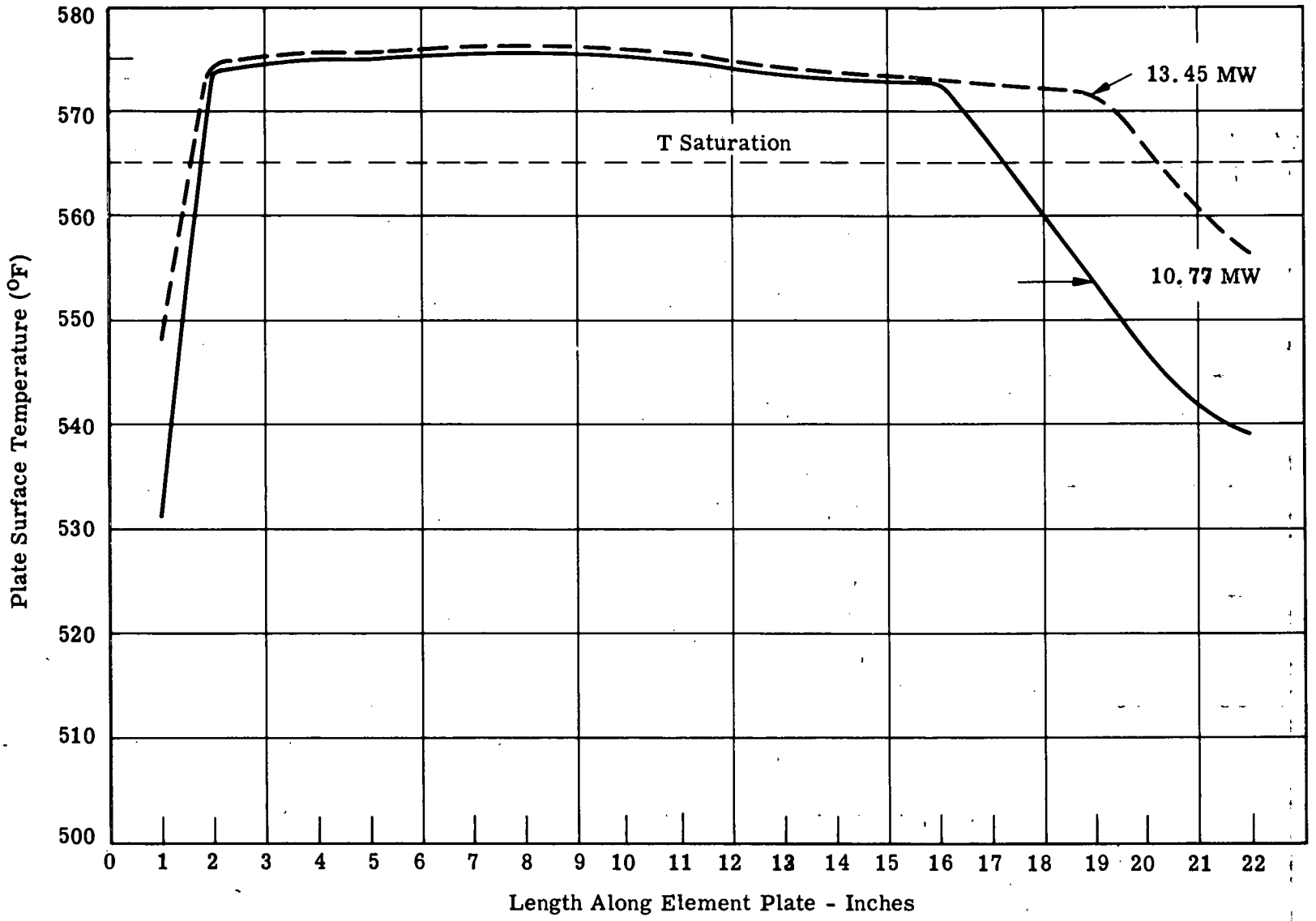

Figure 1.13

Plate Surface Temperature of Type 3 Elements in the SM-1 Core
Core Position 61

1.8 STEADY STATE PERFORMANCE OF TYPE 3 ELEMENTS IN THE SM-1A REACTOR

A steady state thermal analysis was performed on 10 element positions within the SM-1A core. These elements were selected based on their burnout indexes presented in Table 1.11.

The analysis included studies at both design power 20.2 MW and at scram power 24.2 MW with average core heat, fluxes of 120,320 Btu/hr-ft^2 and 144,143 Btu/hr-ft^2, respectively. Plate surface temperature, bulk water temperature, departure from nucleate boiling and quality boiling were calculated for one inch increments up the 22-in. channel.

The results of this analysis at 20.2 MW are shown on Table 1.15 and at 24.2 MW on Table 1.16. There is no indication of local boiling at design power conditions. However, local boiling is indicated at the extreme exit end of control rod elements 33 and 55 at scram power conditions. The inception of local boiling with its characteristic flat surface temperature profile is shown on Fig. 1.14 for element 33. Element 72 shown on Fig. 1.15 represents the stationary element with the lowest DNBR. The flat profile for plate surface temperature indicates that this element is marginally away from local boiling with 13 degrees of superheat.

The results of this analysis indicate that no SM-1A element is in danger of burnout at design conditions of 20.2 MW, since the most critical control rod element 33 and the most critical stationary element 72 exhibit minimum DNBR's of 2.39 and 2.70, respectively. These elements also meet a minimum DNBR of 1.5 at scram power conditions 24.2 MW

1.9 STEADY STATE PERFORMANCE OF TYPE 3 ELEMENTS IN THE PM-2A REACTOR

A steady state thermal analysis was performed on 10 elements within the PM-2A core. These elements were selected based on their burnout indexes presented in Table 1.7.

The analysis included studies at both design power 10.0 MW and at scram power level 12 MW with average core heat fluxes of 68,849 Btu/hr-ft^2 and 82,619 Btu/hr-ft^2, respectively. The results of this analysis at 10.0 MW are shown on Table 1.17 and at 12 MW on Table 1.18. There is no local boiling indicated at either design power or scram power levels. Fig. 1.16 and 1.17 show the plate surface temperature for the two most critical elements in the core, positions 44 and 33. However, element 44 is marginally away from the inception of local boiling at the scram power level with 6.2 degrees of superheat.

The results of this analysis indicate that no PM-2A element is in danger of burnout since the most critical control rod element 44 and the most critical stationary element 33 exhibit at 12 MW minimum DNBR's of 4.66 and 5.00, respectively, both in excess of the design minimum 1.5.

TABLE 1.15
RESULTS OF THE STEADY STATE THERMAL ANALYSIS OF THE SM-1A TYPE CORE, POWER 20.2 MW

Core Position	G-Nominal Channel Flow X 10^6, lb/hr-ft^2	G-Hot Channel Flow X 10^6, lb/hr-ft^2	Hot Channel Bulk Outlet Temp., °F	Hot Channel Maximum Plate Surface Temp., °F	Min DNBR	Qlty.	*Local Boiling
16	1.426	1.337	472.4	577.7	2.70	0	0
27	1.373	1.287	473.5	577.6	2.80	0	0
33	1.692	1.269	473.9	578.5	2.39	0	0
34	1.646	1.543	477.3	578.5	2.77	0	0
43	1.593	1.493	479.5	578.5	2.74	0	0
54	1.625	1.523	478.0	578.5	2.77	0	0
55	1.692	1.269	473.9	578.5	2.39	0	0
61	1.384	1.297	473.1	577.6	2.80	0	0
62	1.331	1.248	469.9	564.6	3.86	0	0
72	1.405	1.317	473.0	577.7	2.70	0	0

* Axial increment at which nucleate boiling begins, measured in inches from the bottom of the element.

TABLE 1.16
RESULTS OF THE STEADY STATE THERMAL ANALYSIS OF THE SM-1A
TYPE 3 CORE, POWER - 24.2 MW

Core Position	G-Nominal Channel Flow X 10^6, lb/hr-ft^2	G-Hot Channel Flow X 10^6, lb/hr-ft^2	Hot Channel Bulk Outlet Temp., ^oF	Hot Channel Max. Plate Surface Temp., ^oF	Min DNBR	Qlty.	*Local Boiling
16	1.426	1.337	479.2	578.2	2.25	0	0
27	1.373	1.287	480.5	578.2	2.33	0	0
33	1.692	1.269	481.1	579.1	1.98	0	21
34	1.646	1.543	485.1	579.1	2.30	0	0
43	1.593	1.493	487.7	579.1	2.27	0	0
54	1.625	1.523	485.9	579.1	2.30	0	0
55	1.692	1.269	481.1	579.1	1.98	0	21
61	1.373	1.287	480.5	578.2	2.33	0	0
62	1.331	1.248	476.3	577.8	3.21	0	0
72	1.405	1.317	480.0	578.2	2.24	0	0

* Axial increment at which nucleate boiling begins, measured in inches from the bottom of the element.

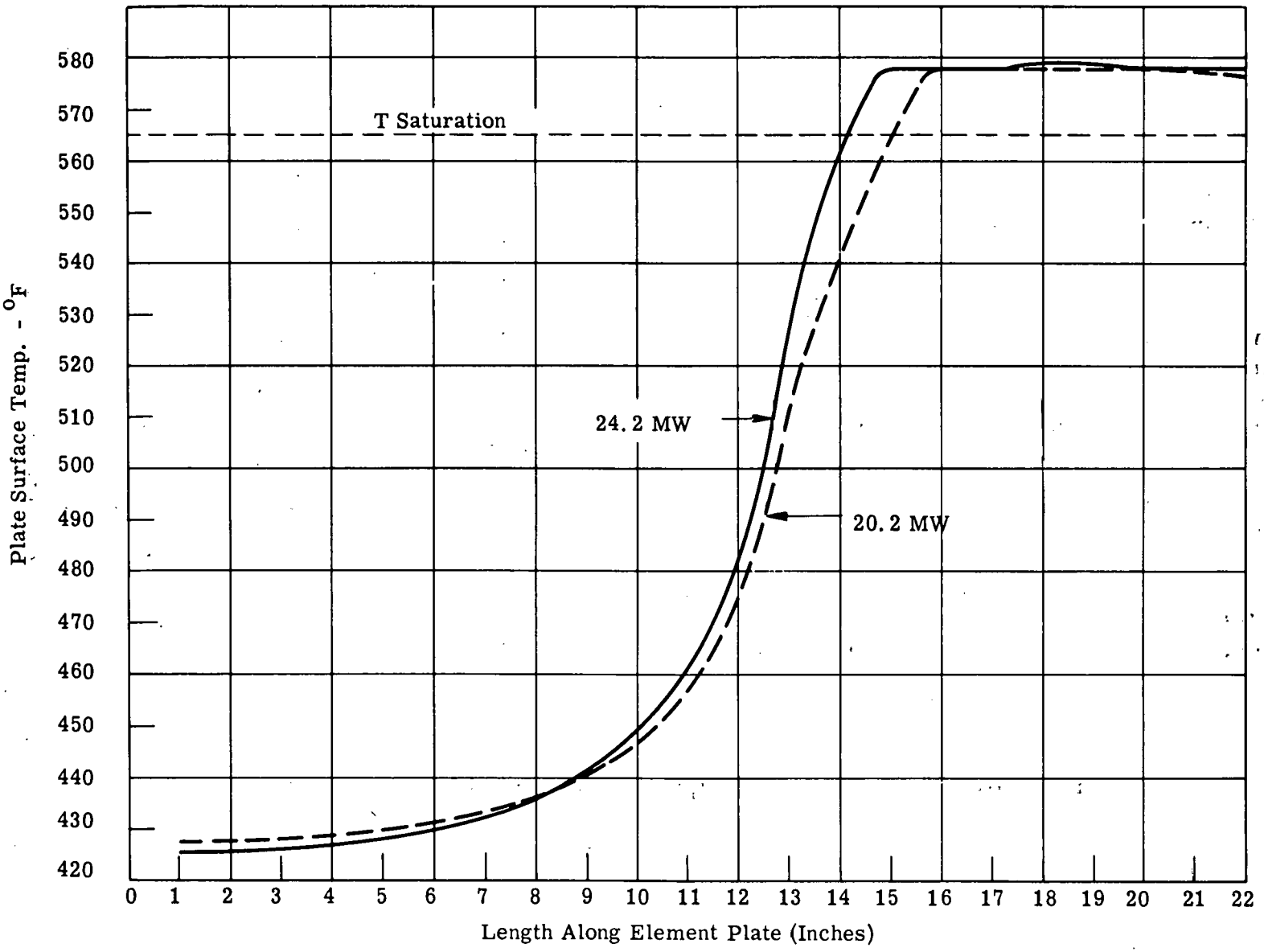

Figure 1.14

Plate Surface Temperature of Type 3 Elements in the SM-1A Core
Core Position 33

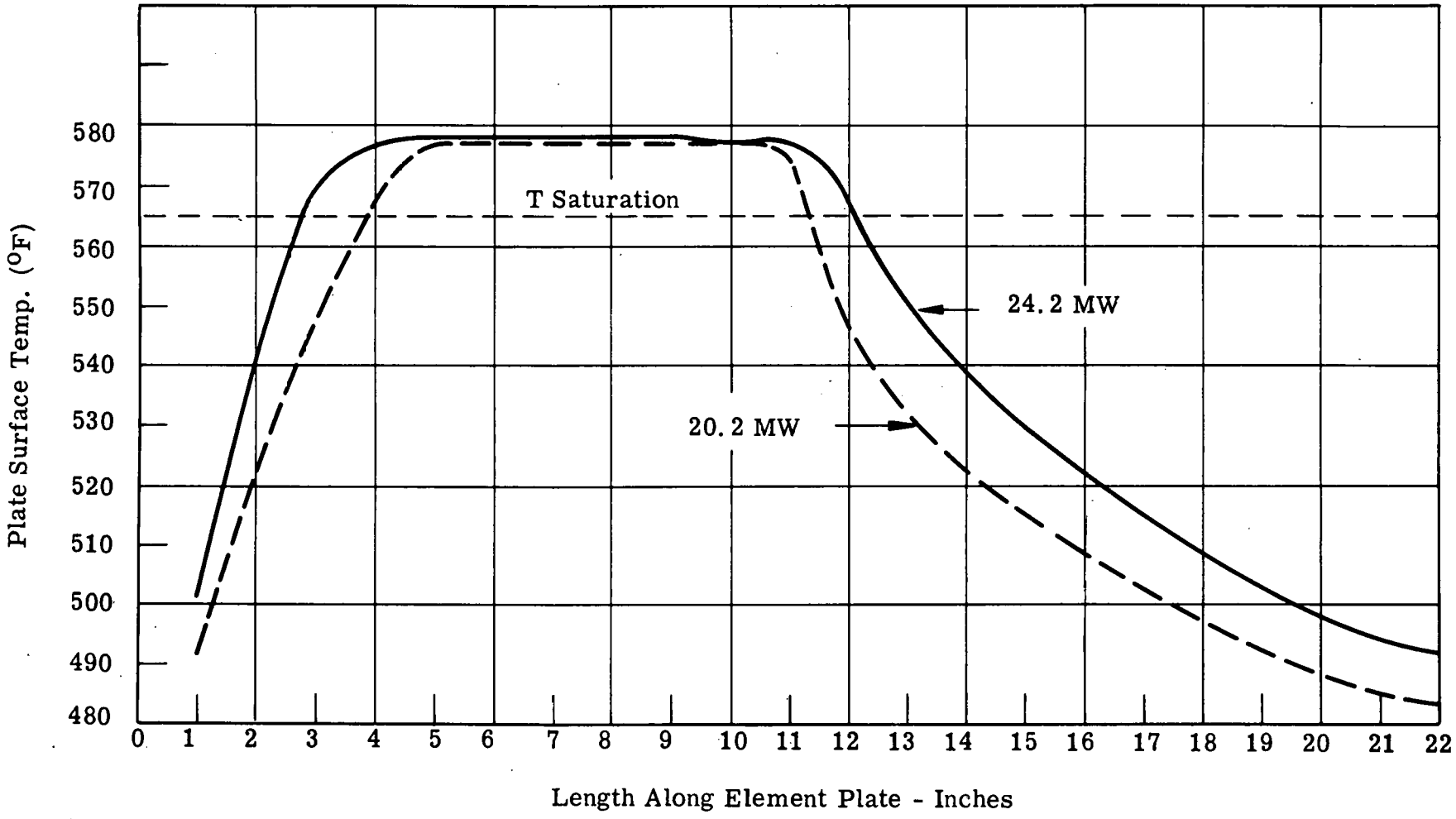

Figure 1.15

Plate Surface Temperature Type 3 Elements in the SM-1A Core
Core Position 72

TABLE 1.17

RESULTS OF THE STEADY STATE THERMAL ANALYSIS OF THE PM-2A TYPE 3 CORE, POWER 10.0 MW

Core Position	G- Nominal Channel Flow X 10^6, lb/hr-ft^2	G-Hot Channel Flow X 10^5, lb/hr-ft^2	Hot Channel Bulk Outlet Temp., ^oF	Hot Channel Max. Plate Surface Temp., ^oF	Min DNBR	Qlty.	*Local Boiling
13	1.112	9.730	539.4	587.6	7.53	0	0
22	1.093	9.564	542.1	599.1	6.03	0	0
26	1.112	9.730	541.5	597.7	6.03	0	0
33	1.112	9.730	538.4	596.6	5.99	0	0
37	1.102	9.642	526.8	572.7	8.02	0	0
43	1.073	9.389	543.0	597.7	6.28	0	0
44	1.168	8.760	545.0	610.3	5.61	0	0
55	1.064	9.310	539.9	600.0	5.99	0	0
62	1.093	9.564	542.1	598.8	6.03	0	0
66	1.102	9.642	541.8	598.4	6.03	0	0

* Axial increment at which nucleate boiling begins, measured in inches from the bottom of the element.

TABLE 1.18
RESULTS OF STEADY STATE THERMAL ANALYSIS OF THE PM-2A
TYPE 3 CORE, POWER 12 MW

Core Position	G-Nominal Channel Flow X 10^6, lb/hr-ft^2	G-Hot Channel Flow X 10^5, lb/hr-ft^2	Hot Channel Bulk Outlet Temp., ^oF	Hot Channel Max. Plate Surface Temp., ^oF	Min DNBR	Qlty.	*Local Boiling
13	1.112	9.730	542.5	594.1	6.28	0	0
22	1.093	9.564	545.7	614.0	5.02	0	0
26	1.112	9.730	544.9	612.4	5.03	0	0
33	1.112	9.730	541.2	611.1	5.00	0	0
37	1.102	9.642	527.4	582.4	6.70	0	0
43	1.073	9.389	546.8	612.4	5.23	0	0
44	1.051	7.589	556.4	620.7	4.66	0	0
55	1.064	9.310	543.0	615.2	4.99	0	0
62	1.093	9.564	545.7	614.0	5.02	0	0
66	1.102	9.642	545.3	613.3	5.03	0	0

* Axial increment at which nucleate boiling begins, measured in inches from the bottom of the element.

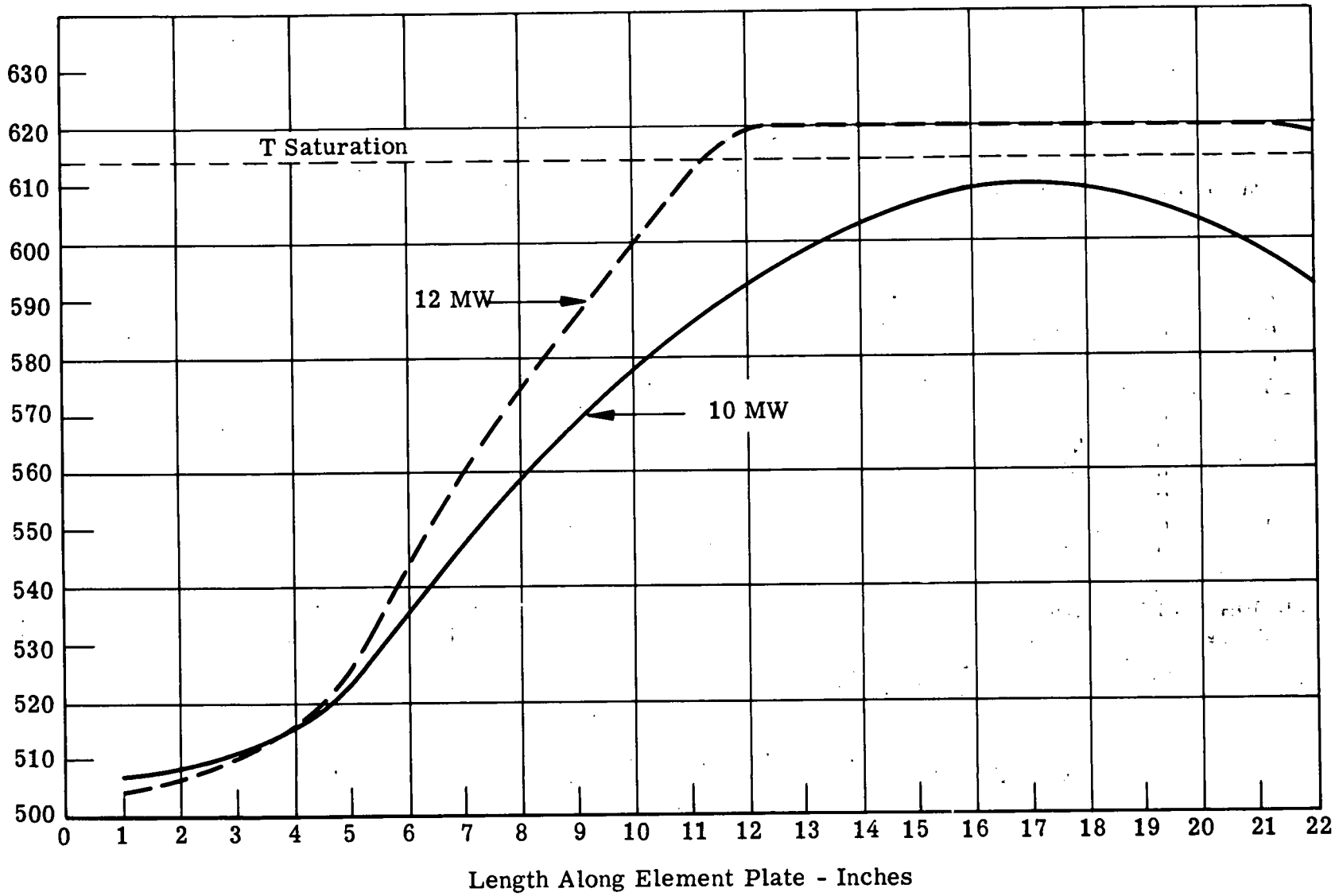

Figure 1.16
Plate Surface Temperature of Type 3 Elements in the PM-2A Core
Core Position 44

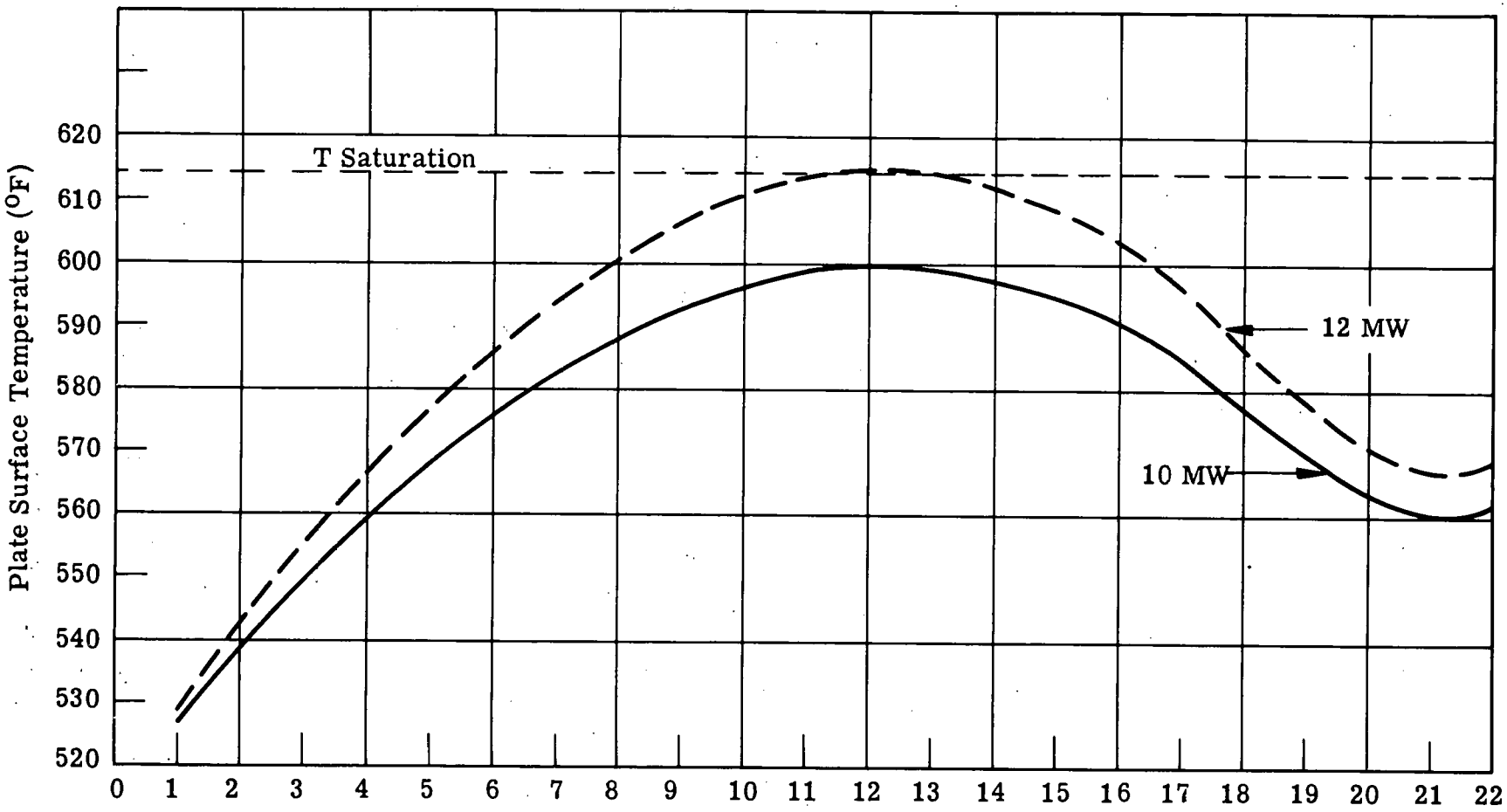

Figure 1.17

Plate Surface Temperature of Type 3 Elements In the PM-2A Core
Core Position 55

1.10 CONCLUSIONS AND RECOMMENDATIONS

1. The SM-1 core with Type 3 elements will operate safely at design conditions with some local boiling in the outermost elements. This situation is slightly worse at scram conditions. There is no evidence of local or bulk boiling for the average channels and minimum DNBR's are well above 1.5.

2. The SM-1A core with Type 3 elements will operate safely at design conditions with no local boiling evident for the average channels with minimum DNBR's for the two hottest elements above 1.5. At scram conditions a minute amount of local boiling was evident at the exit end of the most critical control rod and stationary element. Minimum DNBR's for these elements were within the design minimum of 1.5.

3. The PM-2A core with Type 3 elements will operate safely at both design power conditions and scram power with no local boiling present for either case. The minimum DNBR's for the two hottest elements are greater than 1.5.

4. A decay heat removal study has been omitted from this report, the analysis of which would require an extensive analytical treatment. The decay heat removal models for the SM-1, SM-1A and PM-2A should not change at all since the increase in maximum heat flux within Type 3 cores over the original cores is in general not appreciable. Best judgment indicates the cores will be thermally safe in the decay heat removal condition. All plants are very conservative during this operation.

It is recommended from the above results that:

1. For the SM-1, the amount of local boiling in the hot channels could be reduced with the addition of a flow fix in the inlet end box of the stationary elements to improve the channel-to-channel flow distribution. This was evident from the results of single element flow testing in which an improvement from -55% to -23% in maldistribution was obtained by the addition of an interchangeable conical diffuser in the inlet end box. However, a flow fix is not recommended for the SM-1 elements since the presence of local nucleate boiling is not expected to have any adverse effects on cladding material, the improvement of channel-to-channel flow distribution has an insignificant effect on DNBR, and the insertion of this device in the inlet end box would add complications to the present design.

2. For the SM-1A, no improvement is necessary in the stationary elements; however, a slight improvement with a flow fix could be made in the control rods where maldistributions are in excess of 20%. The improved

flow distribution for this core is attributed to the orifice plate being on the exit side of the elements. Flow fixes are not recommended for the SM-1A control rod elements.

3. For the PM-2A, since channel-to-channel stationary element flow distribution is within 12% and control rod distribution is approximately 20%, flow fixes are not recommended for these elements.

4. Prior to operation of these cores, if analytical proof of adequate thermal margin is required during decay heat removal, an analysis must be performed

2.0 TRANSIENT ANALYSIS

2.1 INTRODUCTION

The thermal analysis of the Type 3 cores in the SM-1, SM-1A and PM-2A during the critical period immediately following a loss of flow accident has been analyzed by means of the ART-02 [17] IBM-704 Code. Determination of the safety of these three cores has been achieved by analyzing the hottest elements in each core as evaluated by the I_{DNBR} (Section 1.6). If these analyzed elements prove to be safe during a loss of flow transient, as measured by the departure from nuclear boiling ratio criteria (DNBR), then the individual cores analyzed will be thermally safe.

2.2 TRANSIENT METHOD OF ANALYSIS

The detailed study of the core during the loss of flow transient has been performed by means of the ART-02 [17] Code. This code utilizes a one-dimensional model to predict the behavior of a water-cooled and moderated reactor with plate type elements during transients which are slower than a prompt excursion. The model utilized in the cases studied was a single pass core operating initially at steady-state conditions. The reactor is then subjected to a variation in flow rate with or without a variation in reactivity as induced by control rod motion to simulate a loss of flow with or without a scram.

The nominal behavior of the individual elements of a core is represented by a single coolant channel in each element. Thermal calculations are also performed on an additional channel which represents the hot channel with its associated extremes in dimensions, pressure drop and heat input.

The version of the ART Code used in the present analysis is based upon fog or homogeneous flow. Though this analysis is somewhat less rigorous than the slip flow model as presented in ART-04 [18] it has been utilized in the absence of good void fraction data. The important correlations and equations used in the code are presented in Appendix C.

2.3 POWER DISTRIBUTIONS

As in the steady state analysis (Section 1.3.2) the loss of flow analysis has been performed at the design power level. However to insure the convervatism of the analysis, an instrumentation tolerance has been applied so that all three cores have been evaluated at the worst feasible condition of the maximum overload or scram power level. The design and scram power along with the reference steady state heat generation per unit area, q_0^* (Eq. C.2) are tabulated below,

Core	Design Power Level	q_0*, Btu/hr, ft^2	Scram Power Level	q_0*Btu/hr, ft^2
SM-1	10.77 MW	64,600	13.45 MW	77,900
SM-1A	20.2 MW	120,300	24.2 MW	144,100
PM-2A	10.0 MW	68,800	12.0 MW	82,600

The axial power distributions in the transient analysis are identical to those used in the steady state analysis (Section 1.3.2) and are plotted for the Type 3 stationary and control rod elements of the three cores, in the following figures:

SM-1	Stationary Element	Fig. 1.6
	Control Rod Element	Fig. 1.3
SM-1A	Stationary Element	Fig. 1.6
	Control Rod Element	Fig. 1.4
PM-2A	Stationary Element	Fig. 1.7
	Control Rod Element	Fig. 1.5

Average radial power peaking factors in the nominal channel ($Q\overline{\Delta}_T$) and hot channel ($Q\Delta_T$) along with local radial peaking factors ($Q_{\Delta\Theta}$)are tabulated in the following tables:

Table of Radial Power Peaking Factors

Core		Peaking Factors	$Q\Delta\Theta$ Max.	Element Core Position	Axial Max.	Approx. Locat. from Bottom of Core	Core Peak to Average
SM-1	Type 3 Core	Table 1.3	2.09	31,57	1.911	7"	3.99
SM-1A	Type 3 Core	Table 1.4	2.24	12,76	1.911	7"	4.28
PM-2A	Type 3 Core	Table 1.5	2.05	44	1.429	10"	2.93

The following tabulation of the peak fluxes at nominal conditions (i.e., SM-1 at 10.77 MW) shows the relation of Type 3 cores to previous cores.

Core	Reference	Peak Flux at Nominal Power, Btu/hr ft^2
SM-1 Core I		
Spiked and		1.881×10^5
Rearranged		3.000×10^5
Core II	APAE No. 85 [8]	2.766×10^5
Type 3 Core		2.578×10^5
SM-1A Core I	APAE No. 17 [19]	3.198×10^5
Type 3 Core		5.149×10^5
PM-2A Core I	APAE No. 39 [7]	1.772×10^5
Type 3 Core		2.016×10^5

The tabulation shows that the Type 3 SM-1 Core represents a 39% increase in the peak flux in relation to the SM-1 Core I. Similarly, Type 3 SM-1A Core is a 61% increase over SM-1A Core I and PM-2A Type 3 Core is a 14% increase over PM-2A Core I. However Type 3 SM-1 Core is a 14% decrease in peak flux in relation to SM-1 Core I Spiked and Rearranged.

2.4 SELECTION OF ELEMENTS

Verification of the safety of the three cores has been achieved by analyzing both a stationary element and a control rod element with the highest ratio of power generation to available flow (I_{DNBR}). If these elements prove to be safe during the loss of flow transient, then each of the cores analyzed will be thermally safe.

By means of the I_{DNBR} index (Section 1.6) the most vulnerable elements in each core are:

SM-1 Type 3 Core

Core Position	Type of Element	I_{DNBR}
61*	Stationary	3.09
27	Stationary	3.07
31	Stationary	3.07
55*	Control Rod	2.61
33	Control Rod	2.61

SM-1A Type 3 Core

Core Position	Type of Element	I_{DNBR}
55*	Control Rod	3.09
33	Control Rod	3.09
43	Stationary	3.05
72*	Stationary	3.01
54	Stationary	3.00
12	Stationary	2.99

PM-2A Type 3 Core

Core Position	Type of Element	I_{DNBR}
44*	Control Rod	2.57
66	Stationary	2.47
55*	Stationary	2.46
62	Stationary	2.48

* Elements investigated during the transient loss of flow analysis.

2.5 FLOW DISTRIBUTIONS

As in the steady state analysis (Section 1.5), the element flow distributions utilized in evaluating the initial flow rates during a loss of flow accident were established by the full scale air flow rigs [11], [12], [13] and are graphically presented in Fig. 1.8, 1.9 and 1.10. The channel-to-channel flow maldistribution (δ) for the various elements investigated during a loss of flow have been evaluated by the latest single element testing .[4] These maldistributions (δ) along with the following maldistribution factors, K_{pf} for friction and K_{pa} for acceleration which are utilized in formulating the pressure drop balance of the hot channel in the ART code (Eq. C.15) are tabulated below:

Core Position	Flow Rate gpm	Channel to Channel Maldistribution (δ), % Wt.	HC $K_{pf} = (1\delta)^{1.8}$	HC $K_{pa} = (1-\delta)^{2.0}$
SM-1 Type 3 Core				
55	89.00	-28.0	.554	.518
61	44.24	-55.0	.237	.203
SM-1A Type 3 Core				
55	147.0	-22.8	.628	.596
72	134.0	-6.7	.883	.870
PM-2A Type 3 Core				
44	110.0	-22.0	.640	.608
55	110.0	-10.9	.812	.794

2.6 HOT CHANNEL FACTORS

The hot channel factors used in this analysis were formulated for average conditions which affect heat generation rates and for local conditions which affect local heat fluxes in the DNB correlations. Numerically, the value of the individual factors used in the transient analysis are equal to those used in the steady state analysis (Section 1.4). However, the input format for the ART code is somewhat different than STDY-3 and the manner of formulating these factors is presented in this section.

The heat generation rate at any particular axial section of the core is expressed in (Eq. C.2) as:

$$q_{ji} = q_o^* f'(Z) \; F_{M\Delta T} \; (P/P_o)_i$$

where $F_{M\Delta T}$, the average power peaking factor, is composed of average engineering hot channel factors ($F_{\Delta T}$), and a radial power peak either in the hot channel $Q_{\Delta T}$ or in the nominal channel $Q_{\overline{\Delta T}}$. The average engineering hot channel factor in turn is composed of average factor for core length deviations ($F_{\text{core length}}$), for clad deviation (F_{clad}), and for average deviations in uranium content and homogeneity (F_{HoM}). Therefore, the average power peaking factor $F_{N\Delta T}$ is

$$F_{M\Delta T} = Q_{\Delta T} \; F_N F_{\text{core length}} F_{clad} F_{Hom} \quad \text{for the hot channel} \tag{2.1}$$

$$F_{M\Delta T} = Q_{\overline{\Delta T}} F_N F_{\text{core length}} F_{clad} F_{Hom} \quad \text{for the nominal channel.}$$

However, the engineering factors in the nominal channel are considered unity and

$$F_{M\overline{\Delta T}} = Q_{\overline{\Delta T}} \; F_N \tag{2.2}$$

The factor which affects the local heat flux ($\frac{\phi^L}{\phi}$ in the DNBR correlations (Eq. C.19) is a <u>multiple</u> of the average radial power peaking factor in steady state:

$$\phi_{jo} = q_{jo}(1-r) \text{ and } \phi^L_{jo} = \left(\frac{\phi^L}{\phi}\right) \phi_{jo} \tag{2.3}$$

or $$\phi_{jo} = \left(\frac{\phi^L}{\phi}\right) q_{jo}(1-r)$$

Using the nomenclature in Appendix B.

$$\frac{\phi^L}{\phi} = \frac{F_{M\Delta\Theta}}{F_{M\Delta T}}$$

where $F_{M\Delta\Theta}$, the local power peaking factor, is composed of local engineering factor, local nuclear uncertainty factor and the (local) hot plate radial power peaking factor.

$$F_{M\,\Delta\theta} = Q_{\Delta\theta}\ F_N^L\ F^L_{\text{core length}}\ F^L_{\text{clad}}\ F^L_{\text{Hom}} \qquad (2.4)$$

and the local heat flux correction factor $(\frac{\phi^L}{\phi})$ is

$$\frac{\phi^L}{\phi} = \frac{Q_{\Delta\theta}\ F_N^L\ F^L_{\text{core length}}\ F^L_{\text{clad}}\ F^L_{\text{Hom}}}{Q_{\Delta T}\ F_N\ F_{\text{core length}}\ F_{\text{clad}}\ F_{\text{Hom}}} \qquad (2.5)$$

Using the numerical values of hot channel factors given in Table 1.6 and Eq. (2.1), (2.2), (2.4), the value of power peaking factors for Type 3 control rods and stationary elements are:

Stationary Elements

Nominal Channel $\quad F_{M\,\overline{\Delta T}} = 1.05\, Q_{\overline{\Delta T}},\ \phi^L/\phi = 1.112\, \frac{Q_{\Delta\Theta}}{Q_{\Delta T}}$

Hot Channel $\quad F_{M\,\Delta T} = 1.087\, Q_{\Delta T},\ \phi^L/\phi = 1.074\, \frac{Q_{\Delta\theta}}{Q_{\Delta T}}$

Control Rods

Nominal Channel $\quad F_{M\,\overline{\Delta T}} = 1.05\, Q_{\overline{\Delta T}},\ \phi^L/\phi = 1.112\, \frac{Q_{\Delta\theta}}{Q_{\Delta T}}$

Hot Channel $\quad F_{M\,\Delta T} = 1.087\, Q_{\Delta T},\ \phi^L/\phi = 1.074\, \frac{Q_{\Delta\theta}}{Q_{\Delta T}}$

Unlike previous thermal analyses (9), there is no hot channel factor formulated for plate spacing deviations as induced by tolerences or rippling. This factor is omitted because the ART Code will accept a local mass velocity correction factor (G^L/G) as direct input to evaluate variations in the local mass velocity (G_i^L). Therefore, the variations in plate spacing which cause variations in local mass velocities are fully covered by the local correction factor (G^L/G) or

$$G_i^L = (\frac{G^L}{G})G_i \qquad (2.6)$$

The local mass velocity correction factor is related to the plate spacing (inclusive of rippling) in the following manner:

$$G = \frac{W}{A} \qquad W = GA$$

where W = flow rate lb/hr, which is constant for a channel

A = Area, ft^2

But A = Sb

b = channel width

s = channel spacing or thickness;

and in thin channels where b the width is very nearly a constant,

$$W = G_1 \, bS_1 = G_2 \, bS_2$$

or

$$\frac{G_2}{G_1} = \frac{S_1}{S_2}$$

The Type 3 element with channel spacings, including rippling as shown below and repeated from Section 1.4.2 has the following local mass velocity correction factor (G^L/G) :

Stationary Elements	Nominal Min Channel Spacing	Max. Local Channel Spacing	G^L/G
Nominal Channel	.123	.127	.969
Hot Channel	.119	.136	.875
Control Rods			
Nominal Channel	.123	.127	.969
Hot Channel	.119	.133	.895

2.7 OPERATING PARAMETERS USED IN THE LOSS OF FLOW ANALYSIS

As in the steady state investigation (Section 1.4), the conservatism of the analysis has been insured by the use of the most adverse operating conditions. The values of the operating parameters (inclusive of instrumentation tolerances) for all the cores studied during a loss of flow analysis were:

	Design Power	Scram Power
SM-1 Type 3 Core		
Core Power, MW	10.77	13.45
Inlet Temperature, ^{o}F	431.7	428
System Pressure, psia	1175	1175
SM-1A Type 3 Core		
Core Power, MW	20.2	24.2
Inlet Temperature, ^{o}F	427	425
System Pressure, psia	1175	1175
PM-2A Type 3 Core		
Core Power, MW	10.0	12.0
Inlet Temperature, ^{o}F	504	500
System Pressure, psia	1715	1715

2.8 FLOW COASTDOWN

The flow coastdown of the reactor which is the driving force for the transient portion of the code, has been represented by decreases in flow in the nominal channel of:

$$\frac{G}{G_o} = \frac{1}{(1 + bt)} 1.25 \qquad (2.7)$$

where t = time, sec

b = constant

For conservatism, the analysis is based on the most adverse pump coastdown, that of a stuck or frozen impeller. For SM-1, the value of b is 2.2 as evaluated by the methods in APAE Memo No. 87, [20] which include a measured term for the pump pressure drop. This is a considerable increase in the severity of the coastdown over that measured in TP-600, [21] in which the impeller was free to rotate.

The value of b used in evaluating the PM-2A is 4.00 as reported in APAE No. 49 [22]. In the case of the SM-1A where the pressure drop in the pump with a frozen impeller is not accurately known, the value of b has been conservatively taken as 4.00. It would appear that the choice of the coefficient b would be very important; but results of the analysis of the SM-1 where b = 2.2 and b = 4.00 in this report indicate only very minor variations in DNBR. Similar effects have been obtained in the loss of flow analysis of the SM-2 [23] with different coastdown rates. A plot of flow as a function of time for the two pump coastdowns considered in the analysis of the Type 3 cores investigated, is given in Fig. 2.1.

2.9 DEPARTURE FROM NUCLEATE BOILING RATIO (DNBR) CORRELATIONS

The latest available data on rectangular channel departure from nucleate boiling heat flux for system pressures below 1850 psia is reported in WAPD-188. [24] In general, this departure from nucleate boiling heat flux has an enthalpy dependence which is less steep than the -2.5 power associated with a system pressure of 2000 psia. However, as the fluid enthalphy increases, the correlation which is associated with enthalpy to the -2.5 power is more applicable and the two types of correlations tend to intersect. Therefore, at all times the STDY-3 Code and ART Code should make an evaluation to determine which correlation produces the more conservative (applicable) results. Fortunately the STDY-3 code does, but the earlier ART code does not have the desired correlations programmed into it and its resulting DNBR's must be re-evaluated. This is presently being performed by means of the ART Reduction IBM-650 code, which corrects the ART DNBR's to the proper correlations in STDY-3.

Mathematically DNB is a function of enthalphy H at the K^{th} temperature.

$$DNB = DNB\ (H_k)$$

Therefore the correction factor

$$C_j = \frac{DNB\ (H_k)\ \text{STDY-3}}{DNB\ (H_k)\ \text{ART-02}} \qquad (2.8)$$

and the corrected DNBR is:

$$DNBR = C_j\, DNBR\ \text{ART-02}$$

or

$$DNBR = DNBR\ \text{ART-02} \left[\frac{DNB(H_k)\ \text{STDY-3}}{DNB(H_k)\ \text{ART-02}}\right] \qquad (2.8A)$$

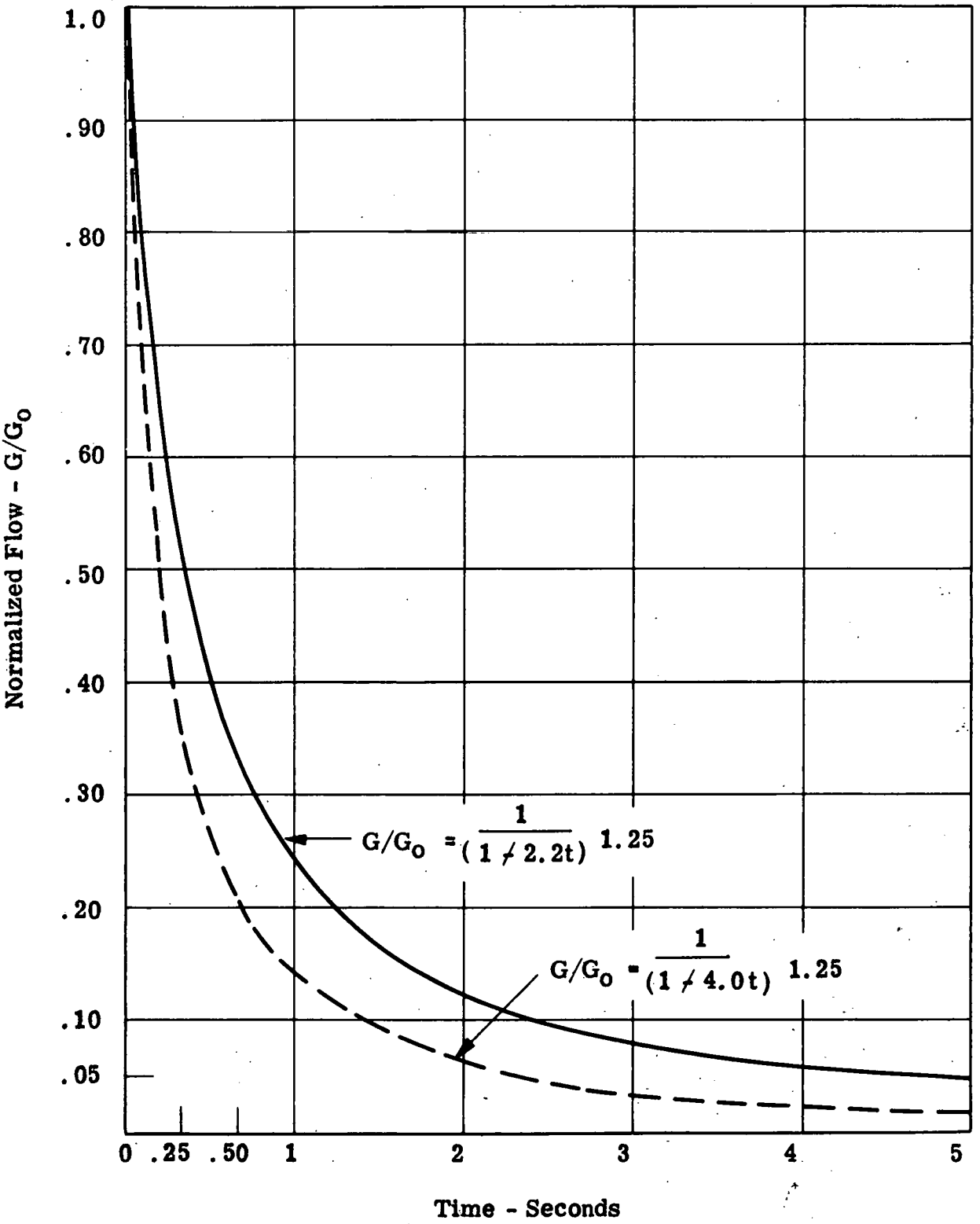

Figure 2.1

Flow Coastdowns Investigated in the Loss of Flow Analysis

For a system pressure of 1175 psia which is applicable to the thermal evaluation of the SM-1 and the SM-1A, the following proper correlations are in the STDY-3 code;

$$\frac{DNB}{10^5} = 3.25 \left[\frac{H_j}{1000}\right]^{-2.5} e^{-0.0012\ L/S}\ F_{(P)}$$

where $F_{(P)} = 1.1875$

$$\frac{DNB}{10^5} = 3.482 \left[\frac{H_j}{1000}\right]^{-2.5} e^{-0.012\ L/S} \qquad (2.10)$$

or

$$\frac{DNB}{10^5} = 8.9 \left[\frac{H_j}{1000}\right]^{-.72} e^{-0.0012\ L/S} \qquad (2.11)$$

where the STDY-3 code takes the minimum value between Eq. 2.10 and 2.11.

However the ART code utilizes the following correlation under a system pressure of 1175 psia.

$$\frac{DNB}{10^5} = 3.86 \left[\frac{H_{ji}}{1000}\right]^{-2.5} e^{-0.0012\ L/S} \qquad (2.12)$$

Equation 2.10 thru 2.12 are plotted in Fig. 2.2 where the geometry factor $e^{-0.0012\ L/S}$ is taken as unity (corresponds to channel length L = 0). It is noted in this particular case that Eq. 2.11 produced more conservative results than Eq. 2.10 for $H \leq 590\ \frac{B}{lbm}$ and it is the STDY-3 solution for DNB, where the enthalpy is less than 590 Btu/lb m

For the PM-2A thermal evaluation where the system pressure is conservatively taken as 1715 psia the STDY-3 code utilizes the following correlations:

$$\frac{DNB}{10^5} = 3.25 \left[\frac{H_j}{1000}\right]^{-2.5} e^{-0.0012\ L/S}\ F_{(P)}$$

where $F_{(P)}$ = function of pressure = 1.042

$$\frac{DNB}{10^5} = 3.386 \left[\frac{H_j}{1000} \right]^{-2.5} e^{-0.0012\ L/S} \qquad (2.13)$$

or

$$\frac{DNB}{10^5} = 8.9 \left[\frac{H_j}{1000} \right]^{-0.72} e^{-0.0012\ L/S} \qquad (2.11)$$

and the ART-02 code uses;

$$\frac{DNB}{10^5} = 3.48 \left[\frac{H_{ji}}{1000} \right]^{-2.5} e^{-0.0012\ L/S} \qquad (2.14)$$

Equations 2.11, 2.13, and 2.14 are plotted in Fig. 2.3. In this particular case Eq. 2.11 is valid to $H_j \leq 581$ Btu/lb_m and Eq. 2.13 is valid for $H > 581$ Btu/lb_m. Therefore, the solution as obtained from the STDY-3 code is a composite of these two correlations dependent upon the fluid enthalphy.

Since the DNB's as obtained from STDY-3 are the desirable correlations as indicated in WAPD-188, ART results are multiplied by the correction factor Eq. 2.8A. A plot of the correction factor vs. fluid enthalphy is presented in Fig. 2.4.

2.10 ALLOWABLE DEPARTURE FROM NUCLEATE BOILING RATIO (DNBR) IN LOSS OF FLOW TRANSIENT

By utilization of the new departure from nucleate boiling correlations for rectangular channels at pressures below 1850 psi (Eq. 2.11, 2.12 and 2.14), as suggested in WAPD-188 [24] the following qualifications, as formulated by Westinghouse are known:

a. The uncertainty associated with the lack of transient burnout or pressure drop data is 1.10.

b. The uncertainty due to meager data on non-uniform heated channels is 1.10. The combined uncertainty factor is multiplative and is equal to 1.10 x 1.10 = 1.21.

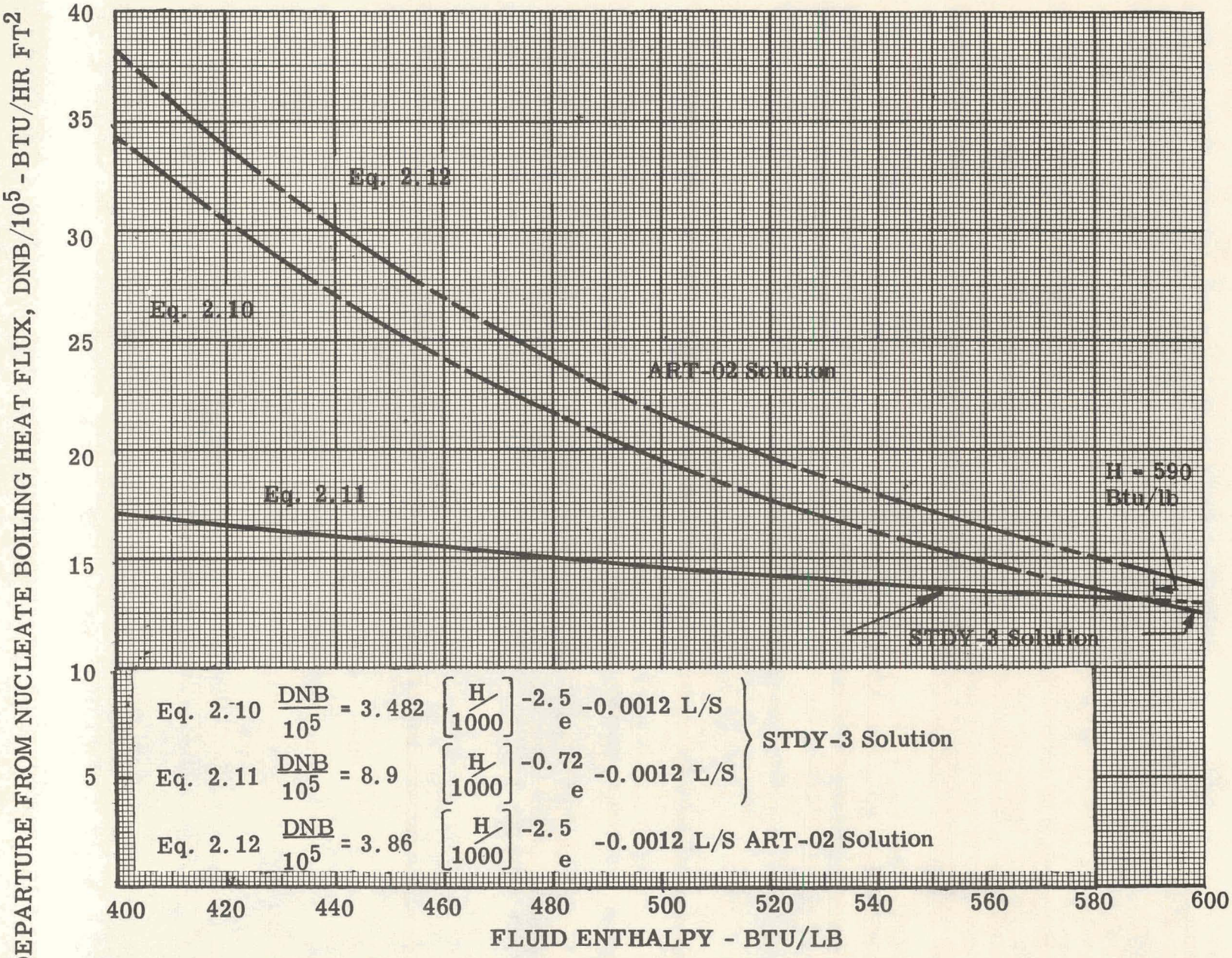

Figure 2.2. DNB Correlations Used in Evaluating the SM-1 and SM-1A

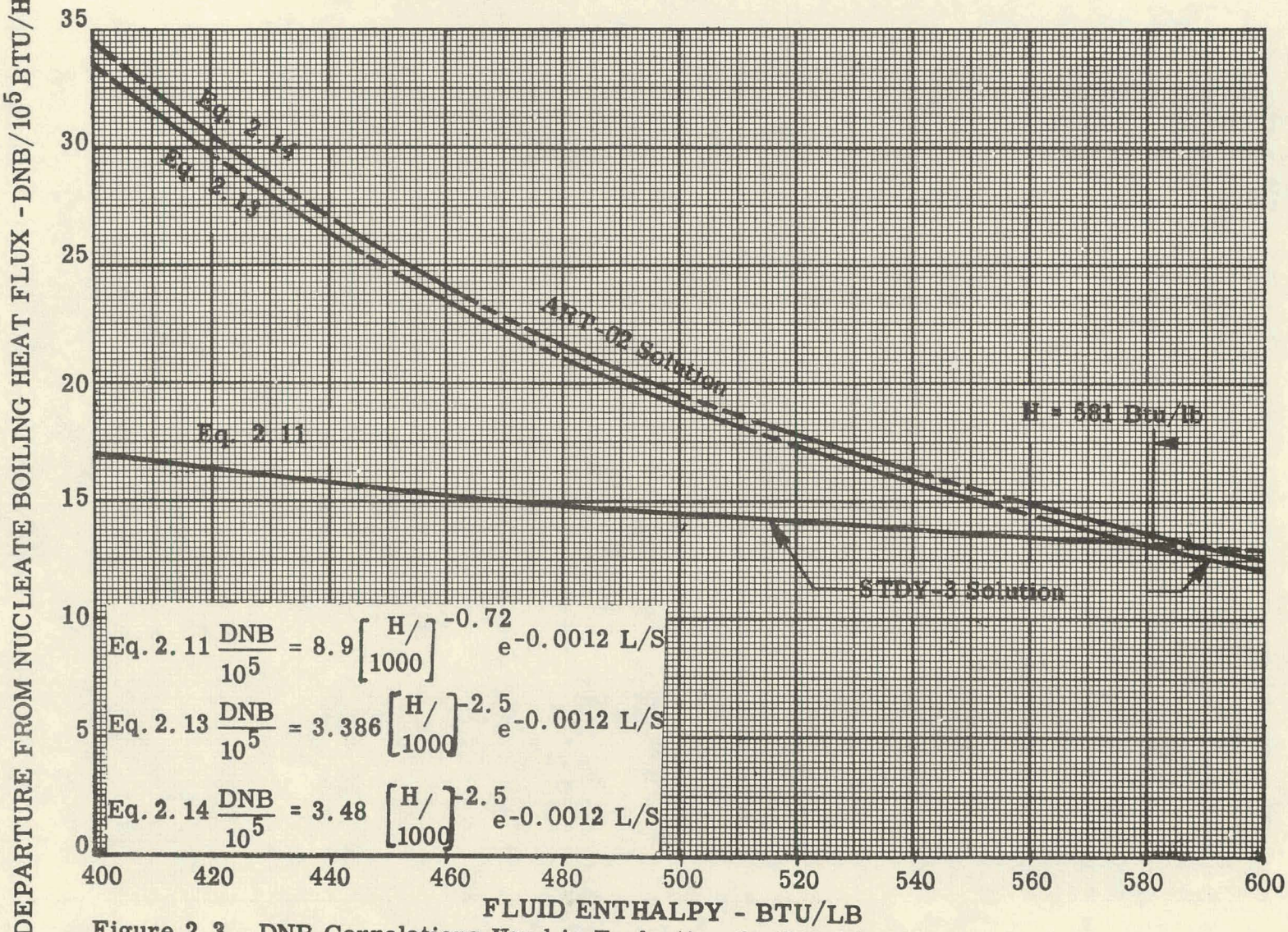

Figure 2.3. DNB Correlations Used in Evaluating the PM-2A

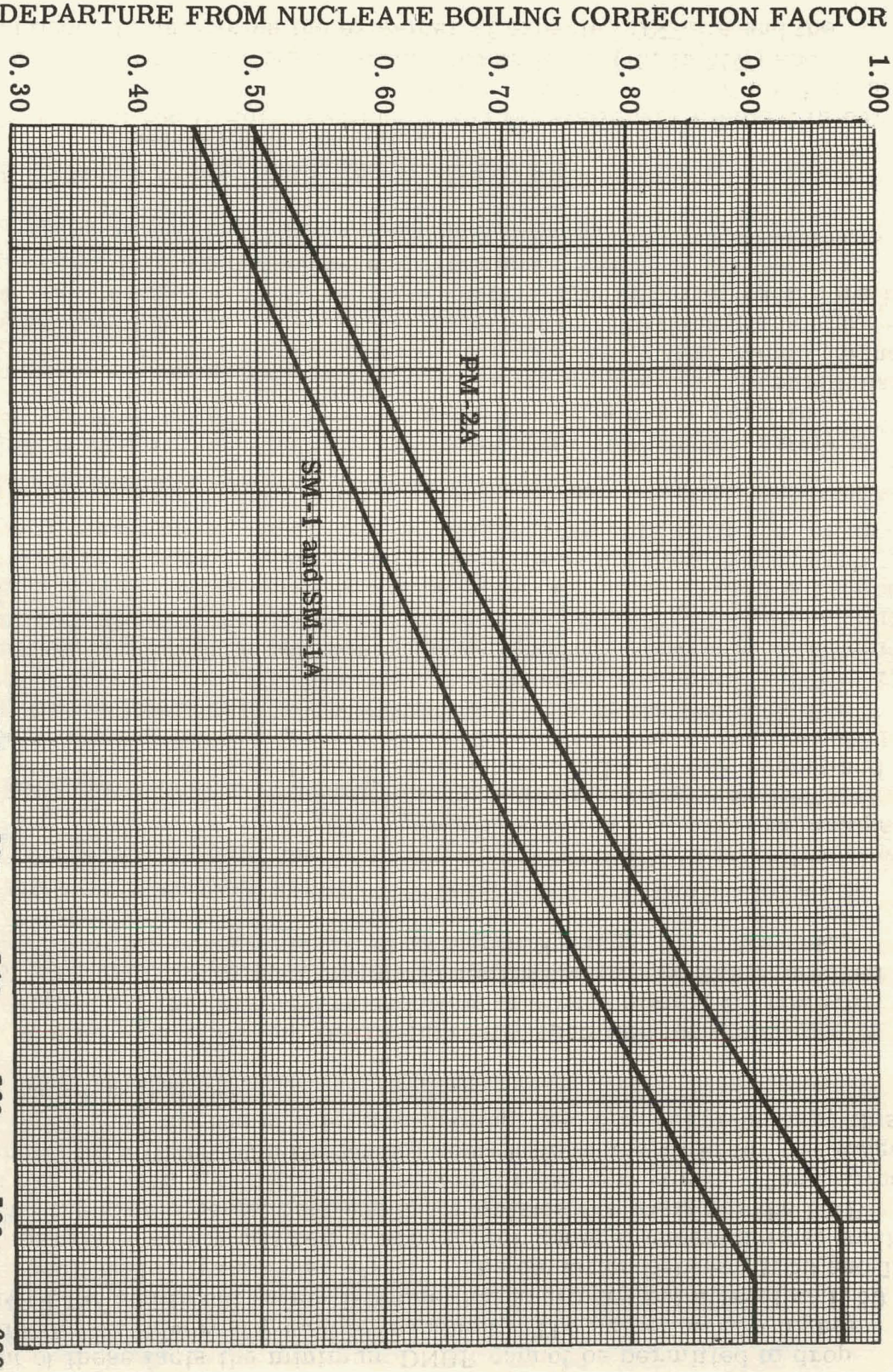

Figure 2.4. ART Code DNB Correction Factor

In light of these facts the minimum DNBR cannot be permitted to drop below 1.21 during the severest possible transient. The selection of a higher minimum DNBR for additional safety is somewhat arbitrary but a level of 1.50 is currently specified for transients [25, 26]. The deviation between 1.50 and 1.21 is the added margin of safety utilized to account for general uncertainties, such as the fact that the experimental data which formulates the basis for the DNB correlations has not been specifically generated for SM type cores. Thus, even though the presently utilized (Westinghouse) correlations are valid for the range of pressure, peak flux, degree of inlet sub-cooling, and channel geometry, this added safety factor is included.

The 1.50 minimum allowable DNBR currently specified for transients is more than adequate for the less severe condition of steady state. If, however, only a steady state analysis is made, a minimum DNBR level of 2.0 is desired to conservatively allow for some potential drop in DNBR during the transient.

This criteria differs from earlier minimum allowable DNBR criteria in that there is no specification for the minimum steady state DNBR when transient analyses are performed. Furthermore, it should be noted that previous analyses have been based on the best fit "departure from nucleate boiling heat flux" equations due to some code limitations. Thermal evaluation in this report and subsequent Alco reports is being performed on the most conservative correlations, namely, the DNB design equations. With the conversion to the use of design equations rather than the best-fit equations, the allowable minimum DNBR of 1.50 during a transient is not only acceptable but conservative. However, some earlier work which either uses the best-fit equations or very old DNB correlations, suffer from updating and their results lead to considerable confusion. For this reason reason Table D.1 in Appendix D, which lists the various hot elements in each core, the report where the information was obtained, the old DNBR and the updated DNBR, is presented in this report.

With this procedure, it is now possible to evaluate the relative safety of the SM-1, SM-1A, PM-2A and SM-2 cores under the same bases since the minimum allowable DNBR in each case is 1.50 during a transient. In particular, the safety of the Type 3 cores is determined if the most critical elements (highest I_{DNBR} Index) do not have a minimum DNBR of less than 1.50 during a loss of flow transient. If the critical elements do not exceed this criteria, each core is deemed safe for the duration of the thermal transient.

2.11 VARIOUS SM-1 TYPE 3 CORE CASES ANALYZED

Both the control rod in core position 55 and the stationary element in core position 61 have been analyzed under the expected flow coastdown of b = 2.2 and the severest conceivable conditions of scram power level (13.45 MW) and no scram. In order to determine the extremes of expected DNBR's and the

effect of variation in flow coastdown on thermal conditions, the control rod in core position 55 has been evaluated with the same severe conditions but with an arbitrary (high) chosen value of b = 4.00.

In order to evaluate the effectiveness of the reactor scram mechanism, the hottest element in the core, the stationary element in core position 61, has been scrammed when at the conservative flow coastdown of b = 4.0. The time delay of 0.060 sec has been conservatively used to represent the time delay prior to activating the 90 percent flow scram setting and the delay in the release mechanism itself. This is a considerably larger time delay than the 0.02 sec that was determined experimentally [27] at the SM-1 site but it is based upon experimental work performed at Alco's Mechanical Engineering Laboratory [28].

To complete the thermal history of the SM-1 Type 3 core, the stationary element in core position 61, and the control rod in position 55 have been evaluated at the nominal power level of 10.77 MW and no scram, with b = 4.0.

The table below is a summary of the cases run on the SM-1 Type 3 core.

Case No.	Core Position	Core Power, MW	Flow Coastdown $G/G_0 = \left(\frac{1}{1 + bt}\right)^{1.25/b}$	Scram Time, Sec	Nominal Channel Flow, GPM	Channel-to Channel Maldistribution %
I	55	10.77	4.0	∞	89.00	- 28.0
II	55	13.45	2.2	∞	89.00	- 28.0
III	55	13.45	4.0	∞	89.00	- 28.0
IV	55	13.45	4.0	06	89.00	- 28.0
V	61	10.77	4.0	∞	44.24	- 55.0
VI	61	13.45	2.2	∞	44.24	- 55.0

Plots of the minimum DNBR in the hot channel are presented in Fig. 2.5 to 2.10.

2.12 VARIOUS SM-1A TYPE 3 CORE CASES ANALYZED

Due to the shortage of IBM-704 time the analysis of both the SM-1A Type 3 Core and the PM-2A Type 3 Core has not investigated the effect of variation in the coastdown function and the safety as induced by the scram mechanism. All efforts were directed toward evaluating the hottest stationary and control rod elements of the cores under the most realistic yet conservative conditions.

In the case of the SM-1A Type 3 Core the hottest elements, the control rod in core position 55 and a hot stationary element in core position 72 have been investigated at the nominal power level of 20.2 MW and the scram power level of 24.2 MW. Both elements were analyzed under the conservative conditions of no scram and a coastdown function with b = 4.0. The table below is a summary of the SM-1A Type 3 core cases run.

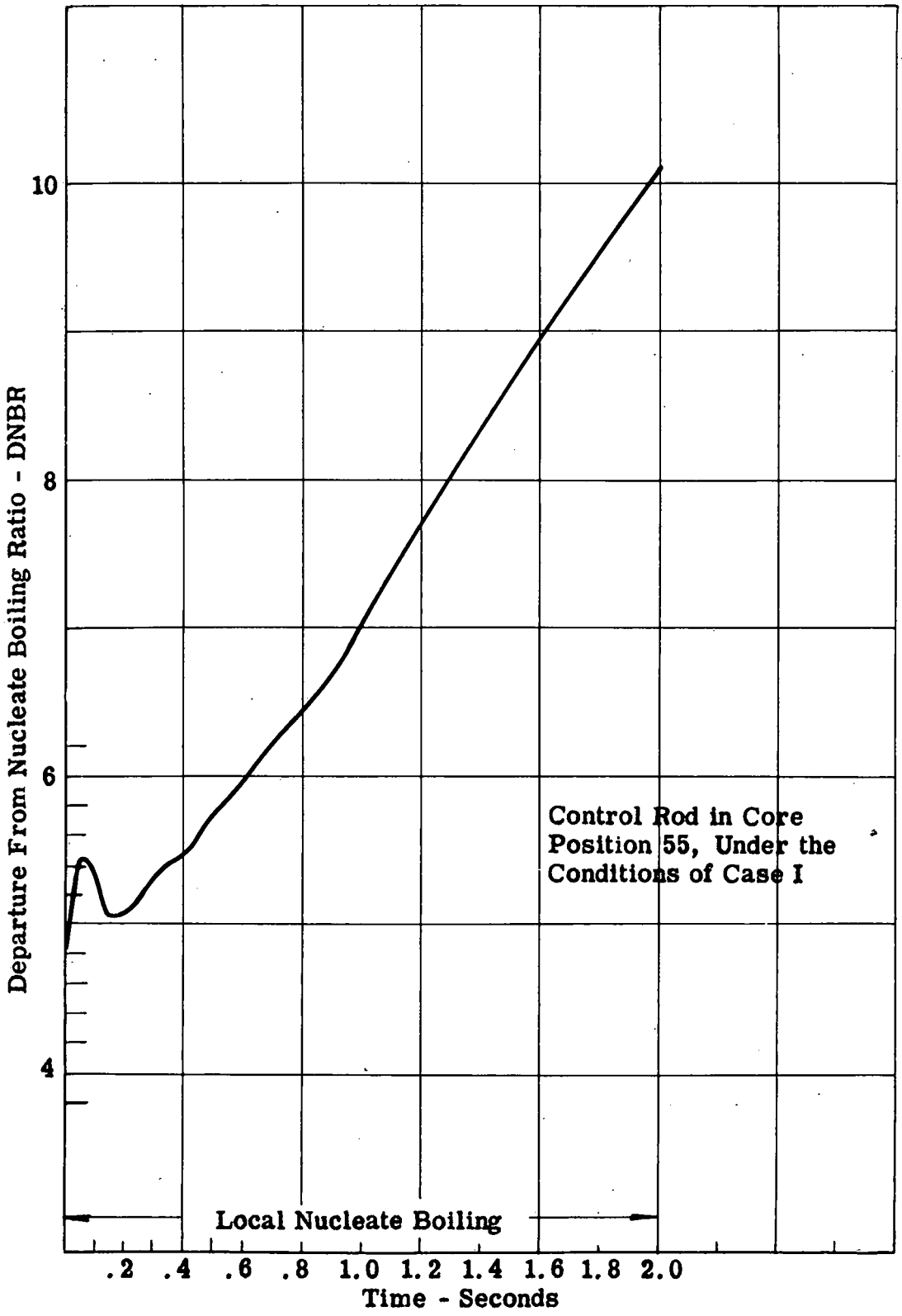

Figure 2.5.
SM-1 Type 3 Core -
Minimum DNBR vs. Time
For The Hot Channel

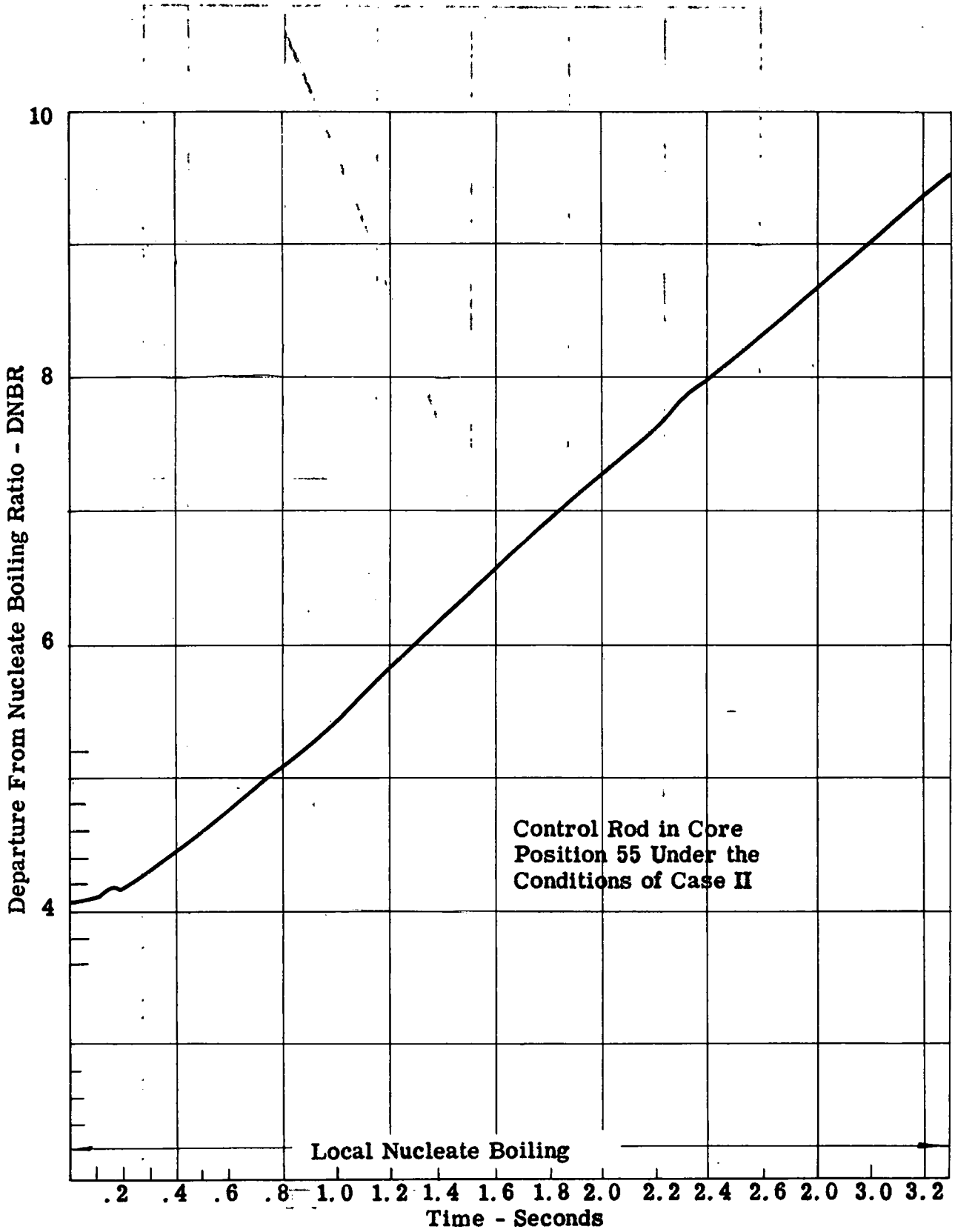

Figure 2.6.
SM-1 Type 3 Core -
Minimum DNBR vs. Time
For The Hot Channel

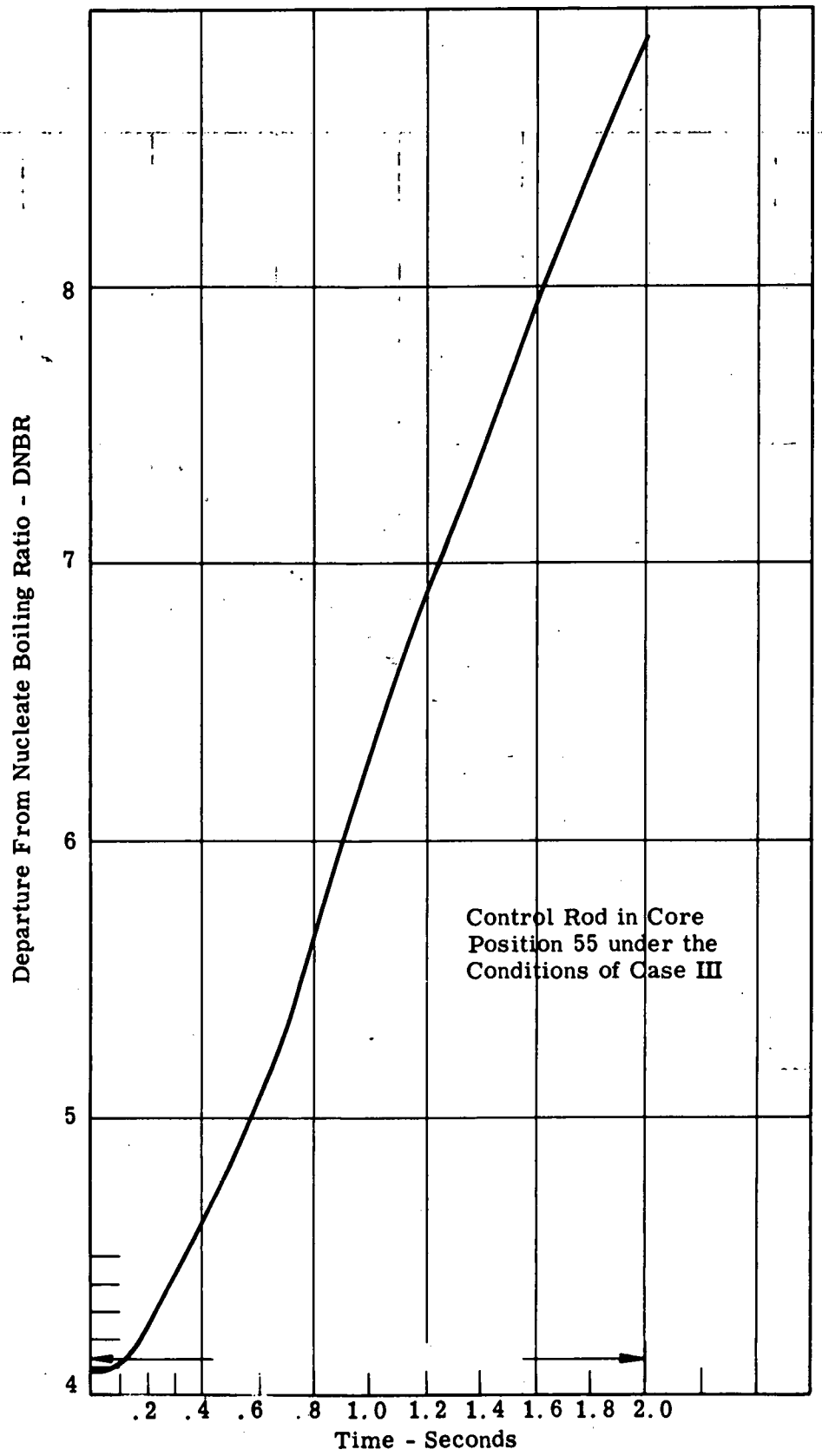

Figure 2.7

SM-1 Type 3 Core Minimum DNBR Vs. Time
For the Hot Channel

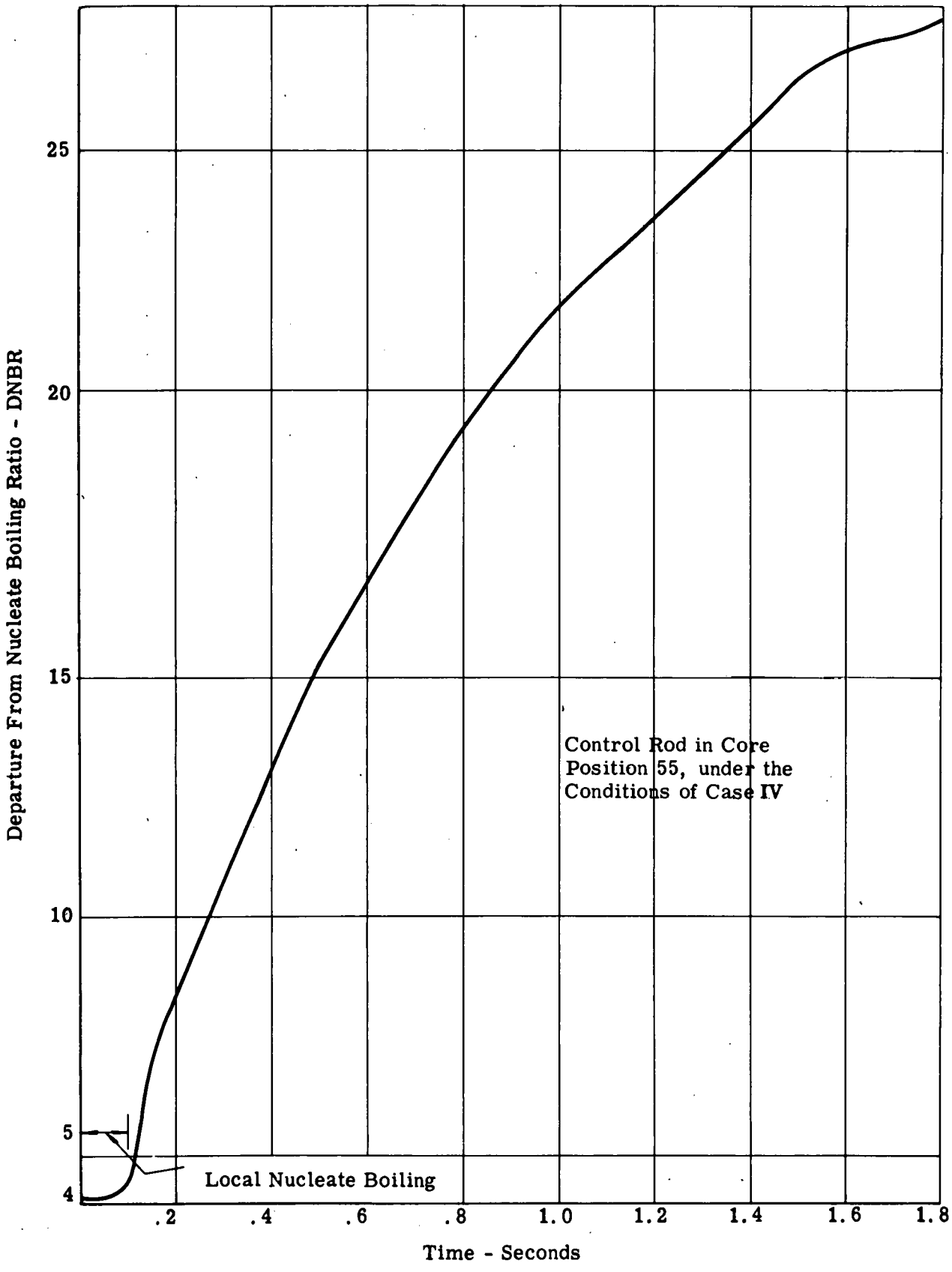

Figure 2.8
SM-1 Type 3 Core Minimum DNBR Vs. Time
For The Hot Channel

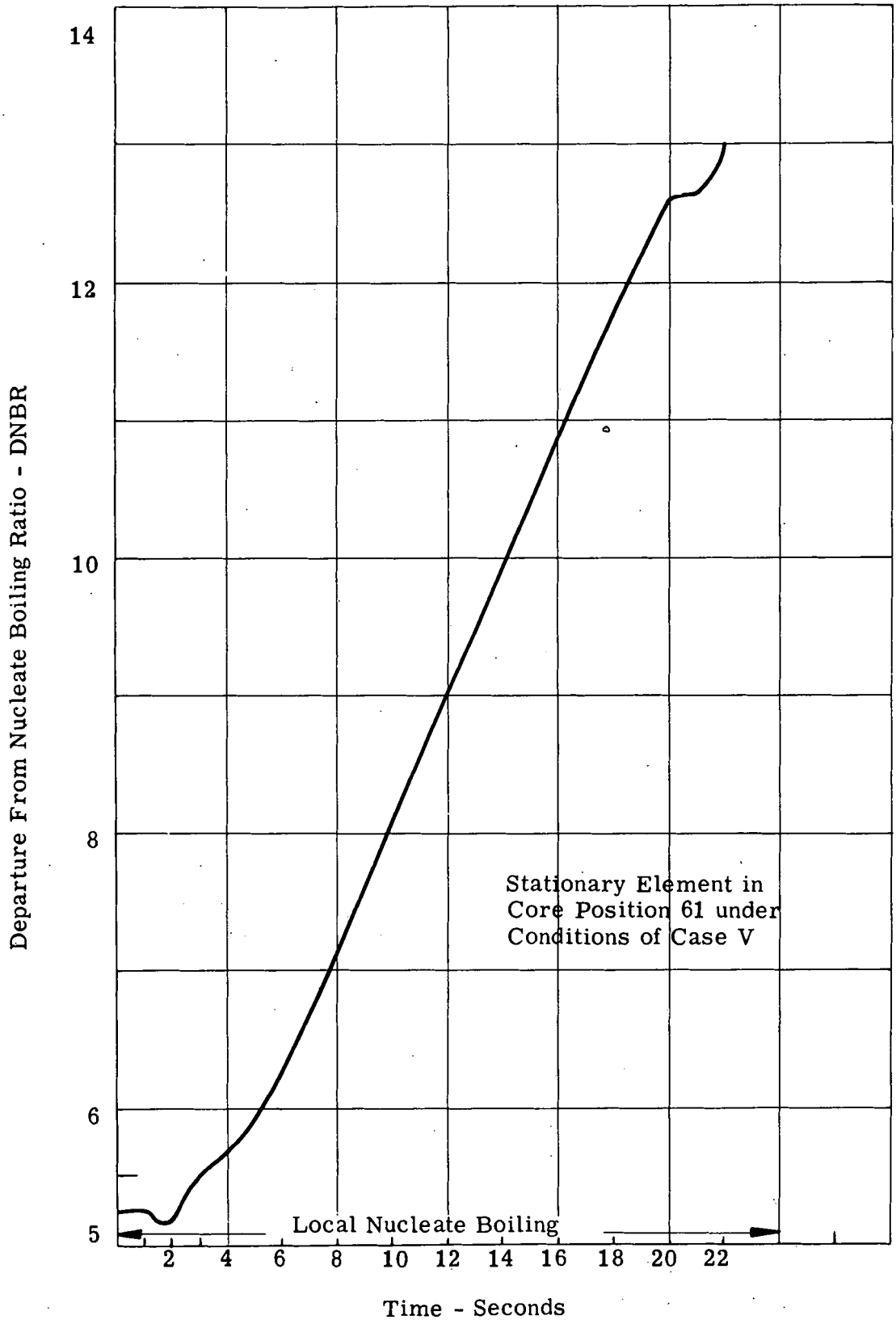

Figure 2.9

SM-1 Type 3 Core Minimum DNBR Vs. Time
For The Hot Channel

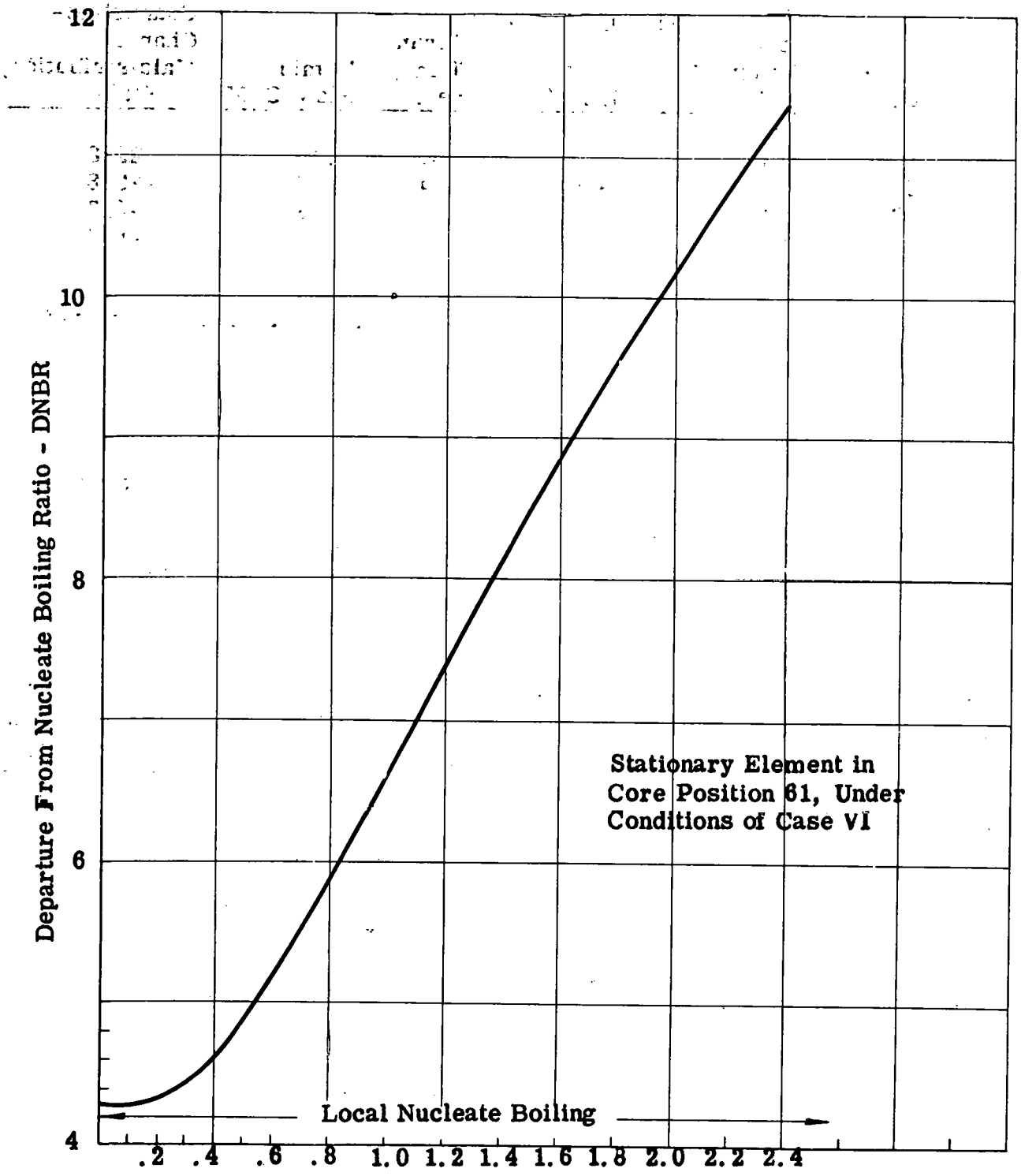

Figure 2.10.
SM-1A Type 3 Core -
Minimum DNBR vs. Time
For The Hot Channel

Case No.	Core Position	Core Power, MW	Flow Coastdown $G/G_o = \frac{1}{(1+bt)}1.25$ $b = 4.0$	Scram Time, Sec.	Nominal Flow, GPM	Channel-to-Channel Maldistribution, Wt %
VII	55	20.2	4.00	∞	147	-22.8
VIII	55	24.2	4.00	∞	147	-22.8
IX	72	20.2	4.00	∞	134	-6.7
X	72	24.2	4.00	∞	134	-6.7

Plots of the minimum DNBR of the hot channel in these cases are presented in Fig. 2.11 thru 2.14.

2.13 VARIOUS PM-2A TYPE 3 CORE CASES ANALYZED

In the analysis of the PM-2A the hottest element in the core, the control rod in core position 44 has been analyzed at the nominal power level of 10.0 MW and the scram power level of 12.0 MW. Similarly the hot stationary element in core position 55 has been analyzed at the nominal power level of 10.0 MW and the scram power level of 12.0 MW. The table below is a summary of the various cases of the PM-2A analyzed.

Case. No.	Core Position	Core Power, MW	Flow Coastdown $G/G_o = \frac{1}{b}\frac{1}{(1+bt)}1.25$	Scram Time, Sec.	Nominal Channel Flow, GPM	Channel-to Channel Maldistribution, Wt %
XI	44	10.0	4.00	∞	110	-22.0
XII	44	12.0	4.00	∞	110	-22.0
XIII	55	10.0	4.00	∞	110	-10.9
XIV	55	12.0	4.00	∞	110	-10.9

Plots in the minimum DNBR of the hot channel in these cases are presented in Fig. 2.15 thru 2.18.

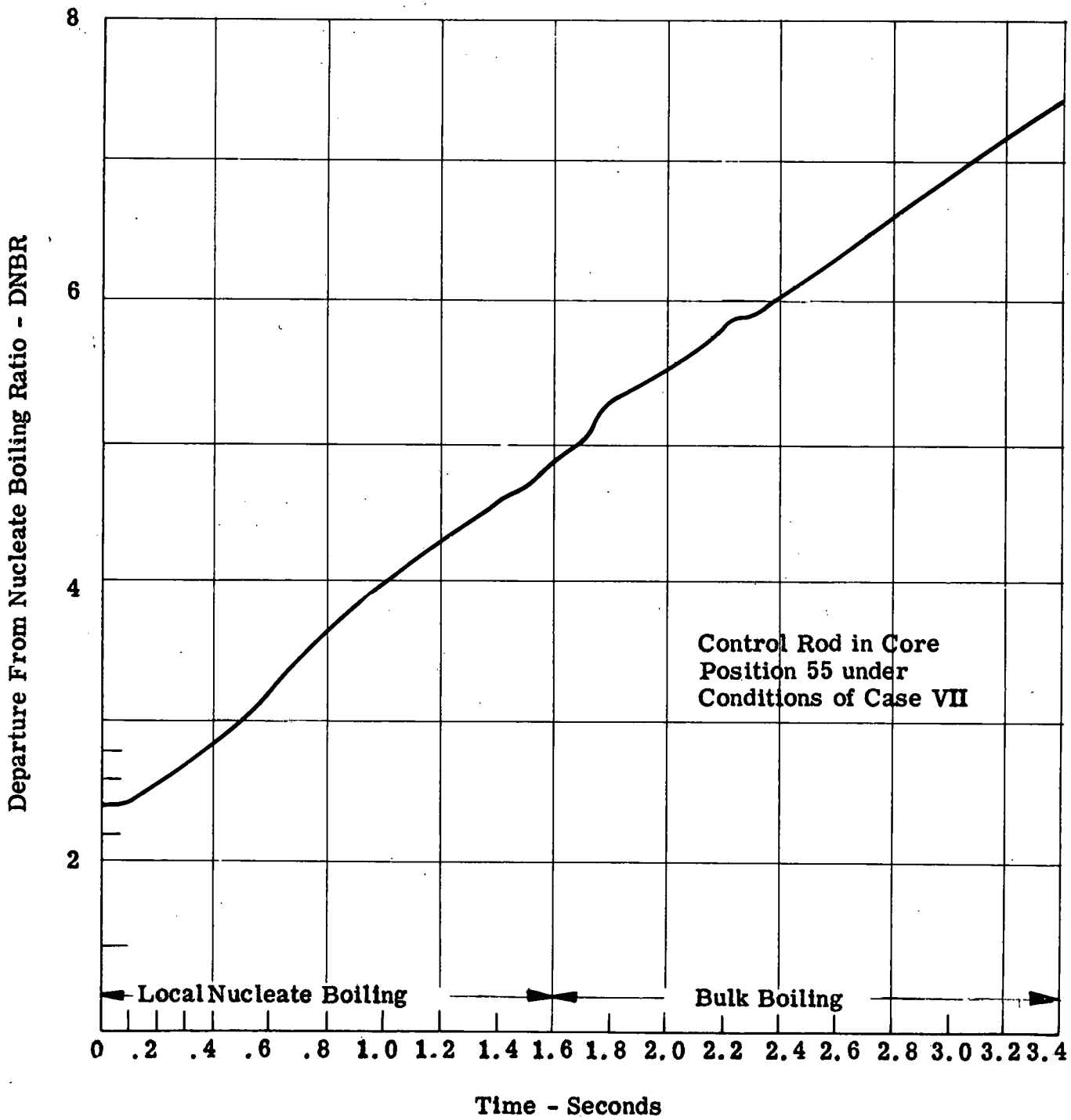

Figure 2.11

SM-1A Type 3 Core Minimum DNBR Vs. Time For The Hot Channel

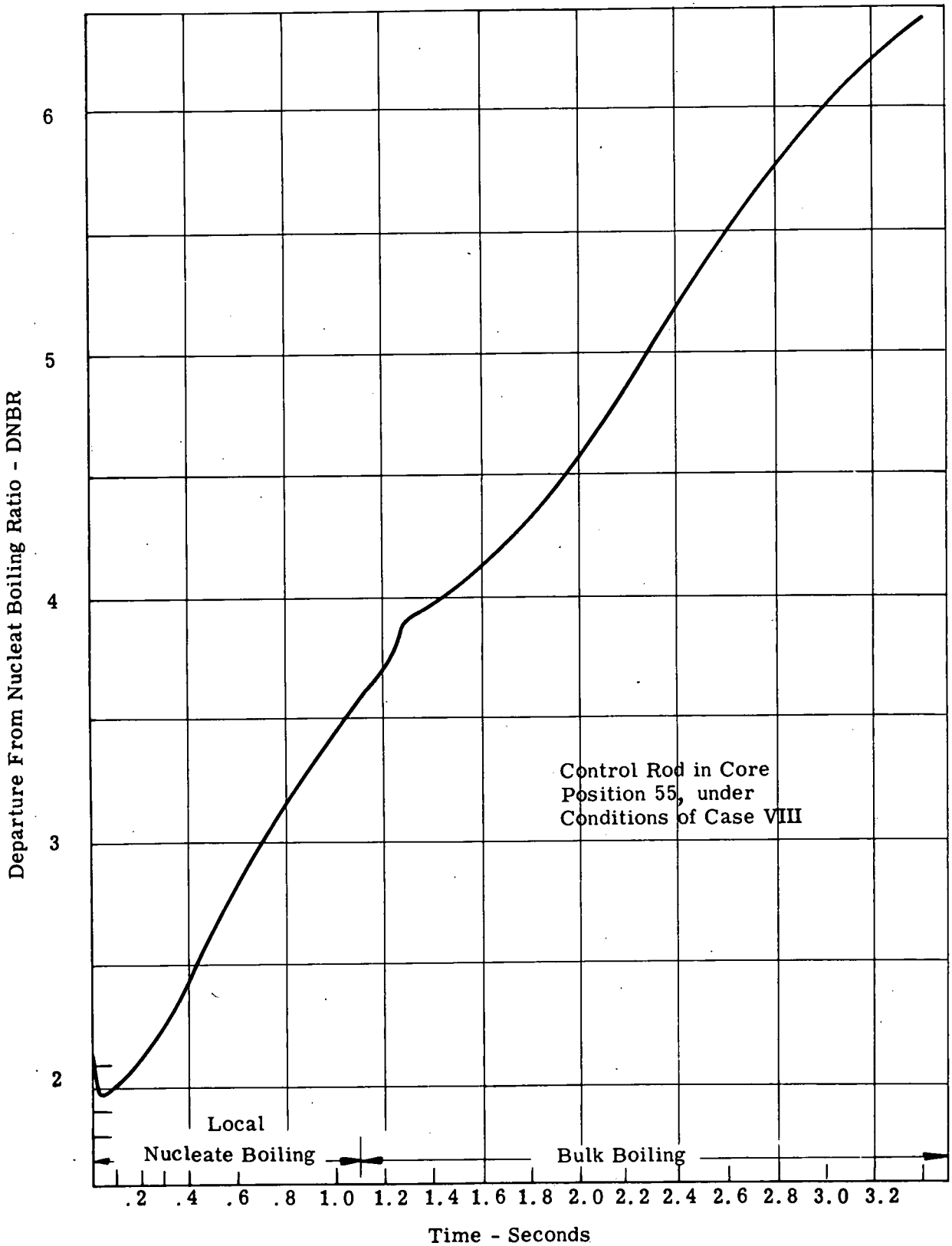

Figure 2.12

SM-1A Type 3 Core Minimum DNBR Vs. Time
For The Hot Channel

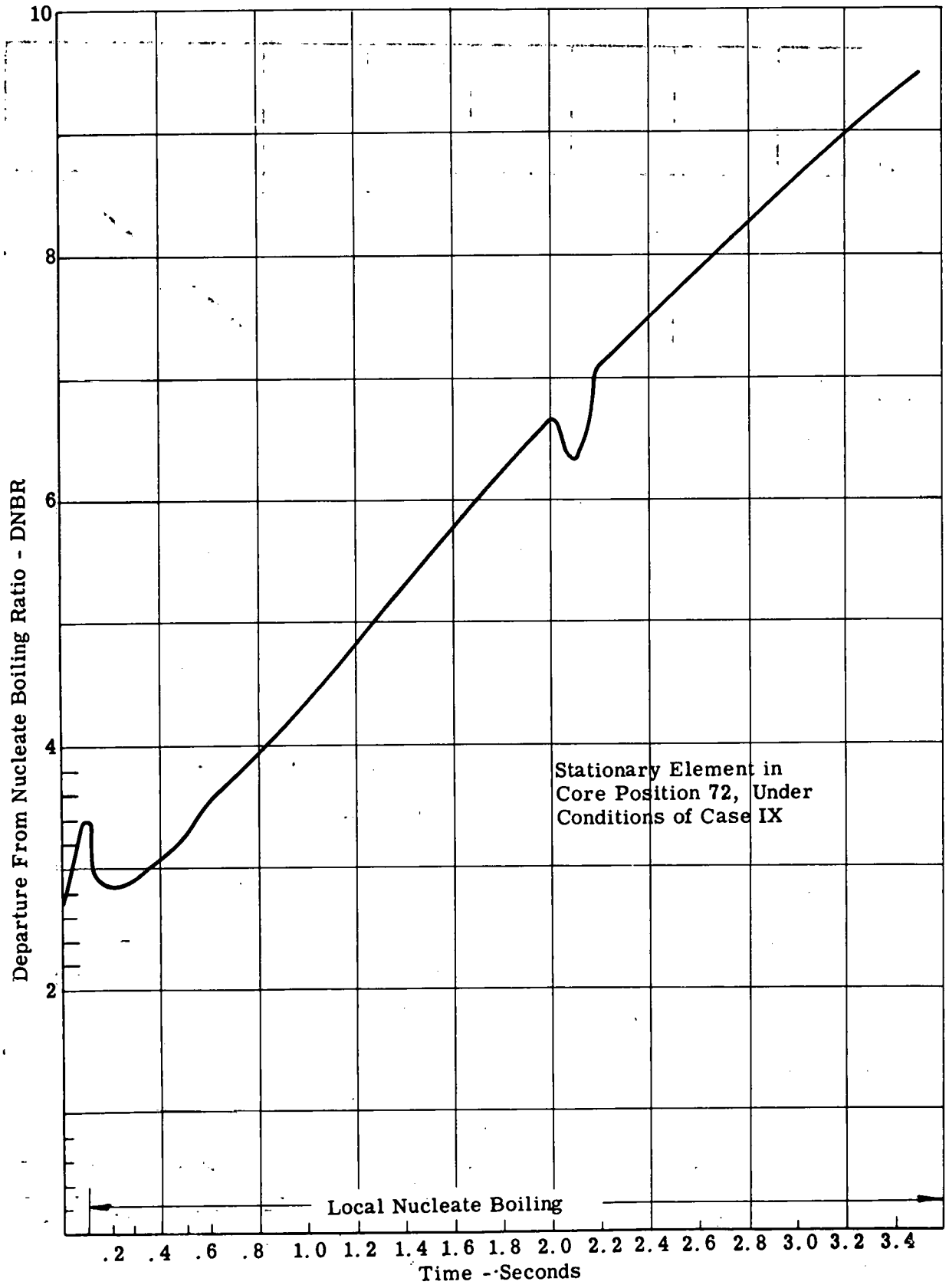

Figure 2.13.
SM-1A Type 3 Core
Minimum DNBR vs. Time
For The Hot Channel

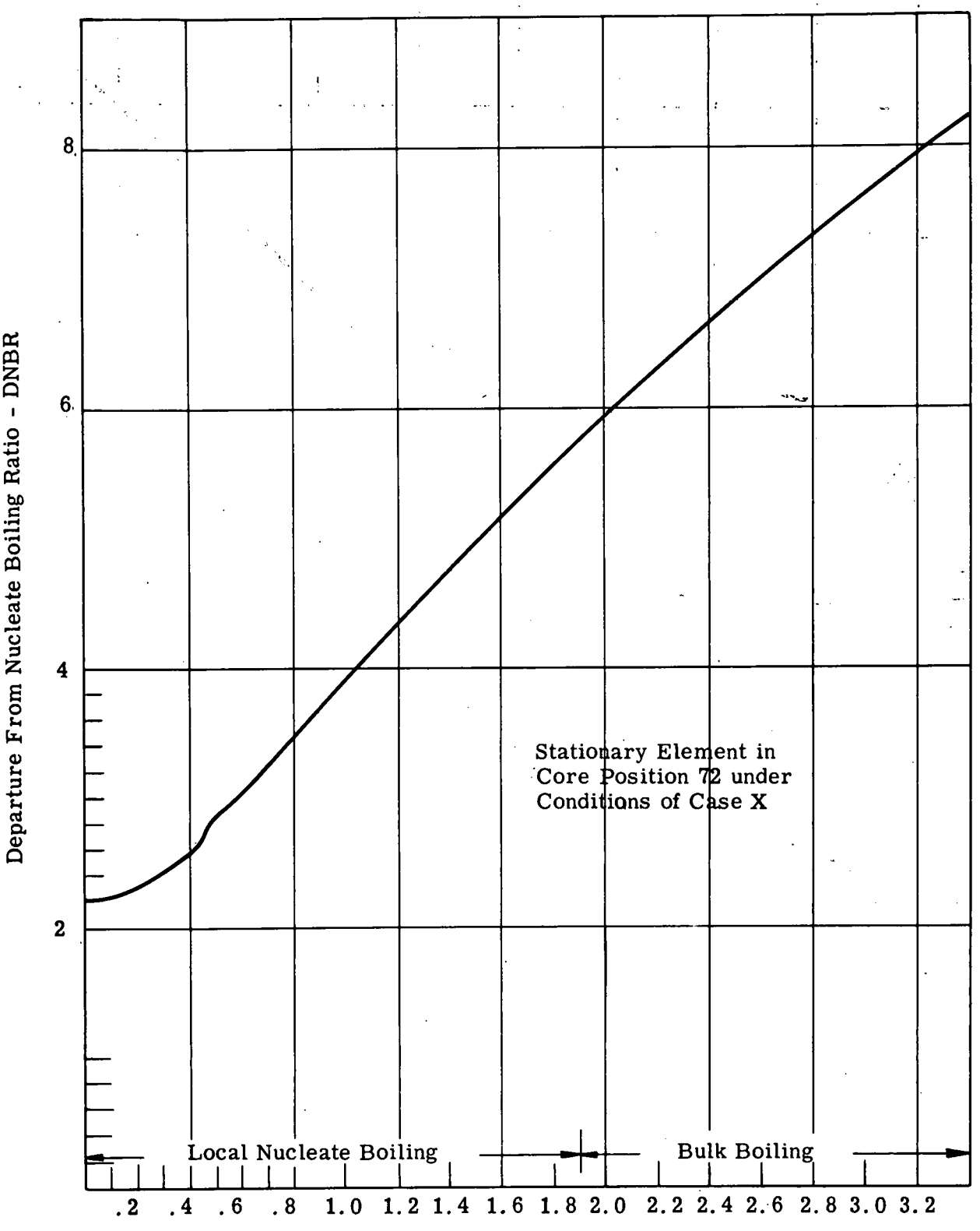

Figure 2.14

SM-1A Type 3 Core Minimum DNBR Vs. Time
For The Hot Channel

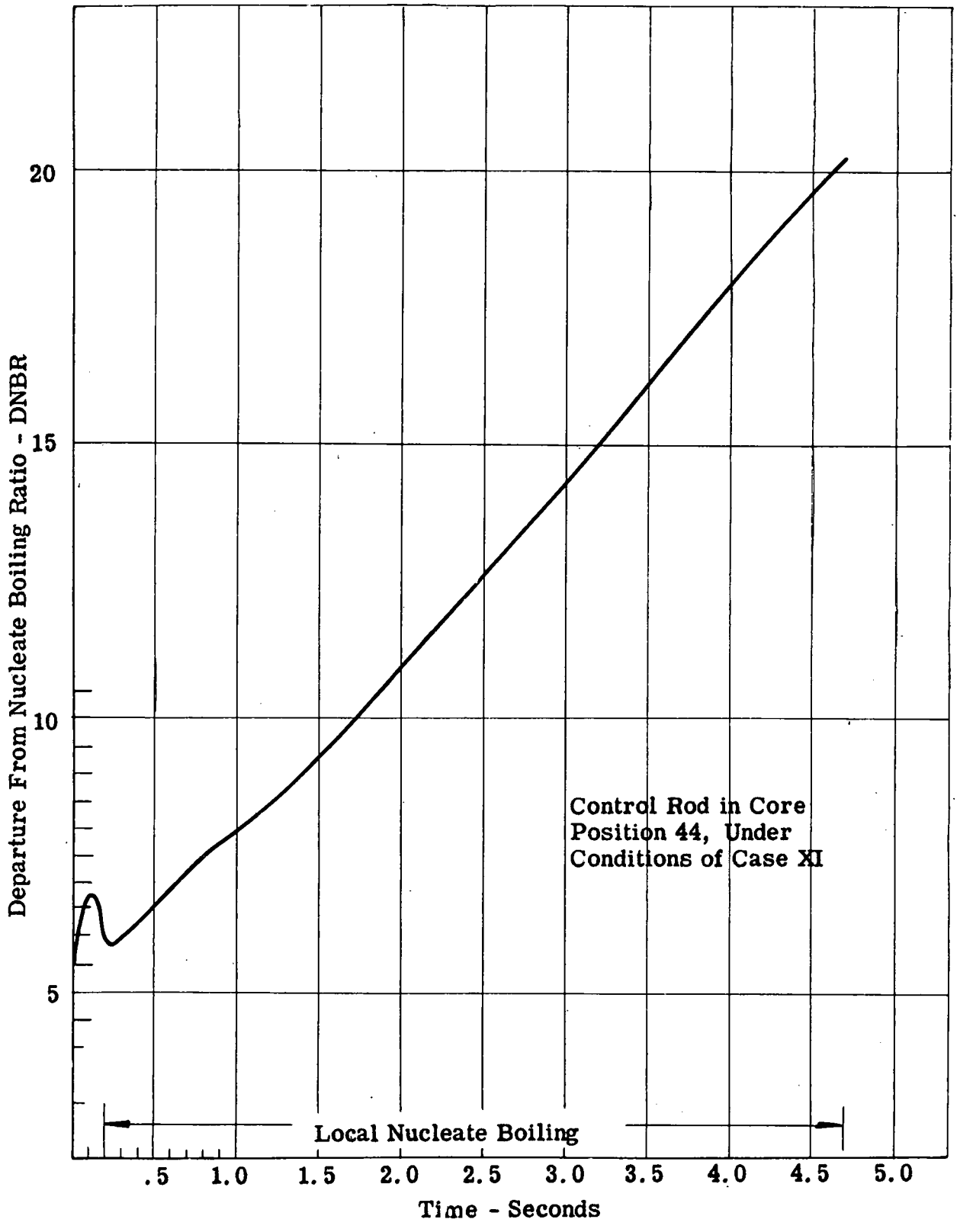

Figure 2.15.
PM-2A Type 3 Core
Minimum DNBR vs. Time
For The Hot Channel

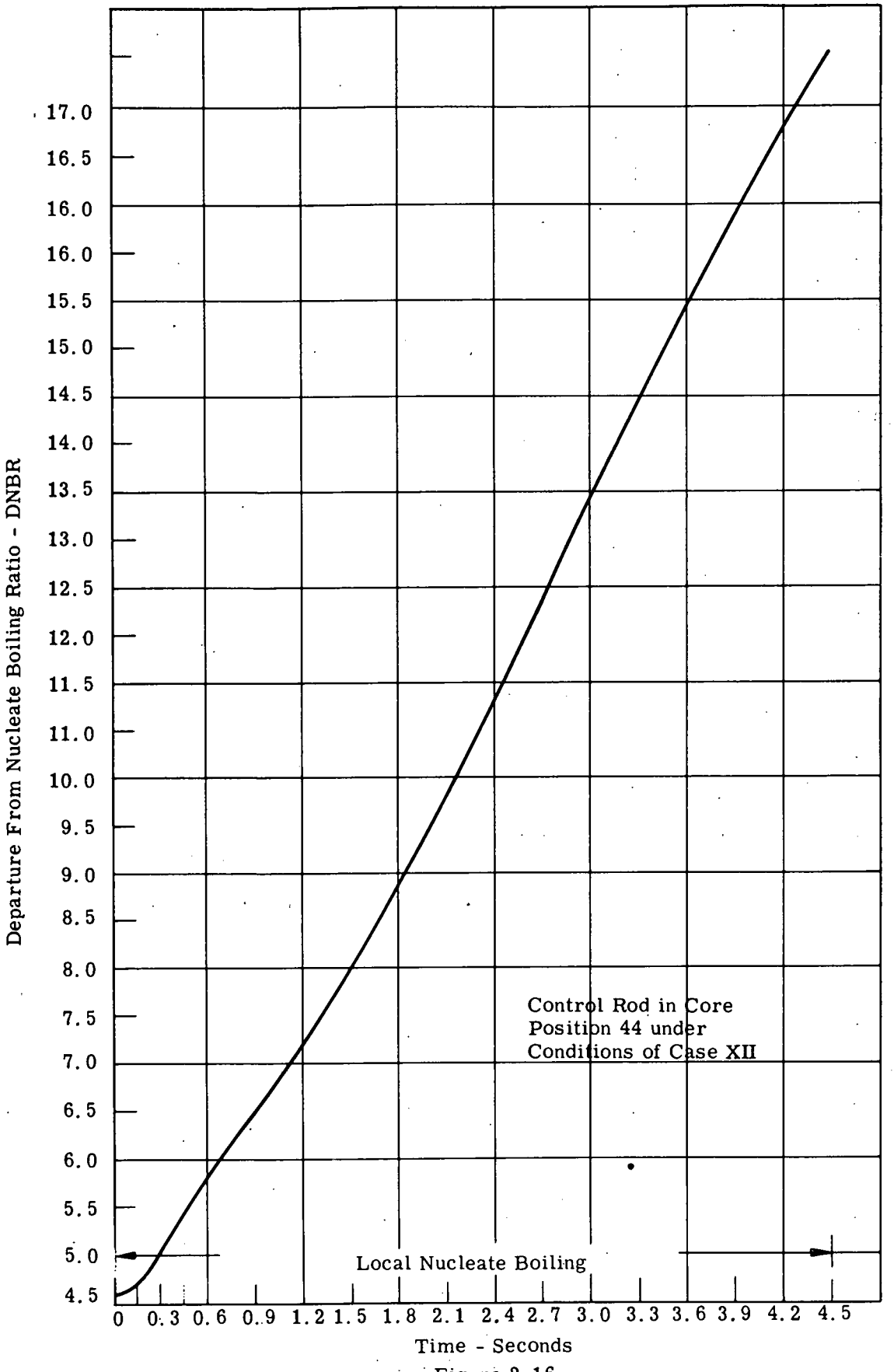

Figure 2.16

PM-2A Type 3 Core Minimum DNBR Vs. Time for the Hot Channel

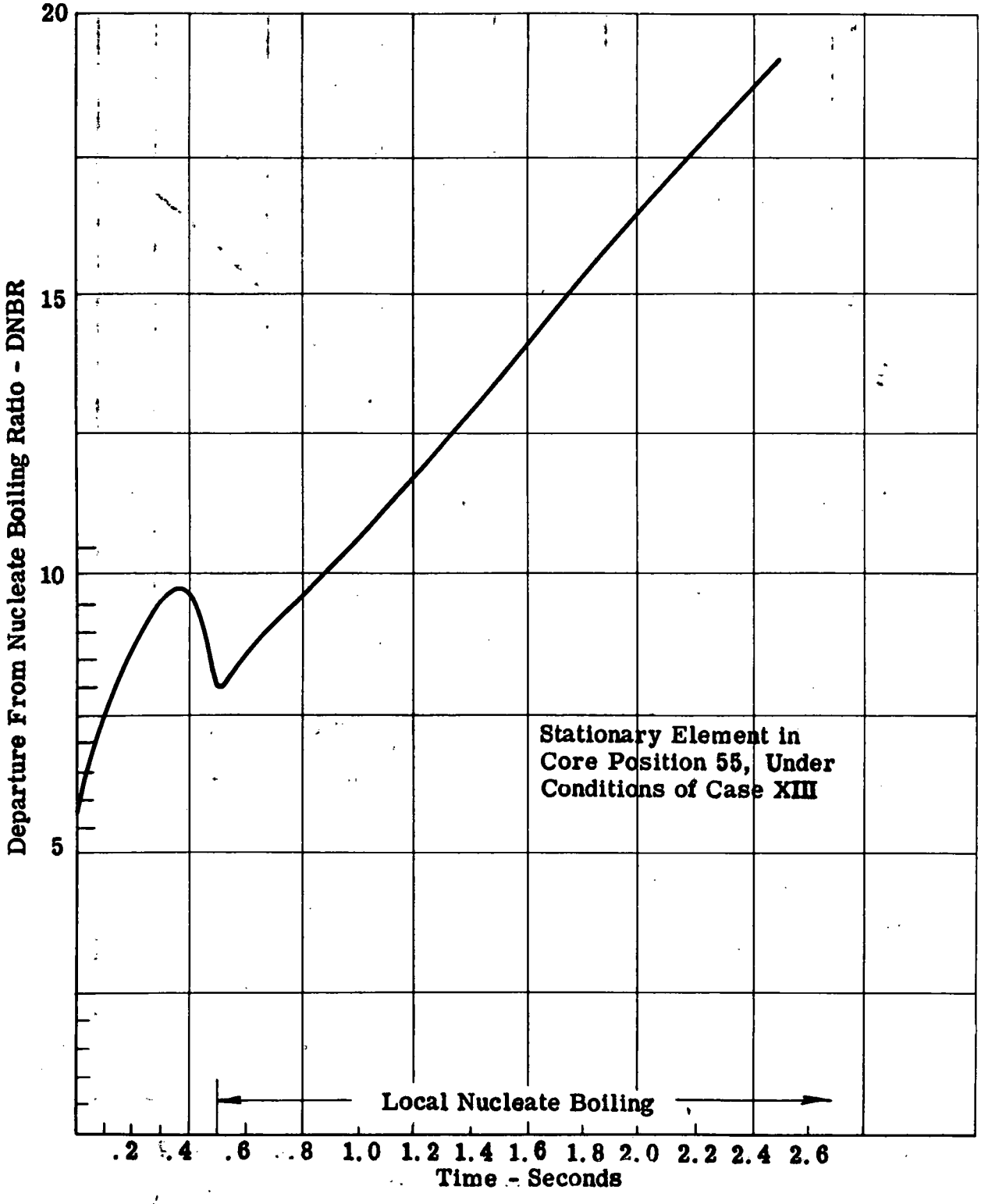

Figure 2.17.
PM-2A Type 3 Core
Minimum DNBR vs. Time
For The Hot Channel

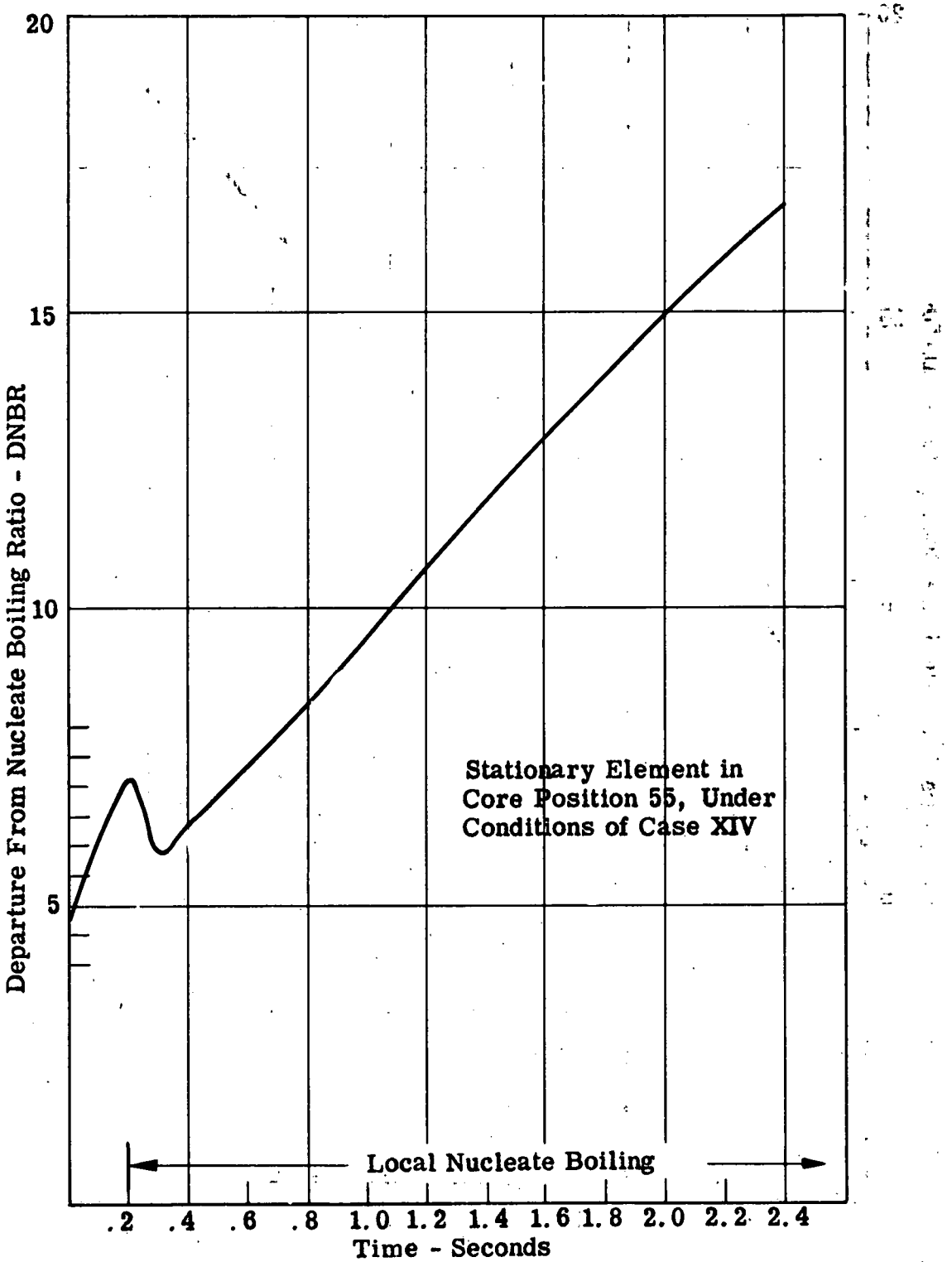

Figure 2.18.
PM-2A Type 3 Core
Minimum DNBR vs. Time
For The Hot Channel

2.14 RESULTS OF THE LOSS OF FLOW ANALYSIS OF THE SM-1 TYPE 3 CORE

The results of the transient analysis of the hottest control rod in core position 55 and the hottest stationary element in core position 61, as presented in Fig. 2.5 to 2.10 and tabulated in Table 2.2 indicate that:

a. There is no effect of the flow coastdown function on the minimum DNBR since the minimum DNBR is the steady state DNBR. This can be seen in Cases II and III. However, the utilization of a fictitiously high coastdown function of 4.0 does cause bulk boiling at 4.2 sec and an exit quality of 0.025 at 5.00 sec.

b. The scram mechanism is not effective during critical early periods of a loss of flow accident since in all cases the minimum DNBR is the steady state minimum DNBR. However, the utilization of the scram mechanism inhibits the bulk temperature rise and the creation of bulk boiling as can be seen by the difference between cases III and IV.

c. All evaluations of the hot stationary element 61 and the hot control rod in core position 55 indicate that at steady state the hot channel is in local nucleate boiling.

Therefore it is concluded that under the realistic conditions of a flow coastdown of 2.2 at the scram power level of 13.45 MW, the hottest element in the core (control rod in core position 55) will have a minimum DNBR of 4.08 when the scram mechanism is not considered to be operative. Similarly, the hottest stationary element, the element in core position 61, will exhibit a minimum DNBR of 4.28 under the same conditions and bulk boiling will occur at 4.43 sec. Since both these elements far exceed the criteria of a minimum transient DNBR of 1.50, these elements and the entire SM-1 Type 3 core is considered safe during a loss of flow transient.

In relation to previous cores and maximum heat flux as tabulated in Section 1.3 and the minimum DNBR's as tabulated in Table D.1, the following is noted:

TABLE 2.1
MINIMUM DNBR'S FOR VARIOUS SM-1 CORES

Core	Peak Heat Flux Btu/hr/ft^2 x 10^5	Core Power, MW	Min. DNBR
I	1.881	10.77	7.60
I	2.349	13.45	6.10
I Spiked & Rearranged	3.000	10.77	4.13
I Spiked & Rearranged	3.747	13.45	3.27
II	2.766	10.77	5.02
II	3.454	13.45	4.00
Type 3	2.578	10.77	4.87
Type 3	3.220	13.45	4.08

The Type 3 cores are considerably cooler than the Spiked and Rearragned Core I and are of approximately the same magnitude as Core II.

2.15 RESULTS OF THE LOSS OF FLOW ANALYSIS OF THE SM-1A TYPE 3 CORE

The results of the transient analysis of the hottest control rod in core position 55 and the hottest stationary element in core position 72 under conservative yet realistic conditions of no scram, with flow coastdown function b = 4.00, are presented in Table 2.3 and Fig. 2.11 to 2.14. These indicate:

a. The hottest element in the core, namely, the control rod in core position 55, exhibits bulk boiling at 1.13 sec and exit quality at 5.0 sec of 0.1275 when the core is at the peak power of 24.2 MW.

b. The control rod in core position 55 indicates a core minimum DNBR of 1.96 when the core is operating at the scram power level of 24.2 MW.

c. The hot control rod in core position 55 and the hot stationary element in core position 72 exhibit local nucleate boiling in the hot channel at steady state when the core is at scram power level.

d. Only the hot control rod in core position 55 exhibits steady state local nucleate boiling in the hot channel when the core is operating at the nominal power level of 20.2 MW.

From this information it is concluded that since the core minimum DNBR (1.96) at the scram power level without a scram exceeds the minimum allowable transient DNBR of 1.50, this element is safe in a loss of flow transient.

In comparison to SM-1A Core I with a nominal peak flux of 3.198×10^5 Btu/hr/ft^2, the SM-1A Type 3 Core with 5.149×10^5 Btu/hr/ft^2 has a much higher heat flux. However, the previously reported [12] minimum DNBR of 1.80 for Core I when operating under the nominal conditions of 20.2 MW must be in error, and the increase to 2.40 can be attributed to improved computation techniques. Therefore even though the SM-1A Type 3 core is somewhat hotter than Core I, it exceeds the minimum transient DNBR criteria and it is considered thermally safe during a loss of flow transient.

2.16 RESULTS OF THE LOSS OF FLOW ANALYSIS OF THE PM-2A TYPE 3 CORE

The results of the transient analysis of the hottest element in the core, the control rod at core position 44 and the hottest stationary element in core position 55 under the conservative yet realistic conditions of no scram, with coastdown function b = 4.0, is presented in Table 2.4 and Fig. 2.15 to 2.18.

The results indicate that:

A. The hottest element in the core, namely, the control rod in core position 44 indicates a core minimum DNBR of 4.59 at the scram power level of 12.0 MW and no scram.

B. The PM-2A core exhibits no steady state nucleate boiling when operating at the nominal core power 10.0 MW.

C. The PM-2A does not exhibit any bulk boiling at 5 sec after the loss of flow transient.

D. Only the hot control rod in core position 44 exhibits local nucleate boiling at steady state when operating at 12.0 MW.

E. The hot stationary element in core position 55 exhibits a minimum DNBR of 4.90 when operating at the scram power level of 12.0 MW without the scram mechanism operative.

Furthermore, it should be noted that in the PM-2A Type 3 Core cases analyzed, the effect of local nucleate boiling on DNBR is graphically demonstrated by the drops in the DNBR under the local boiling conditions as shown in Fig. 2.15, 2.17 and 2.18.

Therefore it is concluded that since the lowest DNBR in the core is 4.59 during a transient with the scram mechanism not operative, the entire core is safe during a loss of flow transient.

In comparison to PM-2A Core I with a nominal peak flux of 1.772 Btu/hr/ft^2 the PM-2A Type 3 Core with a peak flux of 2.016×10^5 Btu/ht/ft^2 has a much higher maximum heat flux. The minimum DNBR in Core I during a transient was 5.53 and logically Type 3 Core with a higher peak heat flux has a minimum DNBR of 4.59. This decrease in DNBR is not hazardous since the DNBR far exceeds the minimum allowable transient DNBR of 1.50; thus the PM-2A Type 3 Core is considered thermally safe.

2.17 CONCLUSIONS AND RECOMMENDATIONS OF LOSS OF FLOW TRANSIENT ANALYSIS

The results of the transient analysis as presented in Tables 2.2 to 2.4 indicate that:

1. All three cores are safe during a loss of flow transient since the minimum DNBR produced is 1.96 in the SM-1A Type 3 Core at the scram power level of 24.2.MW.

2. Only the SM-1A Type 3 Core indicates any bulk boiling during the first 5 sec of a loss of flow accident.

3. At the nominal power levels, SM-1 and SM-1A Type 3 Cores indicate local nucleate boiling while PM-2A Type 3 Core indicates no local nucleate boiling.

4. At the scram power level all three Type 3 cores indicate local nucleate boiling at steady state.

5. A comparison between the minimum steady state DNBR as obtained by means of the STDY-3 and ART-02 codes produces excellent agreement which indicates that the models used in each code are equivalent.

6. Increasing the flow coastdown function b, or scramming the reactor has only the effect of reducing the exit bulk temperature in the case of the SM-1 Type 3 Core.

With the prevalent steady state and transient analysis, the thermal safety of Type 3 cores has been established. Since, the SM-1A Type 3 Core has a minimum DNBR of 1.96, increased confidence can be obtained if a more comprehensive analysis is performed on this core, to remove any conservatism yet insure the thermal safety of the core. Therefore, it is recommended that the SM-1A Type 3 core be investigated under the conditions of:

1. Rod and load perturbations to complete the thermal analysis.

2. An axial flux distribution to account for the shift in distribution corresponding to a maximum xenon override.

3. Utilizing the improved two-dimensional transient codes such as XITE[29] or TITE [30] while incorporating reactivity effects due to boiling.

TABLE 2.2
RESULTS OF THE LOSS OF FLOW ANALYSIS OF THE SM-1 TYPE 3 CORE

Case No.	Core Position	Core Power, MW	Coastdown Function b =	Scram Time sec	Time of Initiation of Nucleate Boiling in the Hot Channel, sec	Minimum DNBR at Steady State (γ=0) By Means of STDY-3 Code	Minimum DNBR at Steady State (γ=0) By Means of ART-02 Code	Minimum Trans. DNBR	Hot Spot Quality or Bulk Temperature	Time Interval of Case Sec.	Initiation of Bulk Boiling, Sec.
I	55	10.77	4.0	∞	0.00	4.91	4.87	4.87	562.65°F	5.00	-
II	55	13.45	2.2	∞	0.00	4.06	4.08	4.08	545.91°F	5.00	-
III	55	13.45	4.0	∞	0.00	4.06	4.08	4.08	.0252	5.00	4.26
IV	55	13.45	4.0	0.06	0.06	4.06	4.08	4.08	476.74°F	2.90	-
V	61	10.77	4.0	∞	0.00	5.21	5.25	5.16	523.10°F	3.36	-
VI	61	13.45	2.2	∞	0.00	4.27	4.28	4.28	.0343	5.00	4.43

TABLE 2.3
RESULTS OF THE LOSS OF FLOW ANALYSIS OF THE SM-1A TYPE 3 CORES

Case No.	Core Position	Core Power, MW	Coastdown Function b =	Scram Time sec	Time of Initiation of Nucleate Boiling in the Hot Channel, sec	Minimum DNBR at Steady State ($\gamma = 0$) By Means of STDY-3 Code	Minimum DNBR at Steady State ($\gamma \neq 0$) By Means of ART-02 Code	Minimum Trans. DNBR	Hot Spot Quality or Bulk Temperature	Time Interval of Case Sec.	Initiation of Bulk Boiling, Sec.
VII	55	20.0	4.00	∞	0.00	2.39	2.40	2.40	.0435	4.4	1.62
VIII	55	24.2	4.00	∞	0.00	1.98	2.02	1.96	.1275	5.0	1.13
IX	72	20.2	4.00	∞	0.15	2.70	2.73	2.73	562.68°F	5.0	-
X	72	24.2	4.00	∞	0.00	2.24	2.23	2.23	590.04°F	5.0	-

TABLE 2.4
RESULTS OF THE LOSS OF FLOW ANALYSIS OF THE PM-2A TYPE 3 CORE

Case No.	Core Position	Core Power, MW	Coastdown Function b =	Scram Time, Sec.	Time of Initiation of Nucleate Boiling in the Hot Channel, sec.	Minimum DNBR at Steady State (τ =0) By Means of STDY-3 Code	Minimum DNBR at Steady State (τ=0) By Means of ART-02 Code	Minimum Trans. DNBR	Hot Spot Bulk Temperatures, °F	Time Interval of Case, Sec.	Initiation of Bulk Boiling, Sec.
XI	44	10.0	4.00	∞	0.10	5.61	5.53	5.53	590.04	5.00	-
XII	44	12.0	4.00	∞	0.00	4.66	4.59	4.59	595.96	5.00	-
XIII	55	10.0	4.00	∞	0.40	5.99	5.88	5.88	607.30	5.00	-
XIV	55	12.0	4.00	∞	0.30	4.99	4.90	4.90	613.76	4.70	-

REFERENCES

1. Davidson, S. L., Oggerino, J. P., "Interim Report on the Use of SM-2 Elements in SM-1, SM-1A and PM-2A Cores," APAE Memo No. 291, June 20, 1961.

2. Oggerino, J. P., "Nuclear Analysis of Type 3 Elements in SM-1, SM-1A and PM-2A Cores," APAE-104 to be issued.

3. Pyle, R. S., "STDY-3 , A Program for the Thermal Analysis of a Pressurized Water Nuclear Reactor During Steady State Operation," WAPD-TM-213, June 1960.

4. Krause, P. S., "Single Element Flow Tests For Type 3 (SM-2) Fuel Elements in SM-1, SM-1A and PM-2A Cores," APAE Memo No. 297, November 27, 1961.

5. Rosen, S. S., "Hazards Summary Report for the Army Package Power Reactor SM-1," APAE 2, Revision 1, May 1960.

6. Gallagher, J. G., "Hazards Summary Report for the SM-1A," APAE No. 13, Supplement 2, Rev. 1, October 7, 1960.

7. "Design Analysis of a Prepackaged Nuclear Power Plant for an Ice Cap Location (PM-2A)," APAE No. 39, Alco Products, Inc., January 15, 1959.

8. Lee, D. H., Robinson, R. A., Segalman, I. "Experiments and Analysis for SM-1 Core II with Special Components," APAE No. 85, April 26, 1961.

9. "SM-2 Core and Vessel Design Analysis," APAE No. 69, Volume I, Alco Products, Inc., March 8, 1961.

10. Birken, S. H., Matthews, F. T., Lee, D. H., "Analysis of Rearranged and Spiked SM-1 Core I," AP Note 243, Alco Products, Inc. April 8, 1960.

11. Ingeneri, S. M., 'Coolant Flow Tailoring Program of the APPR-1 Core Employing a Full Scale Model of the Reactor Vessel," APAE Memo No. 108, November 15, 1957.

12. Matthews, F. T., "Revised Thermal Analysis of the SM-1A Core," AP Note 307, Alco Products, Inc., December 8, 1960.

13. Matthews, F. T., "Results of the Experimental Flow Distribution Program for the PM-2A Reactor - Summary Report," AP Note 266, Alco Products, Inc., May 31, 1960.

14. Krause, P. S., "SM-2 Single Element Final Test Report," APAE Memo No. 267, October 28, 1960.

15. Conner, W. P., "MTR Technical Branch Quarterly Report," Firt Quarter, June 8, 1956.

16. Beck, R. G., "Hydraulics of Modified Fuel Elements for ETR", November 7, 1958.

17. Meyer, J. E., Smith, R. B., Gelbard, H. G., George, D. E., and Peterson, W. D., "ART-02 - A Program for the Treatment of Reactor Thermal Transients on the IBM-704, WAPD-TM-156," November 1959.

18. Meyer, J. E., Peterson, W. D., "ART-04 - A Modification of the ART Program for the Treatment of Reactor Thermal Transients on the IBM-704," WAPD-TM-202, July 1960.

19. Alco Products, Inc., "APPR Field Unit No. 1 APPR-1A," APAE 17, Supp. 1, July 1957.

20. ASTRA, "Pump Failure and the APPR-1." APAE Memo No. 87, May 1956.

21. Morrison, J. H., Lee, D. H., "Final Report Test 600 - Evaluation of Loss of Flow Accident in SM-1," Alco Products, Inc., Test Report, April 1960.

22. Rosen, S. S., "Hazards Summary Report for a Pre-packaged Nuclear Power Plant for an Ice Cap Location (PM-2A)," APAE No. 49, July 1, 1959.

23. Segalman, I., Bradley, P. L., "Steady State and Transient Thermal and Hydraulic Analysis of SM-2 - Termination Report, APAE No. 91, September 8, 1961.

24. De Bortoli, R. A., Green, S. J., LeTourneau, B. W., Troy, M., Weiss, A., "Forced Convection Heat Transfer Burnout Studies for Water in Rectangular Channels and Round Tubes at Pressures above 500 PSIA," WAPD-188, October 1958.

25. Scoles, J. F., "Criteria for Evaluating Hazards Involved in Proposed Tests on and/or Modifications to the SM-1," APAE No. 106, October 18, 1961.

26. Personal Communication by J. G. Gallagher to M. H. Dixon, Alco Products, Inc., on "Thermal Design Criteria and Corresponding End Box Configurations," February 22, 1962.

27. Personal Communication by F. G. Moote, Alco Products, Inc., to W. M.S. Richards, Alco Products, on July 20, 1961 on "Test 600 - Loss of Flow".

28. Krause, P. S., "SM-1A Control Rod Drive Production Test Report," AP Note No. 293, Alco Products, Inc., October 22, 1960.

29. Pyle, R. S., Rose, R. P., "XITE-1 Program, WAPD-R(J)-73, to be issued.

30. Miller, R. I., "A Digital Program for the Prediction of Two-Dimensional, Two-Phase Hydrodynamics," WAPD-TM-240, to be issued.

THIS PAGE

WAS INTENTIONALLY

LEFT BLANK

APPENDIX A
GENERAL DESCRIPTION OF STDY-3 IBM 704 CODE

A. 1 IMPORTANT CORRELATIONS USED IN THE STDY-3 CODE

The burnout correlations used in the code are controlled by the local enthalpy, the channel mass flow rate and system pressure. The general form of the equation selected for system pressures < 1850 psia is given as:

$$\frac{\phi_{DNB}}{10^6} = 0.890 \left[\frac{H_j}{1000}\right]^{-0.72} e^{-0.0012\ L/S} \qquad (A.1)$$

ϕ_{DNB} = departure from nuclear boiling heat flux

H_j = local enthalpy at a specific axial increment

L = channel length

S = channel spacing

The burnout ratio or DNBR is found by dividing the heat flux found in Eq. (A. 1) by $q_o^* F \Delta\theta f'(Z)$

$$DNBR = \frac{\phi_{DNB}}{q_o^* F\Delta\theta f'(Z)} \qquad (A.2)$$

where q_o^* = average core heat flux

$F_{\Delta\theta}$ = local hot channel factor

$f'(Z)$ = axial power at j th elevation

The criteria of local boiling in a channel is based upon a comparison between the average film drop (θ_f) and the film drop as calculated from the Jens-Lottes correlation ($\theta_{J\ \&\ L}$) with bulk parameters. If the average film drop exceeds or equals the film drop as calculated from the Jens-Lottes correlation, the channel is considered to be in local boiling and the proper pressure drop correlations for local boiling are utilized.

Local boiling exists if $\theta_f \geq \theta_{J \& L}$

$$\theta_f = \frac{q_o^* \; F \Delta T \, f'(Z)}{h} \tag{A.3}$$

and

$$\theta_{J \& L} = T_{sat} + \frac{60 \left(\frac{q_o^* \; F \Delta T \, f'(Z)}{10^6} \right)^{1/4}}{e^{P/900}} - T_j \tag{A.4}$$

and

$$h = .023 \; \frac{K}{(De)} \; (N_{RE})^{.8} \; (N_{PR})^{.4} \tag{A.5}$$

where θ_f = Avg. film temperature drop, ^oF

$J \& L$ = Avg. film temperature drop as calculated by the Jens-Lottes, correlation, ^oF

h = Avg. film coefficient, Btu/hr-ft^2 ^oF

T_{sat} = Saturation temperature of the fluid, ^oF

P = System pressure, psia

T_j = Bulk temperature of fluid at specific axial position, ^oF

K = Fluid thermal conductivity, Btu/hr-ft ^oF

De = Average equivalent diameter of channel, ft

N_{RE} = Reynolds Number

N_{PR} = Prandtl Number

Since the purpose of this criteria is not to establish the plate surface temperature but to determine whether the increased pressure drop and decreased flow associated with nucleate boiling occurs, the analysis is based upon bulk or average parameters upon which pressure drop is dependent. However, when calculating plate surface temperature, the film drops are compared as in the previous situation, but local parameters are inserted in Eq. (A. 6) to (A. 8) below.

$$T_S = T_j + \theta^L$$

where $\theta^{L} = \theta_f{}^{L} 1_f \; \theta_f{}^{L} \leq \theta^{L}_{J \& L}$

or $\theta^{L} = \theta^{L}_{J \& L} \; 1_f \; \theta_f{}^{L} > \theta^{L}_{J \& L}$

$$\theta^{L}_{f} = \frac{q_o^* \; F_{\Delta\theta} \; f'(Z)}{h^*} \qquad \text{(A. 6)}$$

$$\theta^{L}_{J \& L} = T_{sat} + \frac{60\left(\frac{q_o^* \; F_{\Delta\theta} \; f'(Z)}{10^6}\right)^{1/4}}{e^{P/900}} - T_j \qquad \text{(A. 7)}$$

and $$h^{L} = .023 \; \frac{K}{(De^*)^{4}_{L}} \; (N^{L}_{RE})^{.8} \; (N_{PR})^{.4} \qquad \text{(A. 8)}$$

where the nomenclature is the same as previously used but the superscript^{L} refers to the local conditions.

With these correlations utilized by the STDY-3 code for defining when nucleate boiling occurs, it is conceivable to have a condition in a channel where some portion of the channel is essentially at a uniform surface temperature with a reasonably high superheat and yet it is not in nucleate boiling. This has been observed in some of the elements investigated which are reported in sections 1.7, 1.8 and 1.9.

A.2 INPUT FORMAT FOR THE STDY-3 CODE

This section discusses the input parameters of the STDY-3 code and how the code uses these parameters to arrive at a solution. For illustrative purposes, control rod element position 44 in the SM-1 core has been selected. Refer to Table A.1.

The STDY-3 code consists of a title card, a control card, a pressure card, a flow card, an inlet temperature card, a core average heat flux card, nominal and hot channel description cards, a plenum card, and axial flux weighting cards.

a. The title card, card number 1, contains up to an eight digit code number and space for an alpha-numeric title. This card is required for the compatability of input with the logic deck.

b. The control card, card number 2, reading from left to right contains the number of system pressures, the number of channel mass flow rates,

the number of first pass temperatures, the number of channel flux variations, the number of passes, the number of first pass channels, the number of 2nd pass channels, clad thermal conductivity, meat thermal conductivity, channel length, fraction of flow heated, degree of mixing between first and second pass in order to calculate 2nd pass inlet temperatures, multiplier applied to the average channel flow to obtain a hot channel flow, equation choice (number refers to burnout equations in reference (3), choice of solution, (number refers to solution choice in reference (3).

c. The pressure card, card number 3, contains the numerical value of system pressure. The instrumentation tolerance for the SM-1 primary system pressure is $\pm$ 25 psia.

d. The 1st pass flow card, card number 4, contains the numerical value of channel mass flow rates. Note that the code accepts five different mass flow rates.

e. The first pass inlet temperature card, card number 6, contains the numerical value of first pass inlet temperature. The instrumentation tolerance for the SM-1 primary system inlet temperature is $\pm$ 4°.

f. The average core heat flux card, card number 71, contains the average core heat flux based on the thermal output of the core and the core heat transfer area. A 3.5% instrument tolerance was accounted for in calculating the SM-1 average core heat flux.

g. The nominal channel description card, card number 81, contains the following items reading from left to right: channel average thickness, channel local thickness, contraction coefficient, expansion coefficient, constant (K_1) to describe the nominal channel friction factor and constant (K_2) to describe the nominal channel friction factor, both to account for variation in friction factor with Reynolds number, clad thickness, meat thickness, fuel plate bundle entrance area ratio, fuel plate bundle exit area ratio, the combined product of the specified hot channel factors affecting average flux, the combined product of the specified hot channel factors affecting local flux.

h. The hot channel description card, card number 82, has the same items as described above in (g).

i. The plenum maldistribution factor card, card number 91, contains the plenum factors which are used to modify the nominal channel pressure drop to account for the following changes in the hot channel:

1. Changes in channel length affecting elevation and friction losses.
2. Changes in acceleration losses.
3. Changes in channel flow rate affecting friction losses.

Of these three losses, only differences in flow rate between the hot and nominal channels have been considered in the presently designed Alco reactors. The channel-to-channel flow maldistribution is caused by the element inlet end box. This factor was obtained from single element flow testing.[4]

j. The axial flux weighting cards, card 01 through 06, appear as the last set of input data. The values given are the average heat flux axially for both the nominal and hot channel. These are obtained from an axial power distribution curve as calculated by digital techniques[2]. The axial power is plotted versus core length and an average obtained by weighing each increment of core length.

In order to evaluate the thermal performance of a core, the STDY-3 code first determines the hot channel flow. The code obtains this hot channel flow from the core average heat flux, card number 71, and enthalpy conditions at a particular axial increment. Enthalpy conditions are obtained from the pressure and temperature input cards, 3 and 6. Within the element there is a channel with adverse mechanical dimensions, a theoretical hot channel. The local and average dimensions for this channel are located on card 82. The fuel plates adjacent to this channel have, in addition to adverse mechanical dimensions, increased fuel concentrations and other factors that tend to increase the heat generation. These factors and dimensions also appear in card 82 as a combined mechanical hot channel factor. Flow maldistribution due to plenum effects is taken into account by card number 91. Channel pressure drop is calculated by the code from the channel length given in control card 2, and channel inlet and exit coefficients, channel width, and variation of Reynolds number with friction factor given in card 82. The flow maldistribution factor listed on card 91 reduces the channel pressure drop, resulting in the available pressure drop for the hot channel. The STDY-3 code iterates until the hot channel flow equivalent to available flow given in flow card number 4 satisfies the hot channel pressure drop. The code gives for each axial point in the hot channel, bulk enthalpy, bulk temperature, plate surface temperature, steam quality, meat centerline temperature and minimum burnout ratios. If local or bulk nucleate boiling exists, the axial position at which the phenomenon exists is designated.

TABLE A.1
SAMPLE INPUT - STDY-3 CODE

Card		Card No.	
Title	-	900	Run 1 Task 3.3 SM-1 Core With SM-2 Elements Pos. 44 10.77 MW STDY-3
Control	-	2	1 5 1 1 1 2 0 22 11.2 9.68 22.0 0 0 1.25 2 3
Pressure	-	3	1175
Flow	-	4	1.076E 06 9.680E 05 8.610E 05 7.530E 05 6.460E 05
Temp. In	-	6	431.7
Flux	-	71	6.4557E 04 6.4557E 04
Channel Description	-	81	0.123 0.123 0.065 0.058 0.192 0.210 0.005 0.030 0.760 0.760 1.42 2.00
Channel Description	-	82	0.119 0.133 0.065 0.058 0.192 0.210 0.005 0.030 0.760 0.760 1.71 2.12
Plenum Factor	-	91	0.5540 1.000 1.000 1.000
Flux Weighting	-	01	0.0030 0.0060 0.0090 0.0140 0.0200 0.0300 0.0440 0.0650 0.0950 0.1400
Flux Weighting	-	02	0.2080 0.314 0.5150 0.9450 1.2300 1.470 1.6640 1.8010 1.8900 1.9110
Flux Weighting	-	03	1.8570 1.7640 -0.0 -0.0 -0.0 -0.0 -0.0 -0.0 -0.0 -0.0
Flux Weighting	-	04	0.0030 0.0060 0.0090 0.0140 0.0200 0.0300 0.0440 0.0650 0.0950 0.1400
Flux Weighting	-	05	0.2080 0.314 0.5150 0.9450 1.2300 1.470 1.6640 1.8010 1.8900 1.9110
Flux Weighting	-	06	1.8570 1.7640 -0.0 -0.0 -0.0 -0.0 -0.0 -0.0 -0.0 -0.0

APPENDIX B
HOT CHANNEL FACTORS

B.1 URANIUM CONTENT DEVIATION

B.1.1 Average Hot Channel Factor

Both fuel elements forming the hot channel are assumed to contain the maximum allowable uranium density per plate. If, on the average, the uranium content is higher by a certain percentage than the nominal, this will increase the water temperature, since more heat will be sent into the coolant moving between the two plates.

$$F_{\Delta T} = \frac{W_{ha}}{W_n} = \frac{W_n (1 + \delta)}{W_n} = 1 + \delta$$

where δ is the fractional deviation in the positive direction on uranium density.

B.1.2 Local Hot Channel Factor

In addition to the fraction of uranium content deviation per plate, which affects the total sensible heat in the channel, there exists some possibility of having a non-homogeneous mixture which might have deviations also. Designating the deviation in the positive direction as being $+\gamma$, (the fractional deviation), and assuming that a maximum positive homogeneity can occur simultaneously with δ, the γ will then essentially designate the criteria for affecting the local heat flux at the hot spot.

Therefore, the effect of $+\gamma$ is on the film temperature rise, which is

$$F_{\Delta\theta} = 1 + \gamma$$

B.2 ACTIVE CORE LENGTH DEVIATION

For a given volume of meat per plate, a negative deviation in active length increases the amount of meat per unit length and therefore per unit heat transfer area. This affects both the bulk coolant temperature rise and the film gradient, based on the conservative approach that the decreased length increases only meat thickness and not active width.

$$F_{\Delta T} = \frac{L_n}{L_{min}} = F_{\Delta\theta}$$

B. 3 CLAD THICKNESS DEVIATION FACTORS

If the two clad thicknesses of a fuel plate are unequal, a greater portion of the total heat generated in the meat will pass out through the thinner clad because of lower thermal resistance. A hot channel, therefore, is defined as being composed of two fuel plates whose inner and outer clad thicknesses are at the minimum and maximum observed values, respectively. Both the average and local hot channel factors are then equal to the proportional increase in the heat transmitted through the inner sides. The water temperature and film coefficients are assumed equal on both sides of the fuel plate shown below.

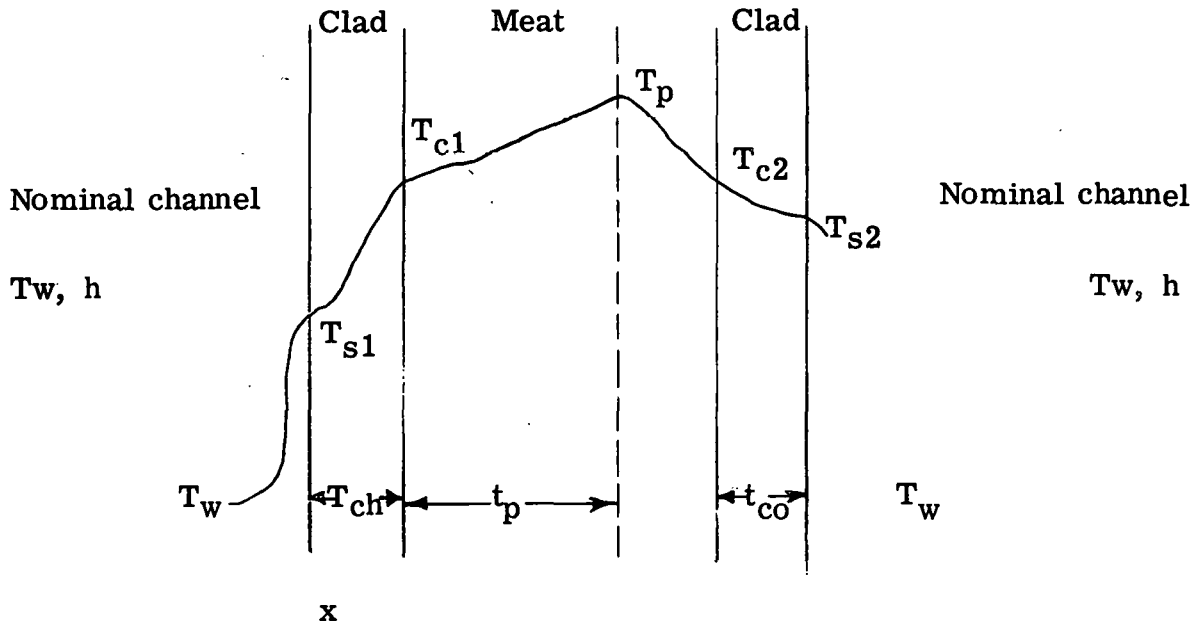

The differential equations describing the mode of conduction heat transfer for the plate are:

$$\frac{d^2T_1}{dx^2} = 0, \qquad 0 \leq X \leq t_{ch} \tag{B.1}$$

$$\frac{d^2T_m}{cx^2} = \frac{-Q}{k} \qquad t_{ch} \leq X \leq t_{ch} + t_m \tag{B.2}$$

$$\frac{d^2T_2}{dx^2} = 0 \qquad t_{ch} + t_m \leq X \leq t_{ch} + t_m + t_{co} \tag{B.3}$$

In the meat region (i.e., $t_{ch} \leq X \leq t_m + t_{ch}$)

at $X = t_{ch}$, $T_m = T_{c_1}$; at $X = t_{ch} + t_m$, $T_m = T_{c_2}$

Solving (B. 2) and the appropriate boundary conditions, the heat flux into the hot channel is

$$q_h = \frac{\frac{Qt_m}{2} + \alpha Q_{km}}{1 + \frac{k_m}{t_m}\beta} \qquad \text{where } \alpha = \frac{1}{h} + \frac{t_{co}}{k_c}$$

$$\beta = \frac{2}{h} + \frac{t_{ch} + t_{co}}{k_c}$$

But nominally the heat flow to either surface would just be $\frac{Q_{tm}}{2}$ if the clad thickness were the same

$$\therefore F = \frac{q_h}{q_n} = \frac{t_m + 2\alpha k_m}{t_m + k_m\beta}$$

if $\beta = 2$ (where $t_{co} = t_{ch}$) then F = 1 as expected.

The hot channel factor for this eccentricity of heat flow can therefore be defined as

$$F\Delta T = \frac{q_h}{q_n} = \frac{t_m + 2\alpha k_m}{t_m + k_m\beta}$$

The local factor, $F\Delta\theta$, is computed similarly except that different values of and α corresponding to the local point conditions are used.

THIS PAGE

WAS INTENTIONALLY

LEFT BLANK

APPENDIX C
DESCRIPTION OF THE EQUATIONS IN ART-02 IBM-704 CODE

C.1 ENERGY BALANCE

The sketch below shows a typical axial increment (ΔZ) of a reactor channel.

An energy balance can be written as heat stored equals heat generated minus heat out, where the heat generated in the plate and water in the j^{th} axial section and at time i is $q_{ji} \Delta Z 1_5$, but a fraction (r) of this total is generated directly in the water and the heat generated in the plate is $(1-r) q_{ji} \Delta Z 1_5$. The total heat flow out of the plate to the water is $\phi_{ji} \Delta Z 1_5$.

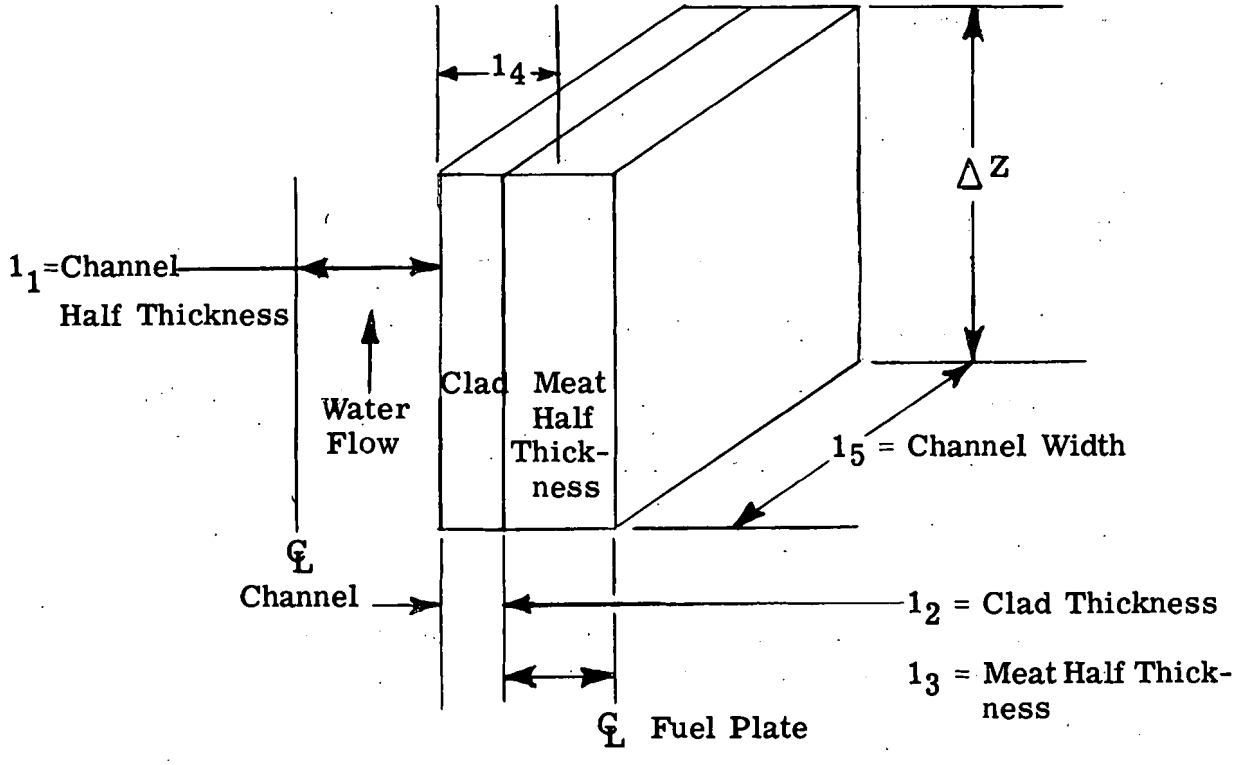

The heat capacity of the plate is $\Delta Z 1_5 (\rho C)_c 1_2 + (\rho C)_m 1_3$,

where $(\rho C)_m$ = heat capacity of the meat per unit volume

$(\rho C)_c$ = heat capacity of the clad per unit volume

Therefore, the energy balance for the plate result in the following differential equation for the mean plate temperature (T_{mj})

$$\Delta Z\, 1_5 \left[(\rho C)_c\, 1_2 + (\rho C)_m\, 1_3 \right] \frac{d\, T_{mj}}{dt} = (1-r)\, qj\, \Delta Z\, 1_5 - \phi_j\, \Delta Z\, 1_5$$

or in finite difference form,

$$(T_m)_{j,\,i+1} = (T_m)_{ji} - \frac{\Delta ti}{\left[(\rho C)_c\, 1_2 + (\rho C)_m\, 1_3 \right]} \left\{ \phi_{ji} - q_{ji}\,(1-r) \right\} \qquad \text{(C. 1)}$$

where

q_{ji} = Total heat generation rate per unit area, Btu/hr-ft^2

r = fraction of heat generated in water

ϕ_{ji} = heat flux, Btu/hr-ft^2

and

$$q_{ji} = q_o^{*}\, f'(Z)_j\, F_{M\Delta T}\, (P/P_o)_i \qquad \text{(C. 2)}$$

where

q_o^{*} = Steady state reference heat generation per unit area= total core power/core heat transfer area, Btu/hr-ft^2

$f'(Z)_j$= local to average axial power ratio at the j^{th} position

$F_{M\Delta T}$=Average power peaking factor inclusive of average engineering Hot channel factors nuclear uncertainty factors, and average hot channel radial power peaking.

$(P/P_o)_i$ = Power coastdown function at the i^{th} time increment.

The correlation for the heat flux from the plate to the water at steady state is equal to the heat generated in the plate:

$$\phi_{jo} = q_{jo}\,(1-r)$$

During the transient, this equality is not valid, since the heat flux is a function of the average meat temperature bulk fluid temperature, etc., and it is evaluated in the ART code as the larger of the following expressions.

$$\phi_{ji} = U_i \left[(T_m)_{ji} - (T_w)_{ji} \right] \qquad \text{(C. 3)}$$

$$\phi_{ji} = \frac{K_q}{1_4} \left[(T_m)_{ji} - (T_c)_{ji} \right] \qquad \text{(C. 4)}$$

where U_i the over-all heat transfer coefficient

$$U = \frac{1}{\left[\frac{1_4}{K_c} + \frac{1}{h_i}\right]} \text{ Btu/hr-ft}^2 - {}^{o}\text{F} \qquad \text{(C. 5)}$$

K_c = Thermal conductivity of the clad Btu/hr-ft^{o}F

1_4 = Equivalent plate conduction length where the mean plate temperature exists, ^{o}F

h_i = the average water film coefficient evaluate at the i^{th} time increment when the average channel mass velocity is G_i, Btu/hr-ft^2 ^{o}F

$(T_w)_{ji}$ = bulk fluid temperature corresponding to the enthalpy H_{ji}, ^{o}F

$(T_c)_{ji}$ = local boiling surface temperature predicted from the Jens-Lottes correlation as is used in STDY-3 code.

$$(T_c)_{ji} = T_{sat} + \frac{60}{e^{P/600}} \left[\frac{\phi_{j,\, i-1}}{10^6} \right] \qquad \text{(C. 6)}$$

where T_{sat} = fluid saturation temperature, ^{o}F

P = System pressure, psia

and as long as nucleate boiling does not occur the actual surface temperature $(T_s)_{ji}$ is evaluated as

$$(T_s)_{ji} = (T_m)_{ji} - \frac{1_4\, \phi_{ji}}{K_c} \qquad \text{(C. 7)}$$

In a similar manner, an energy balance is performed for the water contained in the j^{th} axial section to obtain the enthalpy (and temperature) of the fluid.

Heat generated directly in the water - $rq_{ji}\ \Delta Z\ 1_5$

Heat flux added to the water = $\phi_{ji}\ \Delta Z\ 1_5$

Heat convected away by the water = $G_i\ 1_5\ 1_1\ (H_{ji} - H_{j-1,\, i})$

and in a constant pressure process the stored energy = $\rho_j \Delta Z_j\ 1_1\ 1_5 \frac{dH_j}{dt}$

Writing the energy balance in finite difference terms,

$$H_{j,i+1} = H_{ji} + \frac{v_{ji}\,\Delta t_i}{1_1}\left[(\phi_{ji} + rq_{ji}) - \frac{G_i\,1_1}{\Delta Z}(H_{ji} - H_{j-1,i})\right] \qquad (C.8)$$

where v_{ji} = the specific volume, $\frac{ft^3}{lb}$

C.2 PRESSURE DROP

The pressure drop for any given channel is broken into the following terms:

1. Losses resulting from entrance and exit terms and frictional pressure drop $(\Delta P_f)i$
2. Losses resulting from change in elevation $(\Delta P_{el})\,i$
3. Pressure drop from spatial acceleration $(\Delta P_{a2})\,i$
4. Transient acceleration drop resulting from mass velocity changes with time $(P_{a1})\,i$

$$\text{or } \Delta P_i = (\Delta P_f)i + (\Delta P_{e1})i + (P_{a1})i + (P_{a2})\,i \qquad (C.9)$$

$$\text{where } (\Delta P_f)i = K_e\left(\frac{v_{oi}\,G_i^2}{2}\right) + K_e\left(\frac{v_{ni}\,G_i^2}{2}\right) + \left[\frac{(f_{o1}\,v_{o1})}{2} + \sum_{j=1}^{N-1} f_{ji}\,v_{ji} + \frac{(f_{n1}\,v_{n1})}{2}\right]\left[\frac{(G_i^2\,\Delta Z)}{2D_h}\right] \qquad (C.10)$$

where K_c and K_e = Unrecoverable loss coefficient for the channel entrance and exit.

v_{oi}, v_{ni} = Specific volume of the fluid at the i^{th} time increment just inside the channel inlet and exit, respectively, ft^3/lb

D_h = Channel hydraulic diameter, ft.

f_{oi} f_{ni} = friction factor used to predict frictional resistance to fluid flow at the i^{th} time increment just inside the channel inlet and exit respectively.

As in the STDY-3 code the friction factor f_{ji} is given by

$f_{ji} = (f_{iso})_i \, (f/f_{iso})_{ji}$ for a subcooled liquid, $H_{ji} < H_f$

and $f_{ji} = (f_{iso})_i \, (v_f/v_{ji}) \, (\phi^2_{Lo})_{ji}$ for a steam-water mixture, $H_{ji} \geq H_f$

where v_f = specific volume of a saturated liquid, ft^3/lb

H_f = enthalpy of a saturated liquid, Btu/lb

$(f_{iso})_i$ = Isothermal friction factor at the i^{th} time increment

$(\phi^2_{Lo})_{ji}$ = Function to fit saturation region pressure drop

$(f/f_{iso})_{ji}$ = Function to fit subcooled nonisothermal,pressure drop

$$f/f_{iso} = \left[F_H \quad 1 + .93 \left(\frac{1-[\theta^*_{ji}/\theta_{ji}]}{(G_i/10^6)^{2/3}} \right) \right] \qquad \text{(C. 11)}$$

where F_H = Heat contribution to subcooled pressure drop which equals the smaller of the two

$$F_H = \begin{cases} 1.0 \text{ or} \\ 1.5\,(1-.0025\,\theta^*_{ji}) \end{cases}$$

and θ^*_{ji} = Actual film drop as used in pressure drop calculations which is defined as the smaller,

$$\theta^*_{ji} = \begin{cases} \theta_{ji} = \phi_{ji}/(h_f)_i & \text{or} \\ (T_c)_{ji} - (T_w)_{ji} \end{cases}$$

where θ_{ji} = Film drop used in pressure drop calculations based on the film coefficient $(h_f)_i$, But/hr-ft^2

$(h_f)_i = 1.58\, h_i$

The development of the 1.58 coefficient is given in WAPD-TH-300

The pressure drop resulting from change in elevation is

$$(P_{e1})_i = g\Delta Z \left[(1/2\ (^{1/v}{}_{oi}) + \sum_{j=1}^{n-1} 1/v_{ji} + 1/2\ (^{1/v}{}_{ni}) \right] .. \quad (C.12)$$

where g is the component of the acceleration of gravity acting in the axial direction, = 32.174 ft/sec^2

Pressure drop resulting from mass velocity changes with time

$$(\Delta P_{a1})_i = h\,\Delta Z\,(G_{i+1} - G_i) / \Delta t_i \quad (C.13)$$

and the final pressure drop term for spatial acceleration

$$(\Delta P_{a2})_i = -(1 + \sigma_o{}^2) \left(\frac{v_{oi}\ G_i^2}{2} \right) + (1 + \sigma_n{}^2) \left(\frac{v_{ri}\ G_i^2}{2} \right) \quad (C.14)$$

where σ_o and σ_n = area ratio at entrance and exit respectively

$$\sigma^2 = \left(\frac{\text{area inside channel}}{\text{area in plenum region}} \right)^2$$

C.3 HOT CHANNEL FLOW

For each hot channel in parallel with the nominal channel, it is assumed in ART that the total hot-channel pressure drop $(\Delta P)_i^{HC}$ is related to the nominal channel pressure drop $(\Delta P)_i^{NC}$ by

$$(\Delta P)_i^{HC} = K_{pf}^{HC}\ (\Delta P_f)_i^{NC} + K_{pa}^{HC} (\Delta P_{a1})_i^{NC} + (\Delta P_{a2})_i^{NC} + (\Delta P_{e1})_i^{NC} \quad (C.15)$$

where K_{pf}^{HC} and K_{pa}^{HC} are the plenum maldistribution factors for pressure loss and acceleration terms respectively. They are evaluated:

$$K_{pf}^{HC} = (1 - \delta)^{1.8}$$

$$K_{pa}^{HC} = (1 - \delta)^{2.0}$$

where δ is the percent hot channel flow maldistribution.

The mass velocity in the hot channel is established by:

$$G^{HC}_{i+1} = G^{HC}_{i} + \frac{\Delta t_i}{n \Delta Z} \left(\Delta P_{al}\right)^{HC}_{i} \qquad \text{(C. 16)}$$

C. 4 DEPARTURE FROM NUCLEATE BOILING CORRELATIONS

The departure from nucleate boiling correlations used in the ART code are similar to those used in the STDY-3 code (refer Eq. (A. 1). However the correlations used in STDY-3 are the latest available information as discussed in WAPD-188[24] and the ART results have been corrected to account for the discrepancies in the DNB and as is discussed in Section 2. 9. The equations programmed in the ART-02 for $G^{L}_{i} \leq 1.6 \times 10^6$ lb/hr-ft^2 and system pressures below 1850 psia are:

For SM-1 and SM-1A, where P = 1200 psia design (acutal P = 1175 psia)

$$\left(\frac{\phi_{DNB}}{10^5}\right)_{ji} = 3.86 \left[\frac{H_{ji}}{1000}\right]^{-2.5} (F_C)_2 \qquad \text{(C. 17)}$$

For PM-2A, where P = 1750 psia design (actual P = 1715 psia)

$$\left(\frac{\phi_{DNB}}{10^5}\right)_{ji} = 3.48 \left[\frac{H_{ji}}{1000}\right]^{-2.5} (F_C)_2 \qquad \text{(C. 18)}$$

where

ϕ_{DNBR} = Departure from nucleat boiling, heat flux, Btu/hr-ft^2

G^{L}_{i} = Local mass velocity, lb/hr-ft^2

$$G^{L}_{i} = \left(\frac{G}{G}^{L}\right) G_i$$

where $\frac{G^{L}}{G}$ = local mass velocity correction factor

evaluated by $\left[\frac{(D_h \text{ avg. min}}{D_{h \text{ local max}}}\right]$ Since in narrow rectangular channels, the area is directly proportional to the channel spacing.

The DNB ratio is calculated by

$$DNBR = \frac{\phi_{DNB}}{\phi^{L}_{Ji}} \qquad \text{(C. 19)}$$

where ϕ^{L}_{Ji} is the local heat flux evaluated as

$$\phi^{L}_{Ji} = \left(\frac{\phi^{L}}{\phi}\right) \phi_{ji}, \text{ Btu/hr-ft}^2$$

where ϕ^{L}/ϕ local heat flux correction factor evaluated as

$$\phi^{L}/\phi = \frac{F_{M\Delta\theta}}{F_{M\Delta T}} \qquad \text{(C.20)}$$

$F_{M\Delta\theta}$ = Local power peaking factor inclusive of engineering hot channel factors, nuclear uncertainty factor and local hot plate radial power peaking factor.

C.5 REACTOR KINETICS

The ART code assumes the heat generation at any point within the core is proportional to a single power coastdown function(P/P_o). That is, the heat generation rate (q_{ji}) is given by:

$$q_{ji} = f'(Z)_j \, F_{\Delta T} \, q_o^* \left(\frac{P}{P_o}\right)_i \qquad \text{(C.21)}$$

$$\text{where } \left(\frac{P}{P_o}\right)_i = \alpha_o \left[\frac{\alpha}{\alpha_o}\right]_i + (1 - \alpha_o) N_i \qquad \text{(C.22)}$$

α_o = Steady state fraction of power produced by decay heating.

α/α_o = Decay power coastdown function

N_i = Neutron power coastdown function

Therefore, it is seen that the power coastdown function is divided into a decay heat contribution and a neutron power contribution. The neutron power coastdown, N_i, is itself divided into two parts, the prompt neutron contribution and the delayed neutron contribution. The standard reactor kinetics equation for neutron level as a function of time is:

$$\frac{dN}{dt} = \left[\frac{\delta K - \beta}{\ell^*}\right] N + \sum_{d=1}^{d=L} \frac{\bar{\beta}_d \chi_d}{1^*} \qquad \text{(C.23)}$$

where ℓ^* = prompt neutron lifetime

$\bar{\beta}$ = effective delay neutron fraction which is the sum of the fractions of each delayed neutron group

χ_d = Normalized concentration of precursors

and $\frac{d\chi_d}{dt} = \lambda_d (N - \chi_d)$ (C. 24)

$$\bar{\beta} = \sum_{d=1}^{de} \bar{\beta}_d$$

where λ_d = decay constant

The solution to these equations is:

$$N_i^{K+1} = N_i^K \left[1 + \frac{(\Delta t_r)}{2\,1^*} i \left[\delta K_i^K - \bar{\beta} \right] + \frac{(\Delta t_r)}{2\,1^*} i \sum_{d=1}^{de} \bar{\beta}_d \left[(\chi_d)_i^{K+1} + (\chi_d)i^K \right] \right] \Bigg/ \left[1 - \frac{(\Delta t_r)_i}{2\ell^*} \left(\delta K_i^K - \bar{\beta} \right) \right] \quad \text{(C. 25)}$$

$$\delta K_i^K = (\delta K_r)_i^K + (\delta K_t)_i$$

where (Δt_r) = Time increment

$(\delta K_r)_i$ = Excess reactivity resulting from rod motion

$(\delta K_t)_i$ = Excess reactivity resulting from temperature change

The neutron power coastdown as given in (C.25) results from two negative reactivity effects. The immediate effect is the negative temperature coefficient of reactivity δK_t when the nominal channel temperature rises. The second effect, δK_r, which occurs at a preset (delay) time, t_3, is caused by a scram and its associated control rod insertion.

The temperature dependent portion of the reactivity is given by

$$(\delta K_t)_i = \frac{\partial(\delta K)}{\partial T_w} \left\{ \sum_{J=1}^{n} \alpha_j \left[(T_w)_{ji} - (T_w)_{jo} \right] \right\}^{NC} \qquad \text{(C. 26)}$$

where $\frac{\partial(\delta K)}{\partial T_w}$ is the temperature coefficient of reactivity, and the a_j's are the temperature weighting factors, chosen so that $\sum_{J=1}^{n} (aj) = 1$

APPENDIX D
UPDATED DEPARTURE FROM NUCLEATE BOILING RATIO FOR THE HOT ELEMENT OF VARIOUS CORES

TABLE D.1

UPDATED DEPARTURE FROM NUCLEATE BOILING RATIO FOR THE HOT ELEMENT OF VARIOUS CORES

				Old DNB Correlations		Updated DNBR Correlations	
Core	Report	Core Position	Core Power, MW	Steady State Min. DNBR	Transient Min. DNBR	Steady State Min. DNBR	Transient Min. DNBR
SM-1Core I	APAE No. 85[8]	44	10.77	11.7	11.73*	7.6	7.63*
SM-1 Core I	APAE No. 85[8]	44	13.45	9.4	9.42*	6.1	6.12*
SM-1 Core I Rearranged & Spiked	APAE No. 85[8]	65	10.77	6.4	6.36*	4.2	4.13*
SM-1 Core I Rearranged & Spiked	APAE No. 85[8]	65	13.45	5.1	5.03*	3.3	3.27*
SM-1 Core II	APAE No. 85[8]	65	10.77	7.8	7.73*	5.1	5.02*
SM-1 Core II	APAE No. 85[8]	65	13.45	6.2	6.15*	4.0	4.00*
SM-1 Type 3	APAE Memo No. 291[1]	44	10.77	8.2	-	5.3	-
SM-1 Type 3	APAE Memo No. 291[1]	44		6.5	-	4.2	-
SM-1A Core I	AP Note 307[12]	44	20.20	2.9	2.8*	1.9	1.8*
SM-1A Type 3	APAE Memo No. 291[1]	67	20.20	3.9	-	2.5	-
SM-1A Type 3	APAE Memo No. 291[1]	67	24.20	3.2	-	2.1	-
PM-2A Core I	APAE No. 39[7]	Hot Stationary Element	10.00	7.1	-	7.7	-
PM-2A Type 3	APAE Memo No. 291[1]	23	10.00	7.9	-	5.1	-
PM-2A Type 3	APAE Memo No. 291[1]	23	12.00	6.6	-	4.3	-
SM-2 Core I	APAE No. 91[23]	44	28.00	2.18	1.82	2.18	1.82
SM-2 Core I	APAE No. 91[23]	44	35.00	1.60	-	1.60	-

*Indicates pseudo-transient analysis